Alma Mater Studiorum – Università di Bologna

DOTTORATO DI RICERCA IN

CHIMICA

Ciclo XXVII

Settore Concorsuale di afferenza: 03/A1- CHIMICA ANALITICA

Settore Scientifico disciplinare: CHIM/01-CHIMICA ANALITICA

ULTRASENSITIVE CHEMILUMINESCENCE BIOASSAYS BASED ON MICROFLUIDICS IN MINIATURIZED ANALYTICAL DEVICES

Presentata da: Zangheri Martina

Coordinatore Dottorato

Chiar.mo Prof. Aldo Roda

Relatore

Prof.ssa Mara Mirasoli

Esame finale anno 2014/2015

Alla mia famiglia

Indice

CHAPTER 1

Introduction

The development of an accurate and user-friendly diagnostic device for point-of-care (POC) applications is one of the most challenging tasks in the field of analytical chemistry. The POC approach provides fast and reliable analytical results in a rapid and easy way. In order to be considered a real POC system, the device must fulfill minimum requirements [1], in particular it should:

- allow the direct introduction of the sample with a minimum or nul sample pretreatment
- be portable with a small size, reduced weigh and autonomous electrical power
- be user-friendly in order to be used by non-skilled personnel outside well-equipped laboratories
- offer qualitative or quantitative results, as required, by treating the primary measurement output provided by the detection system.

Moreover an ideal POC device should be based on low cost and disposable elements and it should ensure stability and durability from the fabrication to their use. Other important characteristics of a POC device are the possibility to automate the analytical procedure (from sampling to results generation), to provide wide measurement range and multiplexing capability (simultaneous determination of multiple analytes), as well as device robustness, such as the tolerance to changes in air humidity and temperature [2].

The possibility to scale down traditional bench-top analytical procedures and to transfer them in a portable miniaturized and self-operating system can pave the way for extra-laboratory analyses in

clinical chemistry, environmental monitoring, food analysis, and bio-warfare protection [3].

The challenging objective in this field is the achievement of low limits of detection, since small sample volumes imply that only few molecules of analyte are available for detection, and the possibility to shorten time and cost of the analysis. The sensitivity of the device depends on the analytical technique employed for the recognition of the analyte and on the detection principle. Among the different analytical techniques, those based on biospecific molecular recognition reactions (like immunological or genic reactions) are suitable for this purpose, because of their high specificity and sensitivity, which makes it possible to detect analytes even at low concentrations and in complex matrices. By coupling these methods with optical detection it is possible to obtain high sensitivity, non-invasiveness, rapidity and easy implementation [4]. Among optical detection techniques, fluorescence is by far the most commonly employed one. On the other hand, chemical luminescence is particularly advantageous because it offers high detectability even in low volumes. Since excitation is not required, problems frequently encountered in photoluminescence, such as light scattering, source instability and high backgrounds due to unselective photoexcitation are absent in chemical luminescence [5,6]. Moreover the instrumentation for the measurment of chemical luminescence is very simple and it can be easily miniaturized, fitting the POC purposes.

1.1 Chemical Luminescence systems

Chemical luminescence consists in the production of light via a chemical reaction and it can be distinguished in different subtypes depending on the type of stimulus able to trigger the reaction: chemiluminescence (CL) and bioluminescence (BL) are referred to the chemical production of light started by mixing the reagents, the latter exploiting enzymes and photoproteins isolated from living organisms [7]; electrogenerated chemiluminescence (ECL) is the luminescence generated by relaxation of exited state molecules produced during an electron-transfer reaction that occurs at the surface of an electrode [8]; thermochemiluminescence (TCL) is the emission of light produced by the thermally-induced decomposition of a molecule.

For a chemical reaction to produce light, some essential requirements should be met [9]:

1. To populate an electronically excited (singlet) state the reaction has to be sufficiently exergonic. The free energy requirement can be calculated using:

$$-\Delta G \geq \frac{hc}{\lambda_{ex}} = \frac{28600}{\lambda_{ex}}$$

Therefore, chemiluminescence reactions producing photons in the visible (400–750 nm) range require around 40–70 kcal mol^{-1}.

2. This electronically excited state has to be accessible on the reaction coordinate.

3. Photon emission from the excited state has to be a favorable energy release route. This means that either the product of the reaction has to be fluorescent or – if by energy transfer – an excited state can be populated (this energy transfer can occur intra- or intermolecularly).
The chemical luminescence quantum yield, defined as the number of photons emitted per reacting molecule, can be expressed as:

$$\Phi_{CL} = \Phi_R \Phi_{ES} \Phi_F$$

where Φ_R reflects the chemical yield of the reaction, Φ_{ES} is the fraction of the product entering the excited state and Φ_F is the fluorescent quantum yield.

The oxidation of luminol is one of the oldest described CL reactions.
Luminol can be considered a diprotic acid with pK_A of 6 and 13, respectively. During the CL reaction under basic conditions in presence of H_2O_2, luminol is oxidized to luminol radical anion in its excited state, which releases a photon while decaying to the ground state (Fig. 1). The light is emitted at 428 nm (blue light emission) with a relatively low quantum yield of 1% [10]. The reaction can be catalyzed by horseradish peroxidase (HRP) that is commonly used as a label in binding assays thanks to its signal amplification capability [7].

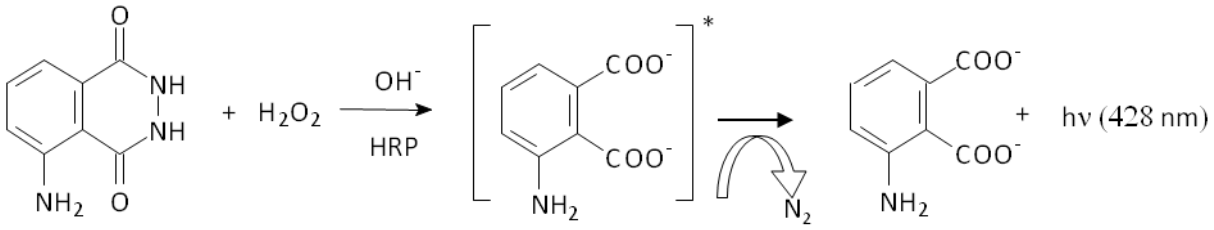

Figure 1: HRP-catalyzed oxidation of luminol.

When enzyme labels are employed, care must be taken to avoid any situation in which the enzyme activity can be disrupted by experimental conditions and, as the enzyme activity depends on temperature, a thermostated read-out cell should be employed. The possibility to use an enzyme like horseradish peroxidase (HRP) or alkaline phosphatase (AP) as a label allows to amplify the CL signal, since in the presence of an excess of CL substrate many product molecules are generated from one enzyme molecule [11]. Moreover, the achievement of a steady-state of the CL emission allows the standardization of the experimental conditions and quantitation of the labeled probe under investigation, since the steady-state light intensity is directly related to the enzyme activity. Several efforts were dedicated to the improvement of the analytical performance of the HRP-catalyzed CL oxidation of luminol. Indeed it is possible to add to the CL cocktail some enhancers like p-iodophenol (PIP), 4- (1-imidazolyl)phenol, [12] and other p-phenol derivatives, [13] para-phenylphenol and sodium tetraphenylborate as synergistic enhancer, [14] or $K_3Fe(CN)_6$ as electron mediator [15]. These enhancers allow to amplify and stabilize the CL signal making it easier to measure the analytical signal [16].

The analytical interest of chemical luminescence detection techniques mainly arises from their ability to produce photons with no need for photoexcitation, as it occurs in fluorescence detection, thereby avoiding problems arising from light scattering, background fluorescence or light source instability. Therefore, instrumentation for chemical luminescence measurements is in principle very simple, since no excitation source is required. In addition, when chemical luminescence detection is employed in conjunction with imaging detection systems, such as charge coupled device (CCD) or complementary metal-oxide semiconductor (CMOS) cameras, flexible configurations of the reading cell (e.g., the spatial distribution of microarray spots on a functionalized surface) are possible, provided that cross-talk phenomena are controlled. Finally, chemical luminescence detection showed wide dynamic ranges, thus facilitating analysis of samples with very different analyte concentrations. On the other hand, the main pitfall of these detection techniques is the potential effect of sample matrix constituents on the chemical reaction, which can either enhance or inhibit the light producing reaction. These effects are by definition unpredictable, and may lead to artefacts or spurious results. Furthermore, due to the high detectability of the chemical luminescence labels, non-specific binding must be carefully controlled to avoid high background signals and thus surfaces functionalization strategies are crucial for the success of the assay [17]. Another aspect that needs to be taken into account, especially when signal acquisition is performed in a flow regimen, is the a kinetics of photons emission that varies depending on the chemistry employed

(ranging from flash- to glow-type). As the chemical luminescence signal is not stable over time, the light-emitting species are subjected to diffusion phenomena in solution, thus causing a loss in resolution [18].

1.2 Biospecific molecular recognition reaction

Molecular recognition refers to the specific interaction between two or more molecules that exhibit molecular complementarity [19,20]. Molecular recognition plays an important role in biological systems, such as the interaction between antigen-antibody or DNA-protein. These recognition is based on noncovalent bonding like hydrogen bonding, hydrophobic forces [21,22], van der Waals forces, π-π interactions, halogen bonding, electrostatic and/or electromagnetic effects. In addition to these direct interactions, the solvent can play a dominant indirect role in driving molecular recognition in solution. [23,24]. Molecular recognition reactions are usually exploited in the field of analytical chemistry as a sensitive and specific biosensing tools, allowing to generate assays that are widely applied for pharmaceutical analysis, toxicological analysis, bioanalysis, clinical chemistry, environmental and food analysis [25].

1.2.1 Immunoassays

Immunoassays (IA) are well established bioanalytical methods widely employed for screening procedures offering high sample throughput, high sensitivity and reduced requirements for sample pre-analytical preparation, owing to the high specificity of antigen-antibody binding

reaction [3]. Appropriate antibodies bind with high selectivity to their antigen and it is possible to design IA for a wide range of analytes. The antibody is a protein that is able to recognize and bind selectively its own specific antigen by an affinity reaction. The chemical structure of the antigen allows its binding to the paratope of the antibody with high affinity, establishing an equilibrium reaction. This reaction depends on the concentration of the analytes if the antibody and the other reagents are present in constant concentrations. There are a great variety of antibodies that can be raised up for different kind of analytes such as small organic molecules (i.e. pesticides, hormones, pharmaceuticals or toxic small molecules), biopolymers (peptides, proteins, DNA) or the outer membrane of cells or organelles (viruses, bacteria, spores, fungi, protozoa, eukaryotic cells), thus allowing the development of rapid and sensitive immunoassay for biological, environmental or food analysis. Monoclonal (mAb) and polyclonal (pAb) antibodies are available for immunoassays [26]. Since the preparation of antibodies requires difficult and expensive procedures, recently, alternative recognition elements like recombinant antibodies (rAbs) or even artificial recognition elements like aptmers, have been developed with potential improved properties [27].

The detection of the formed immune-complex is commonly performed through the use of labeled reagents. Nowadays, 80% of immunoassays for routine clinical analysis are based on the use of enzymatic labels [28]. Enzymes can be chemically coupled to primary detection antibodies, to antigens, to a secondary antibody (which binds to the

unlabelled primary antibody), or to streptavidin (which binds to biotinylated antibodies) to obtain enzymatic tracers.

Immunoassays can be classified into competitive and non-competitive formats. While the non-competitive IAs (also known as "sandwich immunoassays") are based on the directly detection of the immune-complex, in the competitive format an analyte derivative is added and competes with the analyte present in the sample for binding to the antibody. The selection of the format depends on the analyte size, competitive immunoassays being applied for the detection of small analytes containing one binding site for antibody recognition, while sandwich immunoassays are applied to high molecular weight molecules that consist of two or more binding sites [29].

Since the labelling process reduces the activity of antibodies, high amounts of antibodies are needed, which is expensive, especially for sensitive detection antibodies. So, as an alternative, it can be useful to label secondary antibodies (anti-human, anti-rabbit, anti-mouse, etc.) that react with unlabelled primary antibodies (human, rabbit, mouse, etc.) at the solid support.

The most commonly immunoassay format for laboratory routine analysis is the microtiter plate-based immunoassay. This format uses a solid support for the antibody–antigen reaction and it requires the separation of the antibody-antigen complex from free antibodies. So the procedures are based on sequential reaction steps that provide the immunoreaction by adding sample and labelled reagents, the removal of matrix and unbound reagent through washing, and the detection step. The removal of unbound reagents by washing steps is very

important for the sensitivity of the assay because it can decrease significantly the background increasing the detectability.

1.2.2 Gene probe hybridization assay

Gene probe hybridization assays enable sensitive detection of target nucleic acid (DNA or RNA) sequences through their hybridization with complementary oligonucleotide probes immobilized on a functionalized surface. Nucleic acid hybridization is a fundamental tool in molecular genetics which takes advantage of the ability of individual single-stranded nucleic acid molecules to form double-stranded molecules. For this to happen, the interacting single-stranded molecules must have a sufficiently high degree of base complementarity. Standard nucleic acid hybridization assays involve the use of a labeled nucleic acid probe to identify related DNA or RNA molecules within a complex mixture. Nucleic acid hybridization assays are based on the interaction between a probe, which typically consists of a homogeneous population of identified molecules (e.g. cloned DNA or chemically synthesized oligonucleotides) and a target which typically consists of a complex, heterogeneous population of nucleic acid molecules. If either the probe or the target is initially double-stranded, the individual strands must be separated, generally by heating or by alkaline treatment. After mixing single strands of probe with single strands of target, strands with complementary base sequences can be allowed to reassociate. By using a label that can evidence the hybridization between probe and target, it is possible to perform a hybridization assay. Traditionally, labeling of nucleic acids

has been conducted by incorporating nucleotides containing radioisotopes. Such radiolabeled probes contain nucleotides with a radioisotope (often 32P, 33P, 35S or 3H), which can be detected specifically in solution or, commonly, within a solid specimen. Another nonisotopic labeling widely used is the biotin-streptavidin system that utilizes the extremely high affinity of two ligands: biotin (a naturally occurring vitamin) which acts as the reporter, and the bacterial protein streptavidin, which is the affinity molecule. Biotinylated probes can be made easily by including a suitable biotinylated nucleotide in the labeling reaction. As for the immunoassay the commonly laboratory format used for hybridization assay is the microtiter plate-based that involves in immobilizing the target DNA on a solid support that binds the complementary single-stranded DNA readily. Attachment of labeled probe to the immobilized target DNA can then be followed by removing the solution containing unbound probe DNA, extensive washing and drying in preparation for detection [30]. Gene probe hybridization assays frequently take advantage of a preliminary PCR amplification of the target sequence to improve detectability (thanks to the exponential amplification factor of PCR) and specificity (joining the selective PCR amplification of target sequences with their subsequent specific capture by immobilized oligoprobes).

1.3 Microfluidic chip

Microfluidic technologies have a great potential for developing portable analytical devices due to the advantages in size, volume requirements and time for the analysis [31-35]. Traditional multiwell

plates format commonly used in laboratory analysis are based on the binding between the analytes in sample solution and the capture molecules immobilized on solid surfaces while the analytes not bound to the capture molecules are removed during washing steps. These methods usually need relatively long incubation times and several hours are required to complete an analysis (from 1 to 24h). This is mainly due to the fact that the rate of capture of analytes on functionalized solid surfaces is usually limited by the diffusion of analytes from the bulk phase to the boundary layer [36]. Microfluidic immunosensors are able to overcome this limitation, since the increased surface-to-volume ratio makes it possible to have a more efficient transport in the immunoreactions, leading to a faster analysis. Indeed under flow in microchannels, this transport process is thought to be kinetically rapid due to the proximity of the analytes to the surface, [37] and the rapid replenishment of depleted analytes in the boundary layer by convective flow (Fig.2) [38]. Moreover a miniaturized microchannel dimension provides the reduction of consumption of samples and reagents and automated integration with other functions, such as valves, pumps, mixers, and detectors allow achieving a POC goal [39,40]. For these reasons microfluidic systems have recently attracted great deal of attention as immunosensor platforms [41]. Microfluidic chips allow to develop arrays of specific capture probes on a functionalized surface, without impairing their binding ability. This system makes it also possible to perform multiplex analyses by spatially separating several reaction area, each of one

specific for a different analyte that is recognized by its specific position.

Among the several material suited for functionalization and for the development of microfluidic chips, such as glass, silicon or polymer materials, the polydimethylsiloxane (PDMS) is characterized by simple fabrication process (e.g., molding, embossing and printing) and low cost [42,43]. Initially, PDMS proved to be particularly adapted for the development of microfluidic assays because of its flexibility, optical transparency, biocompatibility, and low-autofluorescence properties. Another advantage of PDMS is that it can be easily bonded to silicon, glass or PDMS itself through oxygen plasma treatment. Nowadays the technology improvements in the microfabrication in polystyrene and other plastics makes the use of PDMS less attractive [44].

Different methods can be employed to move liquids in microfluidics, such as pressure-driven flow, electro-osmosis, or acceleration. Ideal microfluidics are simple to utilize, reliable, fast, sensitive, versatile, and cheap. One of the simplest approaches for producing flow in microchannels is to use capillary forces [45]. Capillary-driven flow requires no peripheral equipment, and this concept is used for portable immunodiagnostic tests [46]. An emerging microfluidic platform based on capillary forces, are those based on porous materials, in which capillary action to generate the flow of fluids does not require external forces, like pumps or syringes. Hydrophobic barriers patterned into a porous, hydrophilic material provide channels for the controlled and autonomous wicking of fluids to testing zones within a device. These materials operate independently of

equipment and therefore make excellent substrates for the development of point-of-care diagnostic devices. Among porous materials, paper is an attractive substrate which allows producing diagnostic devices employing minimal infrastructure (e.g., a wax printer to pattern microfluidic channels and a pipette to dispense reagents) and inexpensive raw materials (ca. cents per device). In addition devices can be prototyped rapidly (ca. minutes from design to production) [47]. To date, a number of testing formats have been demonstrated using patterned paper devices, which include clinical chemistry assays [48-50], immunoassays [51], and electrochemical assays [52-54]. Paper-based microfluidics has become a dynamic area of research, but the majority of the activity in this field began only recently [55].

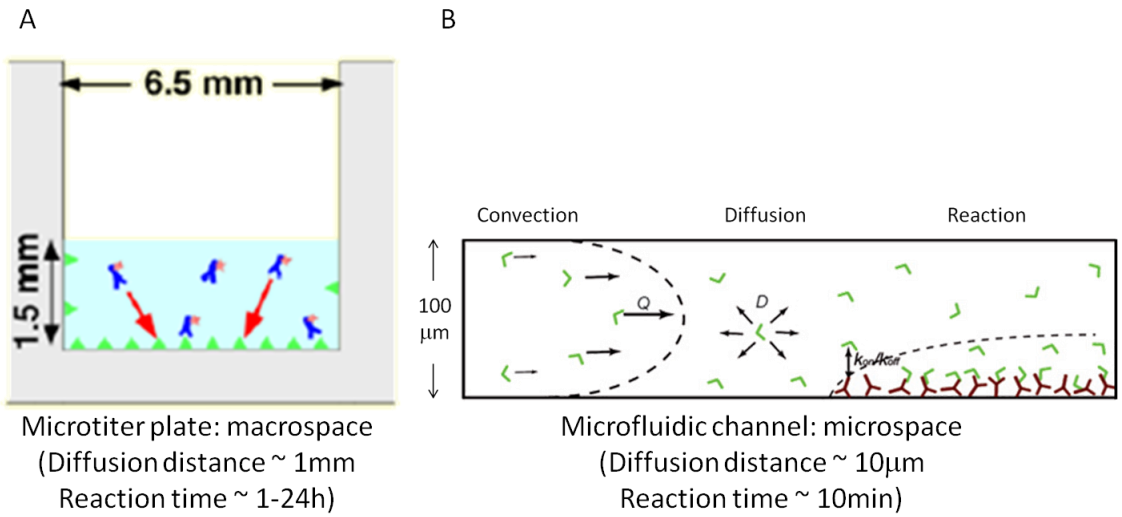

Figure 2: Schematic diagram of the differences between microtiter plate (A) and microfluidic channel (B) formats.

1.3.1 Lateral Flow Immunoassay

Lateral Flow Immunoassays (LFIA) are based on the use of a nitrocellulose test strip as a migration membrane on which reagents are driven by capillary forces. Specific immunoreagents are immobilized in definite reactive areas, while a reporter probe, able to interact with the immobilized immunoreagents and to produce a detectable signal in response to the analyte presence, is deposited on a pad at one side of the strip. Traditionally the LFIA strip is composed by the assembly of different materials, each serving one or more purposes (Fig.3). The parts overlap onto one another and are mounted on a backing card using a pressure-sensitive adhesive [56]. When a test is run, sample is added to the proximal end of the strip, the sample pad. Here, the sample is treated to make it compatible with the rest of the test. The treated sample migrates through this region to the conjugate pad, where a reagent conjugated to a label has been immobilized. This label has been conjugated to one of the specific biological components of the assay, either antigen or antibody depending on the assay format. The sample re-mobilizes the dried conjugate, and the analyte in the sample interacts with the conjugate as both migrate into the next section of the strip, which is the reaction matrix. This reaction matrix is a porous membrane, typically nitrocellulose, onto which the other specific biological component of the assay has been immobilized. These are typically proteins, either antibody or antigen, which have been laid down in bands in specific areas of the membrane where they serve to

capture the analyte and the conjugate as they migrate by the capture lines. The areas in which the reagents are immobilized are called Test-line (T-line), which is used for analyte detection, and Control-line (C-line) that typically comprises a species-specific anti-immunoglobulin antibody, for capturing the excess of conjugated detection immunoreagent. The signal on the C-line must always appear, confirming that the assay has been performed correctly. Finally the reagents move past the capture lines and are entrapped in the wick or absorbent pad. Results are interpreted on the reaction matrix as the presence or absence of signal in correspondence of T- and C-lines. The assay formats can be either non-competitive or competitive. Non-competitive assays are typically used when testing for larger analytes with multiple antigenic sites and, in this case, a positive result is indicated by the presence of a test line. Competitive formats are typically used when testing for small molecules with single antigenic determinants, which cannot bind to two antibodies simultaneously. In this format, a positive result is indicated by the absence of a test line on the reaction matrix. In both non-competitive and competitive format, the C-line should appear, irrespectively of the result on the test line. The detection of the lines can be performed either by eye or using a reader, depending on the label used. In most cases, gold nanoparticles are employed as labels and results, usually obtained in the form of bands visible at the naked eye on the test strip, are readily available. Since conventional colorimetric LFIA only yield subjective and semiquantitative information and show limited sensitivity, various strategies were pursued to enhance analytical performance and to

obtain a quantitative information, including the use of different labels, such as paramagnetic particles, fluorescent dyes or chemiluminescent enzyme (e.g., HRP). Chemiluminescence LFIA were developed for cardiac troponin I [57], myoglobin [58], pathogen bacteria [59], explosives [60] and food contaminants [61].

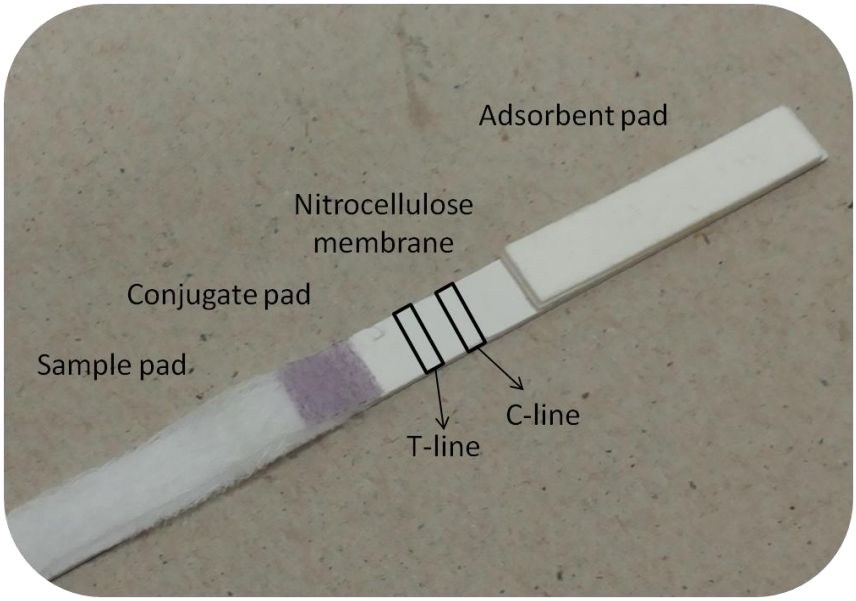

Figure 3: Scheme of the LFIA strip.

References

[1] Aguilera-Herrador E., Cruz-Vera M., Valcarel M.; (2010) Analyst; 135: 2220-2232

[2] Von Lode P.; (2005) Clin. Biochem.; 38: 591–606

[3] Mirasoli M., Guardigli M., Michelini E., Roda A.; (2014) J Pharmaceut Biomed; 87: 36-52

[4] Myers F.B., Lee L.P.; (2008) Lab Chip; 8: 2015–2031

[5] Rongen H. A. H., Hoetelmans R. M. W., Bult A., Vanbennekom W. P., (1994) J. Pharm. Biomed. Anal.; 12: 433-462

[6] Dodeigne C., Thunus L., Lejeune R., (2000) Talanta; 51: 415-439

[7] Roda A., Guardigli M., (2012) Anal Bioanal Chem 402: 69–76

[8] Hu L., Xu G., (2010) Chem Soc Rev; 39: 3275–3304

[9] Chemiluminescence and Bioluminescence: Past, Present and Future, Edited by Aldo Roda, Royal Society of Chemistry 2011, Published by the Royal Society of Chemistry

[10] Creton R., Jaffe L. F., (2001) BioTechniques; 31: 1098-1105

[11] Roda A., Pasini P., Guardigli M., Baraldini M., Musiani M., Mirasoli M., Fresenius J., (2000) Anal Chem; 366, 752-759

[12] Dotsikas Y., Loukas Y. L.; (2004) Anal Chim Acta; 509: 103-109

[13] Dotsikas Y., Loukas Y. L.; (2007) Talanta; 71: 906-910

[14] Luo J. X., Yang X. C.; (2003) Anal Chim Acta; 485, 57-62

[15] Chouhan R. S., Babu K. V., Kumar M. A., Neeta N. S., Thakur M. S., Rani B. E. A., Pasha A., Karanth N. G. K., Karanth N. G.; (2006) Biosen Bioelectron; 21: 1264-1271

[16] Marzocchi E., Grilli S., Della Ciana L., Prodi L., Mirasoli M., Roda A.; (2008)Anal Biochem; 377: 189–194

[17] Wolter A., Niessner R., Seidel M.; (2007) Anal Chem; 79: 4529–4537

[18] Cheek B.J., Steel A.B., Torres M.P., Yu Y.Y., Yang H.; (2001) Anal Chem; 73: 5777–5783

[19] Lehn J.M.; (1995) Comprehensive Supramolecular Chemistry; Wiley-VCH, Weinheim

[20] Gellman S. H.; (1997) Chem Rev; 97: 1231–1232

[21] Lockett M., Lange H., Breiten B., Heroux A., Sherman W., Rappoport D.; (2013) Angew Chem; 52: 7714–7717

[22] Breiten B., Lockett M.R., Sherman W., Fujita S., Al-Sayah M., Lange H., Bowers C. M., Heroux A., Krilov G., Whitesides G.M.; (2013) J Am Chem Soc, 135: 15579–15584

[23] Baron R.; Setny P.; McCammon J. A.; (2010) J Amer Chem Soc; 132: 12091–12097

[24] Baron R.; McCammon J. A.; (2013) Ann Rev Phys Chem; 64: 151–175

[25] Knopp D.; (1995) Anal Chim Acta; 311: 383-392

[26] Zhao L., Sun L., Chu X.; (2009) Trends Anal Chem; 28, 404-415

[27] Maragos C. M.; (2009) Anal Bioanal Chem; 395: 1205-1213

[28] Roda A., Pasini P., Mirasoli M., Michelini E., Guardigli M., (2004) Trends Biotechnol; 22: 295-303

[29] Marquette C. A., L. J. Blum; (2006) Biosen Bioelectron; 21: 1424-1433

[30] Strachan T., Read A.P.; Human Molecular Genetics. 2nd edition. New York: Wiley-Liss; 1999

[31] Manz A., Eijkel J. C. T.; (2001) Pure Appl Chem; 73: 1555–1561

[32] Lion N., Reymond F., Girault H. H., Rossier J. S., (2004) Curr Opin Biotechnol; 15: 31–37

[33] Beebe D. J., Mensing G. A., Walker G. M.; (2002) Annu Rev Biomed Eng; 4: 261–286

[34] Brody J., Yager P., Goldstein R., Austin R.; (1996) Biophys J; 71: 3430–3441

[35] Chin C. D., Linder V., Sia S. K., (2007) Lab Chip, 7: 41–57

[36] D. Wild, The Immunoassay Handbook, Elsevier Science, Amsterdam, 2005

[37] Rossier J. S., Gokulrangan G., Girault H. H., Svojanovsky S., Wilson G. S., (2000) Langmuir; 16: 8489–8494

[38] Goldstein B., Coombs D., He X., Pineda A. R., Wofsy C.; (1999) J Mol Recognit; 12: 293–299

[39] Bange A., Halsall H.B., Heineman W.R.; (2005) Biosens. Bioelectron; 20:2488–503

[40] Lin C.C., Wang J.H. ,Wu H.W., Lee G.B.; (2010) J Lab Autom; 15:253–74

[41] Kwi Nam Han, Cheng Ai Li, Gi Hun Seong; (2013) Annu Rev Anal Chem; 6:119–41

[42] Becker H., G¨artner C.; (2008) Anal Bioanal Chem; 390:89–111

[43] McDonald J.C., Whitesides G.M.; (2002) Acc Chem Res; 35:491–99

[44] Berthier E., Young E.W.K., Beebe D; (2012) Lab on a Chip; 12: 1224–1237

[45] Zimmermann M., Delamarche E., Wolf M., Hunziker P.;(2005) Biomed Microdevices; 7: 99–110

[46] Apple F.S., Christenson R.H., Valdes R., Andriak A., Berg A., Duh S., Feng Y., Jortani S.A., Johnson N.A., Koplen B., Mascotti K., Wu A.H.B.; (1999) Clin Chem; 45: 199–205

[47] Mace C. R., Deraney R. N.; (2014) Microfluid Nanofluid; 16:801–809

[48] Klasner S.A., Price A.K., Hoeman K.W., Wilson R.S., Bell K.J., Culbertson C.T.; (2010) Anal Bioanal Chem; 397:1821–1829

[49] Dungchai W., Chailapakul O., Henry C.S.; (2010) Anal Chim Acta; 674:227–233

[50] Vella S.J., Beattie P.D., Cademartiri R., Laromaine A., Martinez A.W., Phillips S.T., Mirica K.A., Whitesides G.M.; (2012) Anal Chem; 84:2883–2891

[51] Cheng C.M., Martinez A.W., Gong J., Mace C.R., Phillips S.T., Carrilho E., Mirica K.M., Whitesides G.M.; (2010) Angew Chem Int; 49:4771–4774

[52] Dungchai W., Chailapakul O., Henry C.S.; (2009) Anal Chem; 81:5821–5826

[53] Nie Z.H., Deiss F., Liu X.Y., Akbulut O., Whitesides G.M.; (2010) Lab Chip; 10:3163–3169

[54] Mirica K.A., Weis J.G., Schnorr J.M., Esser G., Swager T.M.; (2012) Angew Chem Int; 51:10740–10745

[55] Martinez A.W., Phillips S.T., Butte M.J., Whitesides G.M.; (2007) Angew Chem Int; 46:1318–1320

[56] Wong R. C., Tse H. Y.; Lateral Flow Immunoassay (2009), Editor Wong R. C., Humana Press, Springer

[57] Cho I.H., Paek E.H., Kim Y.K., Kim J.H., Paek S.H.; (2009) Anal Chim Acta; 632: 247–255

[58] Kim H.S., Ko H., Kang M.J., Pyun J.C.; (2010) BioChip J; 4: 155–160

[59] Park S., Kim Y.T., Kim Y.K.; (2010) BioChip J; 4: 110–116

[60] Mirasoli M., Buragina A., Dolci L.S., Guardigli M., Simoni P., Montoya A., Maiolini E., Girotti S., Roda A.; (2912) Anal Chim Acta; 721:167–172

[61] Mirasoli M., Buragina A., Dolci L.S., Simoni P., Anfossi L., Giraudi G., Roda A.; (2012) Biosen Bioelectron; 32:283–287

CHAPTER 2

Aim of the thesis

The activity carried out during my PhD was principally addressed to the development of portable microfluidic analytical devices based on biospecific molecular recognition reactions and CL detection. In particular, the development of biosensors required the study of different materials and procedures for their construction, with particular attention to the development of suitable immobilization procedures, fluidic systems and the selection of the suitable detectors. Different methods were exploited, such as gene probe hybridization assay or immunoassay, based on different platform (functionalized glass slide or nitrocellulose membrane) trying to improve the simplicity of the assay procedure. Different CL detectors were also employed and compared with each other in the search for the best compromise between portability and sensitivity. The work was therefore aimed at miniaturization and simplification of analytical devices and the study involved all aspects of the system, from the analytical methodology to the type of detector, in order to combine high sensitivity with easiness-of-use and rapidity.

in Chapter 3, an analytical device is proposed that is able to provide both the pre-analytical sample preparation and the analyitical step. In particular, an integrated POCT system based on gravitational field-flow fractionation (GrFFF) and CL detection is presented for the on-line sample pre-analytical treatment and/or clean-up and analysis of biological fluids. As a proof of principle for the new GrFFF-CL POCT system, the automatic on-line analysis of plasma alkaline phosphatase activity, a biomarker of obstructive liver diseases and bone disorders, starting from whole blood samples was developed. The GrFFF-CL POCT

system was able to give quantitative results on blood samples from control and patients with low sample volume (0.5 μL) and reagent consumption, short analysis time (10 minutes), high reproducibility and with a linear range of 50–1400 IU L^{-1}. The system can be easily applied to on-line prepare plasma from whole blood for other clinical biomarkers and for other assay formats, based on immunoassay or DNA hybridization.

In Chapter 4, a miniaturized multiplex biosensor exploiting a microfluidic oligonucleotide array and chemiluminescence (CL) lensless imaging detection is reported for parvovirus B19 genotyping. The portable device consists of a reaction chip, comprising a glass slide arrayed with three B19 genotype-specific probes and coupled with a polydimethylsiloxane (PDMS) microfluidic layer, and a charge-coupled device (CCD) camera modified for lensless CL imaging. Immobilized probes were used in DNA hybridization reactions with biotin-labeled targets, and then hybrids were measured by means of an avidin-horseradish peroxidase (HRP) conjugate and CL detection.

Chapter 5 reported the development of a multiplex chemiluminescent biosensor for on-site simultaneous quantification of Aflatoxin B1 and type B-Fumonisins in maize samples based on CL-Lateral Flow Immunoassay (LFIA), in order to combine the simplicity of the LFIA technique with the advantages offered by CL detection. The biosensor integrates a multiplex indirect competitive lateral flow immunoassay (LFIA) based on enzyme-catalyzed CL detection and a CCD camera, employed in a lensless “contact” imaging configuration. The developed assay requires a simple extraction of the analytes from maize flour

samples followed by their detection with a 30-min assay time. The use of CL detection allowed accurate and objective analytes quantification, enabling simultaneous detection of type B-Fumonisins and Aflatoxin B1 down to 6 μg kg^{-1} and 1.5 μg kg^{-1}, respectively, thus fulfilling the standard imposed by the legislation of European Union.

Chapter 6 reports about a different new CL detector, that is back side illuminated CMOS used in smartphone cameras that can provide a further minizaturization and simplification of the analytical system. Nowadays improvements in the sensitivity of the back side illuminated CMOS used in new generation smartphone cameras make them amenable for detecting CL signals. Moreover, the connectivity and data processing offered by smartphones can be exploited to perform analyses directly at home with simple procedures. We therefore developed a portable analytical device, employing 3D printing technology, that transforms a smartphone into a CL detector for quantitative analysis based on LFIA and we demonstrated the performance of the system by quantitative detection of salivary cortisol, which is considered a biomarker of stress, anxiety, and depression and thus requires highly sensitive and accurate assays in order to detect disease-related variations at nanomolar levels.

In Chapter 7 an innovative detector for CL measurement based on hydrogenated amorphous silicon (a-Si:H) photodiode array was proposed as an alternative to conventional bench-top instrumentation. In order to state the suitability of a-Si:H photodiodes as ultrasensitive detection devices for Lab-on-Chip (LOC) systems, we designed, fabricated and characterized a LOC system with integrated

photosensors and applied it to two different “model” bioassays. The system includes an array of 16 a-Si:H photodiodes deposited on a glass substrate, on which a PDMS unit containing 16 wells was applied to obtain an integrated microcartridge. A custom portable readout electronic board was employed. Firstly, device performances were characterized at the photosensor level and at analytical level in terms of noise, sensitivity, detectability with different CL and BL systems, comparing the analytical performances with reference state-of-the-art laboratory instrumentation. Finally, the device functionality was successfully tested on two model bioanalytical BL (cell toxicity assay) and CL (total antioxidant capacity measurements) assays. This device provides efficient photon transfer between the sample-well and the photosensors, thus increasing assay sensitivity. In addition, the very compact dimensions, favourable for miniaturization, the low-cost and the versatility make it a good candidate for developing miniaturised biosensors with high detectability and sensitivity.

CHAPTER 3

Gravitational field-flow fractionation integrated with chemiluminescence detection for a self-standing point-of-care compact device in bioanalysis

---

Reproduced from: "Gravitational field-flow fractionation integrated with chemiluminescence detection for a self-standing point-of-care compact device in bioanalysis"
Sonia Casolari, Barbara Roda, Mara Mirasoli, Martina Zangheri, D. Patrono, Pierluigi Reschiglian, Aldo Roda
Analyst, 2013, 138, 211–219
Reproduced by permission of The Royal Society of Chemistry
http://pubs.rsc.org/en/content/articlepdf/2013/an/c2an36041a

3.1 Introduction

The “Point-Of-Care Testing” (POCT) approach, based on the development of miniaturized and portable analytical platforms, aims at rapidly performing clinical chemistry assays directly where the sample is obtained. To meet analytical and diagnostic requirements, a POCT device should combine portability, minimum sample pre-treatment, and the possibility to perform highly sensitive simultaneous detection of several biomarkers (multiplexing) in a short assay time.

Sample pre-treatment is the most critical point to reach the needed specificity and detectability in many bioassays conducted on complex biological samples (such as blood, urine, or saliva). Despite this, while great research effort has been directed toward the development of miniaturized analytical devices and biosensors for diagnostic applications, the integration of pre-analytical sample preparation and/or clean-up modules still represents the key bottleneck for realizing a totally integrated analytical device application [1]. In specialized laboratories, blood clinical analyses are commonly carried out on cells and plasma components after their separation, generally through a centrifugation step that requires a volume of whole blood samples in the range of milliliters. Various miniaturized systems have been proposed to prepare cell-free plasma, possibly from small volumes of whole blood, such as microfluidic systems exploiting cross-flow filtration [2,3], “lab-on-a-disc” systems exploiting centrifugal forces [4] and biomimetic microfluidic separation, microstructures, magnetophoresis, acoustophoresis and dielectrophoresis

[5,6]. However, such systems do not provide total recovery of plasma and in most cases the efficiency of separation is not satisfactory. In addition, most of the proposed methods present problems of clogging, lead to the rupture of blood cells owing to high shear forces and do not allow collection of cellular materials for further analysis.

In this context, the field-flow fractionation (FFF) family of flow-assisted separation techniques represents a more versatile and multiplexed solution, being able in the same run both to separate plasma from whole blood and to further fractionate cellular components by a non-invasive process and a simple and easily automatable system setup. In FFF the separation is achieved within a capillary empty channel in which a laminar flow of the mobile phase sweeps sample components down the channel. A field is applied perpendicularly to the parabolic flow to make the analytes be driven into different laminar flows due to their differences in physical properties such as molar mass/ size, density, and surface properties, resulting in different retention times. Thanks to its “soft” separation mechanism, FFF has been successfully applied to a wide range of bioanalytes, from relatively small biomolecules to living cells in complex biological samples, which after separation keep their native characteristics such as enzymatic activity, cell integrity and vitality, or quaternary protein structure [7,8]. The gravitational FFF (GrFFF) variant, exploiting the Earth gravitational field to structure the separation, appears to be particularly suited for its implementation in POCT devices, thanks to the simplicity of its separative device, amenability to miniaturization, and the potential easy on-line integration with specific analytical modules. GrFFF was

extensively used as non-invasive cell sorting techniques [9–11], and we have recently demonstrated the possibility of increasing its selectivity by derivatizing the fractionation device walls with biospecific reagents [12].

Herein, we propose to exploit the potentialities of GrFFF towards the development of an on-line pre-analytical simple module of a POCT device, able to fractionate sample components, thus providing a selectively enriched fraction for the analysis with an increase of the overall analytical output. After fractionation, sample components can be on-line transferred to different analytical modules where analytes are quantified.

GrFFF was coupled with chemiluminescence (CL) detection, which has been shown to be particularly suited for its implementation in miniaturized POCT devices, since it offers high detectability also in small volumes and it avoids the need for photoexcitation and wavelength selection systems [13,14]. We have recently demonstrated the potential analytical applications of GrFFF coupled with CL detection for the development of rapid and ultrasensitive immunoassays [15,16].

As a first approach, we present a novel GrFFF-CL integrated device able to prepare whole blood samples for the automatic on-line measurement of the activity in plasma of alkaline phosphatase (ALP, EC 3.1.3.1), an enzyme produced primarily in the liver and intestine. Measurements of ALP activity in plasma are used as a first level screening test for obstructive liver diseases and bone disorders, elevated levels usually prompting further testing to complete the diagnosis [17]. Most frequently, spectrophotometric techniques are employed, exploiting the ability of the enzyme to catalyze the conversion of p-nitrophenyl phosphate (PNPP) to

p-nitrophenol (405 nm maximum absorbance). Several kits (such as those produced by TC Diagnostic, Anaheim CA; AbCam Inc. Cambridge, MA; QuantiChrom, BioAssays Systems, Hayward, CA) and automatic devices (such as Cobas® by Roche Diagnostics Corporation, Indianapolis, IN) also for POCT applications (such as SpotChem EZ by A. Menarini Diagnostics, Firenze, Italy) based on colorimetric detection are commercially available for ALP activity measurement in serum. Nevertheless, such methods are limited by interferences from absorbing molecules in plasma (e.g., bilirubin, haemoglobin). Other sensitive methods, amenable to miniaturization, were described, such as CL detection [18], or electrochemical detection, although this system was not tested on human serum or plasma samples [19]. However, most of these systems are not applicable to whole blood samples and they require preliminary separation of serum/plasma from whole blood. A method based on voltammetric determination was described to measure ALP activity in whole human blood, which however provided a limit of detection and a linear range not adequate for diagnostic applications [20]. In the proposed GrFFF-CL integrated device, after the injection of a small volume of heparin-treated whole blood, plasma is separated from cells which elute at different retention times and is then addressed by means of a micro□uidic system to the CL-analytical module, where the enzyme activity is measured by means of an on-line flow-through luminometer. To obtain a compact GrFFF device, amenable to miniaturization and easily integrated in a microfluidic system for POCT applications, the channel geometry was modified with respect to the conventional linear

rectangular shape and a more compact GrFFF device containing the separative channel was used. The method has been validated by comparing the results obtained from whole blood samples with those obtained by analyzing serum by a conventional clinical chemistry test routinely used in hospital laboratories.

3.2 Materials and methods

3.2.1 Reagents

The CL substrate Lumi-Phos® Plus, containing Lumigen PPD (4-methoxy-4-(3-phosphatephenyl)spiro[1,2-dioxetane-3,20-adamantane] disodium salt and a patented enhancer in 2-amino-2- methyl-1-propanol buffer (pH 9.6), was purchased from Lumigen Inc. (Southfield, MI, USA). Being Lumigen PPD photosensitive, it was protected from light throughout the analysis. Sodium chloride (NaCl) was acquired from Sigma Aldrich Co. (St. Louis, MO, USA) and the lyophilized calibrator for Automated Systems (C.f.a.s. 10759350), from Roche (Basel, CH, Switzerland), was kindly supplied by the Clinical Chemistry Central Laboratory of the S.Orsola-Malpighi hospital (Bologna, Italy). Saline solution (9 g L^{-1} NaCl in ultrapure MilliQ water) was used for samples and calibrators dilution and as a FFF mobile phase.

3.2.2 Samples

Calibrator:

A stock ALP solution having a certified concentration (460 IU L^{-1}; IU = International Unit for enzymatic activity) was obtained by reconstitution of the lyophilized C.f.a.s. with 3 mL of ultrapure MilliQ water. The stock ALP solution (that is stable for 8 h at room temperature, 2 days at 2–8 °C and one month at -20 °C) was serially diluted with saline solution to provide ALP standard solutions, which was used to obtain calibration curves. Dilutions of the stock ALP solution were also prepared at 1.5, 4.0, and 6.0 IU L^{-1} ALP activity and used as quality control samples.

Control plasma and whole blood:

Five different control plasma samples having ALP enzymatic activity ranging between 0.625 and 7.000 IU L^{-1} were prepared by serially diluting with saline solution a reference plasma (BIO-RAD, Hercules, CA) having a 70 IU L^{-1} certified ALP activity and they were used to check the calibration curve. Control plasma was kindly supplied by the Clinical Chemistry Central Laboratory of the S.Orsola-Malpighi hospital (Bologna, Italy). Fresh human blood samples were collected in heparintreated tubes from 15 healthy donors and 10 patients affected by cholestasis. Prior to inclusion in the study, each subject gave his/her written informed consent.

For each analysis, 0.5 μL of whole blood (or plasma isolated after centrifugation for comparison purposes) were injected upon simply a 1:100 (v/v) dilution with saline solution. For each sample, ALP activity was

calculated by interpolation of the CL signal on the calibration curve and corrected for the sample dilution factor. In addition, for each blood sample, the value of ALP activity in plasma was calculated by considering the dilution factor of plasma in whole blood (blood is composed of 55% plasma and 45% cellular components) [21,22] in order to allow comparison of the results with those obtained in plasma with the reference method. Results obtained by the developed method on control samples and real samples were compared with those obtained by the optimized method Cobas® routinely used in the Clinical Chemistry Central Laboratory of the S.Orsola-Malpighi hospital (Bologna, Italy). This method, based on the colorimetric measurement of ALP activity, is applied to serum samples and it provides a dynamic range of the measurement in the interval 5– 2000 IU L^{-1}, with a run-to-run CV of <0.5%, a day-to-day CV of <2% and a recovery of ±5% of the initial value. Alkaline phosphatase values lower than 270 IU L^{-1} for men and lower than 240 IU L^{-1} for women measured at 37 °C were considered normal values for physiological conditions.

3.2.3 GrFFF-CL POCT system

The GrFFF-CL system was composed of two main integrated modules: the GrFFF device and the CL analyzer, which were online connected as described in the following paragraphs and depicted in Fig. 1.

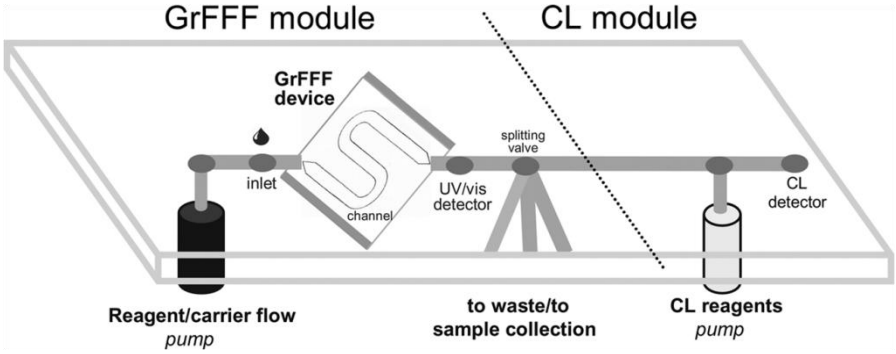

Figure 1: Scheme of the GrFFF-CL system. The GrFFF module is composed of a system for carrier delivery, a tube for sample injection, the GrFFF device (comprising the Sshaped channel and plastic walls), the UV/vis detector, and a splitting valve to drive selected fractions to the integrated CL module (comprising a system for reagents delivery and a CL detector).

GRFFF MODULE. The GrFFF fractionation module (Fig. 1) was based on a new GrFFF channel design with respect to the conventional rectangular geometry. The GrFFF channel, cut from a Mylar spacer, had a curvilinear shape with an S geometry characterized by two curvilinear parts of 3.9 cm with a radius of curvature of 1.25 cm. The channel presented conventional dimensions of 30.0 cm in length (tip-to-tip), 0.018 cm in thickness and 1.0 cm in breadth and it was sandwiched between polycarbonate (PC) and polyvinyl chloride (PVC) walls, both from Plasticenter (Bologna, Italy), thus making the GrFFF device suitable for blood fractionation. The S geometry allowed for obtaining a GrFFF device with a 55% reduction in overall size. In its current configuration, the carrier flow was delivered by a peristaltic pump (Miniplus Gilson Plus), while the GrFFF outlet was fed to the CL-analysis module described below. Samples and standards (injection volume 50 μL) were directly injected into the channel via a PEEK inlet tube

(L = 5 cm, i.d. = 0.750 mm, o.d. = 1/16 in) by means of a Hamilton syringe. They were manually shaken for some seconds before the injection which was performed at a flow rate of 0.2 mL min^{-1} for 15 s. Then the flow was stopped for 2 min to allow sample relaxation. After the stop-flow time, the flow was restarted at a flow rate of 1.0 mL min^{-1} for sample elution.
During the elution, whole blood components were fractionated: plasma was not retained and eluted in the void peak, while cellular components eluted later following the GrFFF fractionation mechanism. The elution process was registered by means of an on-line UV6000 LP, diode array UV/vis detector (Thermo- Quest, Austin, TX), operating at 280 nm and 600 nm.

CL-ANALYSIS MODULE. By means of a splitting L-valve, a fraction of the void peak, containing plasma components of the sample, was on-line sent from the channel outlet to the CL analysis module, where ALP activity was quantified by postcolumn reaction, as described below. The CL analysis module was constituted by an on-line mixer to blend the eluted fraction with the CL enzyme–substrate and by a flow-through CL detector (FB12 luminometer, Berthold Detection Systems, GmbH, Pforzheim, Germany) equipped with a flow-cell specifically modified, as previously described, to perform flow measurements [15]. This cell (186 μL) was created by employing transparent Teflon tubing (L = 23 cm, i.d. = 1 mm, 8.107 μL cm^{-1}) bound on itself and placed in a glass test tube into the luminometer. In a perspective, the L-valve can be used to switch different fractions of the same samples to different analytical modules eventually on-line

connected to the GrFFF device resulting in a multiplexed POCT system. Alkaline phosphatase activity was measured by employing the CL substrate Lumi-Phos-Plus® diluted 1 : 9 (v/v) with saline solution, warmed to 37 °C and delivered by the peristaltic pump (Gilson) at a flow rate of 1.8 mL min^{-1} for 10 s. The proportion between the sample and the substrate into the flow-through CL analyzer was fixed to 1 : 1.8 (v/v), as determined by flow rates of the mobile phase and the CL substrate. These experimental conditions were adopted to minimize the costs of a single run ensuring, at the same time, that the initial reaction speed depends only on enzyme activity. The CL mixture was stopped into the flow-through CL detector cell and the signal was acquired for 3 min; then, the flow was restored to wash out the sample and to make the system ready for further analysis. The value of enzyme activity was calculated from the slope of the CL kinetic curve obtained. After injection of 10 blood samples, the entire analytical system was cleaned by flushing ultrapure MilliQ water at a flow rate of 1 mL min^{-1} for 30 minutes, then a cleaning solution (30% v/v ethanol and 0.5% w/v sodium dodecyl sulphate (SDS) in ultrapure MilliQ water) was flushed at 0.5 mL min^{-1} for 20 minutes. The system was finally rinsed with ultrapure MilliQ water at 1.5 mL min^{-1} for 30 minutes, before restoring the mobile phase.

3.3 Results and discussion

3.3.1 Principle of the assay/preliminary assays

In this work, an on-line GrFFF-CL system was designed and optimized for its applicability in bioanalysis in a POCT setting, by integrating a GrFFF channel in an innovative format with a fluidic CL detection module. Blood ALP activity was used as a model analyte. Preliminary work was conducted to investigate the possibility of a direct measurement of ALP activity in whole blood, by addition of the CL substrate to highly diluted (1:100 to 1:500 v/v) blood samples, exploiting high CL detectability. However, poor reproducibility and sensitivity were obtained (data not shown), thus confirming the need of a simple sample pre-treatment in order to obtain a robust method suitable for diagnostic applications. In view of a POCT application, the GrFFF-CL system was developed by employing an original curvilinear geometry for the GrFFF channel, in order to obtain a compact device. The influence of the new geometry on the fractionation performance was preliminary evaluated on blood samples by employing CL imaging accomplished by placing the GrFFF transparent channel in a dark box and by acquiring, through a highly sensitive, back-illuminated, double Peltier-cooled CCD camera, the CL emission of fractionated analytes at fixed time intervals during the elution, as previously described [23]. No significant difference in the fractionation efficiency was observed with respect to a conventional rectangular GrFFF channel, both in terms of resolution and recovery.

Employing such an original channel design, the fractionation method was optimized as described below in order to obtain a quantitative method with high sensitivity, linear range and reproducibility for the analysis of real samples. The developed procedure can be summarized as follows: a small volume (0.5 μL) of whole blood diluted 1 : 100 (v/v) with saline solution was injected in the GrFFF system for separation of plasma from cells, which elute at different times. At the exit of the GrFFF channel, a fraction of plasma was split to the analytical module, where ALP activity could be measured on-line upon mixing with the dioxyethane-based CL substrate. For method optimization purposes, the UV/vis detector was on-line inserted between the channel outlet and the CL analyzer, however, thanks to the high reproducibility of the fractionation process, the UV-vis detector was eliminated in the final set-up of the GrFFF-CL system.

3.3.2 Method optimization

FRACTION SELECTION. When whole blood is injected into a GrFFF channel, plasma components are not retained by the system and are thus eluted in a single peak corresponding to the void volume, while blood cells are subjected to retention mechanisms and are thus eluted later (and fractionated in cell populations). As a consequence, plasma separation is obtained after GrFFF run, without the need of a centrifuging step and with low shear stress, thus without cell lysis. At the exit of the GrFFF channel, the plasma fraction was split to the CL detection analytical module, while cellular components, which were not of interest in the present work, were separately collected. A representative GrFFF profile obtained upon

injecting whole blood is reported in Fig. 2a, panel I. Since, the whole volume of the void peak was much higher (1.5 mL) than the plasma volume necessary to perform the CL measurement of ALP activity, only a fraction of the void peak was split to the analytical module to reduce CL substrate consumption and measurement times. Even if it is expected that molecules eluted within the void peak are not differently distributed along the peak, since they are not affected by the external field during separation, preliminary experiments were performed aimed at confirming that the distribution of ALP was homogeneous in the void peak (thus no artefact was introduced by analyzing only a fraction of it) and at determining which fraction of the void peak would provide the highest assay sensitivity and reproducibility, with reduced reagent consumption and assay time. For this purpose, after injecting 50 μL of diluted whole blood, four 250 μL fractions of eluting plasma (F1–F4, 15 s collection time for each fraction, Fig. 2a, panel II) were separately addressed to the CL analysis module, where the kinetics of CL emission was monitored for 3 min upon mixing for 15 s with the CL substrate, following the procedure described in Section 2.3.2. For each fraction, the area under the curve measured at l =280 nm (indicating whole protein content, mainly represented by human serum albumin and other plasma proteins) and the slope of the CL emission profile (indicating ALP activity) were correlated. The graph (Fig. 2b) shows a good linear relationship (r = 0.99) demonstrating a uniform distribution of ALP within the void peak and confirming that any of the fractions collected within the void peak could be used for evaluating ALP activity in the blood sample. Fraction 2 of the

void peak, corresponding to the peak maximum and therefore to the highest amount of plasma components, was employed in subsequent experiments to reach higher assay detectability. The optimal splitting time for addressing the central fraction of the void peak towards the analytical module was assessed to be 10 s, providing high assay reproducibility, as shown in Fig. 3, reporting the results of six repeated GrFFF runs and showing that void peaks of different fractograms and CL emission profile time are completely superimposable. It must be noted that a shorter 6 s splitting time provided high CL signals for ALP activity measurements as well, thus potentially low detection limits for ALP activity could also be reached when employing short sampling times. However, low reproducibility was obtained under such conditions in this work, where the instrumental set-up employed, in a prototype level of development, was based on a manual splitting operation. Future automation of the splitting system will most probably enable significant reduction of collection time, thus reagent consumption.

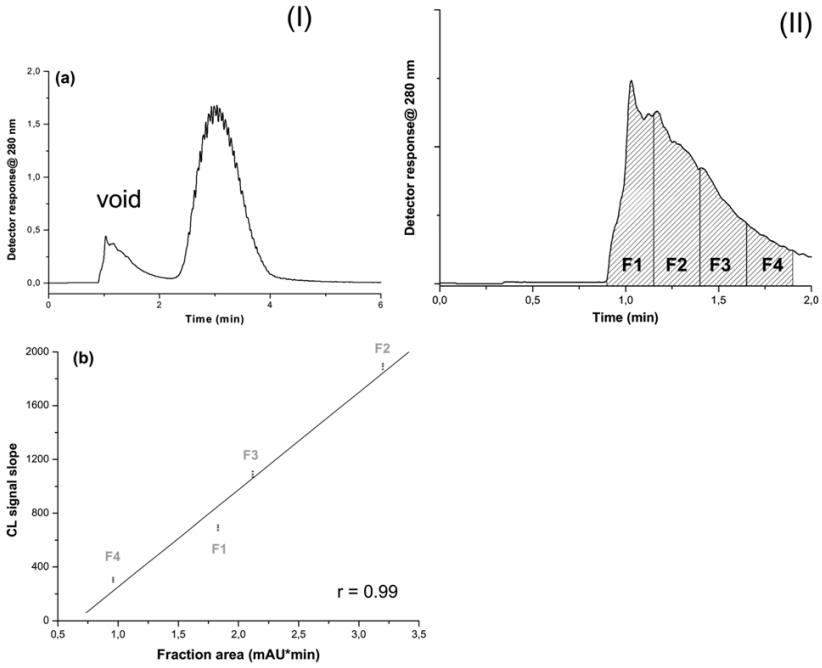

Figure 2: (a) GrFFF fractionation of whole blood (panel I): 50 mL of diluted (1/100 v/v in the mobile phase) whole blood, mobile phase ¼ NaCl 9 g L_1, elution flow rate = 1 mL min^{-1}, relaxation time = 2 min and fractographic profile registered at 280 nm. The first band represents the void peak corresponding to unretained analytes (serum components); the second band corresponds to retained blood cells. Void peak partitioned in 15 s collected fractions (panel II): F1–F4 fractions of the void (serum) peak used for the CL assay. (b) ALP activity (slope of the CL emission profile) for F1–F4 collected fractions vs. area under the curve of the fractographic profile measured at l =280 nm (reflecting the whole protein content in each fraction). The F2 fraction which has the higher band area also shows the higher CL intensity.

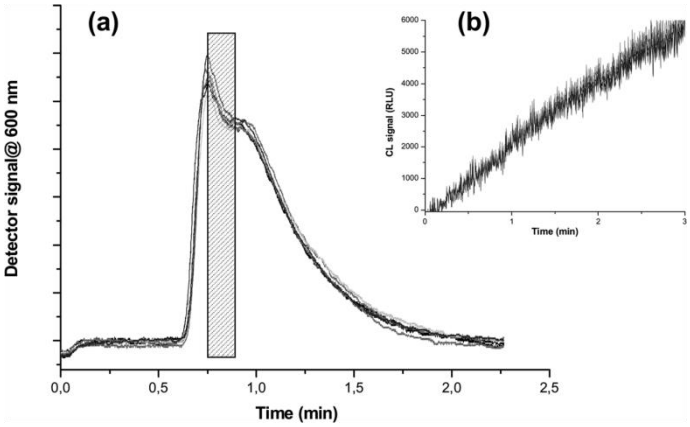

Figure 3: (a) Superimposition of void peaks of the fractographic profiles for six subsequent blood injections in the GrFFF system. The central portion of the void peak (evidenced in grey in panel a) corresponding to a 10 s splitting time was selected as a serum collection time for determination of ALP. (b) Results for chemiluminescence ALP activity measurements on the selected fraction for the six subsequent injections.

EXPERIMENTAL PARAMETERS OPTIMIZATION. Saline solution (9 g L^{-1} NaCl) was employed as a mobile phase and to dilute all samples to maintain physiological conditions during fractionation, thus preserving enzyme activity and cell integrity. As enzyme activity is affected by the temperature, to fulfil international standards for enzymatic measurements in clinical chemistry, the analytical CL module was thermostatted at 37 °C, obviously complicating the instrumental design in a perspective of a POCT application. Explorative tests, performed also at 25 °C, showed that, although a significantly higher signal was obtained for the blank (Fig. 4a), a linear calibration curve was obtained (Y = 86X -15, r = 0.99), indicating the possibility of giving a conversion factor for analysis to be performed at 25 °C. Optimization experiments were performed to minimize the CL substrate consumption while maintaining an excess

substrate to obtain an analytical signal only dependent on enzyme activity. Dilution factors for the Lumi-Phos- Plus substrate with saline solution ranging from 1 : 2 to 1 : 9 (v/v) were tested, the optimal one being assessed to be 1 : 9 (v/v). The memory effect between subsequent runs was also evaluated by measuring the blank signals that, while being very low and constant when a blood sample was injected into a new GrFFF channel, significantly increased after ten repeated blood injections. This memory effect, probably due to the weak adsorption of ALP molecules on the channel walls and their release during the subsequent runs, was eliminated by adopting a short channel cleaning procedure, as described in Section 2.3.2. The procedure was able to eliminate any ALP molecule adsorbed on the channel wall and the resulting memory effect (Fig. 4b). It must, however, be noted that, thanks to the low cost of the GrFFF device, the separative device is suitable for a disposable usage, thus eliminating the memory effect problem.

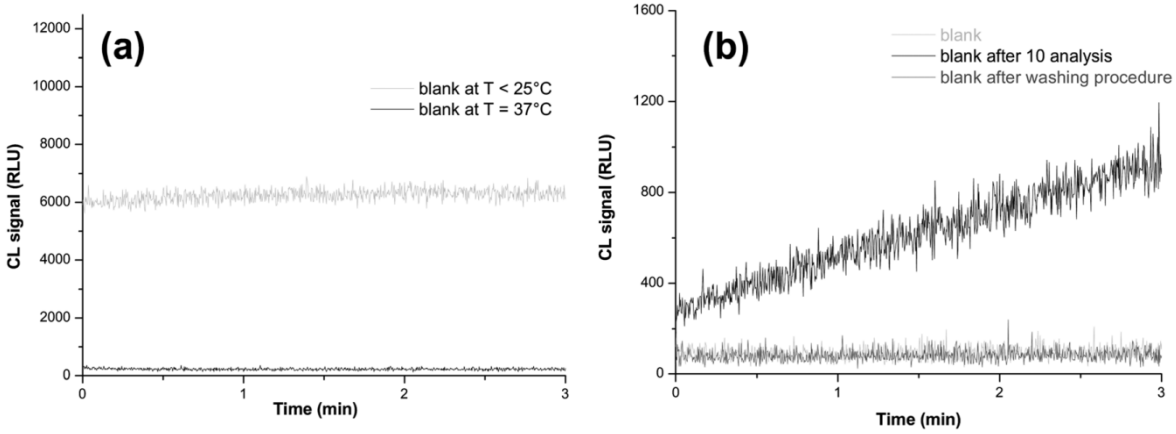

Figure 4: (a) CL signals measured at 25 °C and at 37°C when the assay was conducted in the absence of the blood sample (blank signal) by analyzing 50 μL of the mobile phase under the GrFFF-CL conditions. (b) CL blank signals measured employing a newly prepared GrFFF channel, after 10 subsequent blood analysis, and using the same channel restored by the cleaning procedure described in Section 2.3.2.

3.3.3 Quantitative analysis

CALIBRATION RESULT. A calibration curve was obtained by employing ALP standard solutions, displaying a linear range from 0.5 to 14 IU L^{-1}, which corresponds to 50–1400 IU L^{-1} when considering the 1 : 100 (v/v) dilution factor employed for injected samples. The equation Y = 54.0 (±0.2)X + 8 (±2) was obtained when repeating the calibration 15 times (r = 0.99). It is to be underlined that physiological reference values of enzymatic activity of ALP of the adult healthy subject range from 45 to 270 IU L^{-1}, while higher values (generally up to 1400–2000 IU L^{-1}) are encountered in pathologic situations, such as obstructive liver diseases and bone disorders. The limit of detection (LOD), calculated as the ALP activity

corresponding to the signal of the blank plus three standard deviations, was 28 IU L^{-1}. The dynamic range of the developed method is thus suitable for the analysis of blood samples presenting normal, abnormally elevated, or abnormally low ALP activity levels. Samples characterized by ALP levels lower than the LOD method may be re-analyzed upon a 1 : 10 (v/v) dilution, since we have excluded the presence of matrix effects at this sample dilution (Section 3.3.3).

VALIDATION OF THE CALIBRATION PROCEDURE. The analytical performances of the quantitative method were evaluated by employing two types of samples: quality control samples (prepared by serially diluting the stock ALP solution, having a 460 IU L^{-1} certified ALP activity) and control plasma samples containing also matrix elements (prepared by serially diluting a reference plasma sample, having a 70 IU L^{-1} certified ALP activity). The reproducibility of the method was assessed by analyzing quality control samples at 1.5, 4.0 and 6.0 IU L^{-1} ALP activity (corresponding to 270, 730, and 1090 IU L^{-1} in undiluted plasma, calculated as detailed in Section 2.2). Results are reported in Table 1. The intra-assay CVs across the entire range were below 2% (n = 15), while inter-assay CVs, obtained in five different days, were below 4%. Accuracy was determined by repeatedly analyzing control plasma samples, having a certified ALP activity value in the range (0.65–7.00) IU L^{-1} corresponding to final ALP concentrations in the range (120–1270) IU L^{-1}. Results, reported in Table 2, show recovery values in the range from 110 to 93%, thus confirming the accuracy of an ALP quantification procedure.

The analysis of pathological samples displaying ALP activities higher than 1400 IU L^{-1} can be performed by further diluting the sample prior to analysis.

As stated above, automatization of the system may allow a higher control of the flow and splitting times, with a potential reduction of the sampling time and a consequent increase in the dynamic range of the method.

Real value (IU L^{-1})	Measured value (IU L^{-1})	Mean (IU L^{-1})	Std. dev. (IU L^{-1})	CV% intra	CV% inter
1.50	1.55	1.57	0.02	1.3	1.5
	1.59				
	1.56				
4.00	3.85	3.79	0.07	1.7	3.2
	3.72				
	3.80				
6.00	6.75	6.63	0.13	1.9	3.5
	6.50				
	6.65				

Table 1: Reproducibility of the method: measured ALP activity of quality control samples compared with real values obtained by the reference Cobas® method

Real value (IU L^{-1})	Measured value (IU L^{-1})	Mean (IU L^{-1})	Std. dev. (IU L^{-1})	Recovery (%)
0.65 final c 118	0.63	0.63	0.02	97.0
	0.62			
	0.65			
1.25 final c 227	1.20	1.19	0.03	95.0
	1.16			
	1.21			
2.50 final c 455	2.38	2.29	0.09	93.0
	2.21			
	2.29			
5.00 final c 910	4.90	4.96	0.12	99.0
	4.89			
	5.10			
7.00 final c 1272	7.76	7.73	0.03	110.0
	7.70			
	7.74			

Table 2: Accuracy of the method: repeated analysis of control samples having certified ALP activity (real value)

MATRIX EFFECT EVALUATION. Calibration curves obtained either with external standard (employing ALP standard solutions) or with standard addition procedures (employing a reference blood sample of 61 IU L^{-1} ALP activity, as determined by the reference Cobas- method) were compared, to verify the absence of matrix interferences. Each measurement was performed in triplicate. A dilution of 1/10 (v/v) for injected samples was chosen to stress the study of matrix components. Fig. 5a shows a representative calibration curve obtained with the external standard procedure, in the range 3–32 IU L^{-1} (corresponding to 550 to 5820 IU L^{-1} concentrations in an undiluted plasma sample calculated as detailed in Section 2.2).

A linear relationship was observed between the ALP activity and the CL signal (r =0.99). Finally, when the ALP activity in the reference blood sample (diluted 1 : 10 v/v with saline solution) was calculated by interpolation on the calibration curve, a value of 60 ± 6 IU L^{-1} of ALP activity (calculated as activity in undiluted plasma) was obtained, which was not significantly different from the value obtained by the reference method ($p > 0.01$). The calibration curve obtained by employing the standard addition (Fig. 5b) was produced by addition of ALP standards in the range 6–23 IU L^{-1} (corresponding to 1090–4180 IU L^{-1} in undiluted plasma) to aliquots of the reference blood sample, previously diluted 1 : 10 v/v with saline solution. A linear relationship was observed between the ALP activity and the analytical CL signal ($r = 0.99$) and a value of 58- 5.0 IU L^{-1} of ALP activity was obtained for the blood sample, which is not significantly different from the reference value ($p = 0.05$). In addition, no significant difference was observed between the slope of calibration curves obtained by employing the two methods ($p > 0.05$), thus demonstrating the absence of matrix effects.

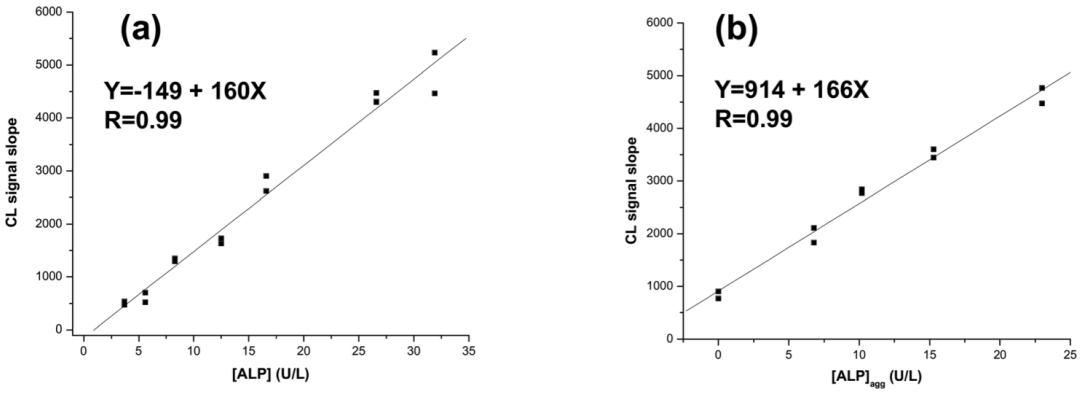

Figure 5: (a) Calibration curve for external standard obtained by analyzing ALP standard solutions in the range 3–32 IU L^{-1}; (b) calibration curve for standard additions obtained by analyzing aliquots of the blood sample fortified with ALP standards in the range 6–23 IU L^{-1}.

3.3.4 Real samples analysis

Fresh human blood samples were drawn from healthy donors (n = 15) and patients affected by cholestasis (n = 10) in heparintreated tubes. The samples had ALP activity in plasma values ranging from 500 to 1200 IU L^{-1}, as determined by the reference Cobas- method. For each sample, 0.5 μL of whole blood diluted 1 : 100 (v/v) was analyzed in the GrFFF system in five replicate analyses. Results (calculated as plasma ALP activity) were compared with those obtained by the reference Cobas® method and a good agreement was observed. Moreover, in order to test the robustness of the method, different dilutions of blood samples and plasma obtained from the same sample were analyzed with the GrFFF-CL system. Representative results for a normal sample and a pathological sample,

reported in Table 3, show that recovery values ranged between 90 and 110%, thus confirming the method accuracy.

	Sample	Real value	Determined value	Mean	Dev. Std.	Relative error	CV% intra	Recovery (%)
Normal sample	Blood diluted 1/100	(93 119)	94.20	94.57	1.29	−11	1.4	90
			93.50					
			96.00					
	Blood diluted 1/25		95.60	95.47	1.31	−10	1.4	90
			94.10					
			96.70					
	Plasma diluted 1/50		97.20	96.23	0.91	−9	0.9	91
			96.10					
			95.40					
	Plasma diluted 1/100		96.70	96.63	0.70	−9	0.7	92
			97.30					
			95.90					
Pathological sample	Blood diluted 1/100	(463 593)	537.00	533.00	4.00	1	0.8	100
			529.00					
			533.00					
	Plasma diluted 1/300		567.00	562.67	4.04	7	0.7	106
			562.00					
			559.00					
	Plasma diluted 1/200		590.00	587.33	2.52	11	0.4	110
			585.00					
			587.00					

Table 3: GrFFF-POCT results for normal and pathological samples

3.4 Conclusion

The results show the potentialities for the quantitative detection of specific analytes in plasma samples after their separation from cellular components employing a simple and compact GrFFF system on-line integrated with a flow-through CL analyzer. Quantitative detection of ALP activity was obtained with high analytical performances comparable to conventional diagnostic systems, with the advantages of lower sample and reagent consumption, shorter analysis time and simple instrumentation acting directly on the blood sample. The developed method was shown able to highly efficiently separate plasma from a very small volume (0.5

μL) of whole blood, in short analysis time (10 minutes) and high reproducibility (run-to-run CD <2%, day-today CV <4%). Such a low sample volume makes the assay compatible with a finger stick blood collection procedure, suitable for a POCT environment. GrFFF thus represents a convenient tool to assist bioanalytical methods acting on plasma or serum, since it easily online isolates plasma components without the need of centrifugation steps. The same approach can be extended to any bioassay terminating with a CL reaction, including also immunoassay and gene probe assays performed in microfluidic platforms and employing CL labels. In principle, with the same injected sample, different analytes could be detected in plasma by splitting different plasma fractions to different specific analytical modules. In addition, the fractionation method used in this work allows preservation of all the native properties of analytes and cells that could be further analyzed with increased analytical information. Finally, due to the simplicity of the proposed system, many detection modules can be simultaneously connected to the GrFFF device, realizing multiplexed analysis. In the present study, an innovative curvilinear geometry for the GrFFF channel was employed to obtain a compact device, while keeping the same fractionation performance obtained by the GrFFF device containing traditional rectangular channels. In the future, further miniaturization may be accomplished by building a microchannel on a support that also integrates microstructures for sample and mobile phase delivery. The use of an array of GrFFF channels will also be considered to increase enrichment productivity and to allow the

development of multiplexed systems based on the same separative principle

References

[1] de Mello A. J., Beard d N.; (2003) Lab Chip, 3: 11N–19N

[2] Aota A., Takahashi S., Mawatari K., Tanaka Y., Sugii Y., Kitamori T., (2011) Anal. Sci.; 27: 1173–1178

[3] Tachi T., Kaji N., Tokeshi M., Baba Y.; (2009) Anal. Chem.; 81: 3194–3198

[4] Lee B. S., Lee Y. U., Kim H.-S., Kim T.-H., Park J., Lee J.-G., Kim J., Kim H., Lee W. G., Cho Y.-K.; (2011) Lab Chip; 11, 70–78

[5] Gossett D. R., Weaver W. M., Mach A. J., Hur S. C., Tse H. T. K., Lee W., Amini H., Di Carlo D.; (2010) Anal Bioanal Chem; 397: 3249–3267

[6] Toner M., Irimia D.; (2005) Annu. Rev. Biomed. Eng.; 7: 77– 103

[7] Reschiglian P., Zattoni A., Roda B., Michelini E., Roda A.; (2005) Trends Biotechnol; 23: 475–483

[8] Roda B., Zattoni A., Reschiglian P., Moon M. H., Mirasoli M., Michelini E., Roda A.; (2009) Anal Chim Acta, 635: 132– 143

[9] Tong X., D. Caldwell,(1995) J. Chromatogr., B: Biomed. Sci. Appl; 674: 39–47

[10] Roda B., Reschiglian P., Zattoni A., Tazzari P. L., Buzzi M., Ricci F., Bontadin A.; (2008) Anal Bioanal Chem; 392: 137–145

[11] Roda B., Reschiglian P., Alviano F., Lanzoni G., Bagnara G. P., Ricci F., Buzzi M., Tazzari P. L., Pagliaro P., Michelini E., Roda A.; (2009) J. Chromatogr; 1216: 9081–9087

[12] Roda B., Casolari S., Reschiglian P., Mirasoli M., Simoni P., Roda A.; (2009) Anal Bioanal Chem; 394: 953– 961

[13] Roda A., Mirasoli M., Dolci L. S., Buragina A., Bonvicini F., Simoni P., Guardigli M.; (2011) Anal Chem; 83: 3178– 3185

[14] Kuswandi B., Nuriman, Huskens J., Verboom W.; (2007) Anal Chim Acta; 601: 141–155

[15] Magliulo M., Roda B., Zattoni A., Michelini E., Luciani M., Lelli R., Reschiglian P., Roda A.; (2006) Clin. Chem., 52: 2151–2155

[16] Roda A., Mirasoli M., Melucci D., Reschiglian P.;(2005) Clin. Chem.; 51: 1993–1995

[17] Lee T. H., Kim W. R., Poterucha J. J., (2012) Clin Liver Dis; 16: 183–198

[18] Girotti S., Ferri E., Ghini S., Budini R., Patrono D., Incorvara L., Roda A.; (1994) Anal Lett; 27: 325– 335

[19] Miao P., Ning L., Li X., Shu Y., Li G.; (2011) Biosens Bioelectron; 27: 178–182

[20] Kim H.-J., Kwak J.; (2005) J. Electroanal Chem; 577: 243– 248

[21] Blood – The Human Heart, The Franklin Institute Inc., 2009

[22] Mitaishvili R., The Human Blood: Composition, Typing, Lab Test Interpretation, RM Global Health (RMGH), 2010

[23] Melucci D., Guardigli M., Roda B., Zattoni A., Reschiglian P., Roda A.; (2003)Talanta; 60: 303–312

CHAPTER 4

Portable chemiluminescence multiplex biosensor for quantitative detection of three B19 DNA genotypes

Reproduced from: "Portable chemiluminescence multiplex biosensor for quantitative detection of three B19 DNA genotypes"
Mara Mirasoli, Francesca Bonvicini, Luisa Stella Dolci, Martina Zangheri, Giorgio Gallinella, Aldo Roda
Analytical and Bioanalytical Chemistry, 2013, 405:1139–1143
Reproduced by permission of Springer (License number 3580690366855)

4.1 Introduction

The parvovirus B19 is a very common virus in the population and it is implicated in a wide spectrum of pathological conditions such as erythema infectiosum, arthropathy, hemolytic anemia and aplastic transitional crisis. The infection is also associated with rare clinical manifestations such as myocarditis, hepatitis, encephalitis, chronic fatigue syndrome and some autoimmune diseases [1]. In pregnant women, the infection can lead to the development of non-immune fetal hydrops, miscarriage and fetal death [2]. The availability of portable and rapid diagnostic systems would allow an early diagnosis of viral infection by means of systems "Point-of-Care Testing" that might be useful start promptly the treatment with consequent reduction of adverse fetal outcomes. Moreover since B19V can be found in three different genotypes (G1,G2, and G3) which epidemiology still needs further studies, virus genotyping represents an interesting issue for monitoring B19 epidemiology. Biospecific binding assays exploiting chemiluminescence (CL) detection represent one of the most promising approaches towards miniaturized multiplex assays characterized by high detectability and rapidity [3]. Recently, a versatile and portable bioanalytical device relying on CL lensless charge-coupled device (CCD)-based imaging was developed to perform hybrid multiplexed assays, enabling detection of enzymes, antigens, and nucleic acids [4]. Digoxigenin-labeled amplified products from parvovirus B19 DNA, selected as a model nucleic acid analyte, were detected by hybridization with an immobilized capture probe and hybrids detection employing a horseradish peroxidase (HRP)-conjugate antibody and a CL substrate. However, the

limit of detection (LOD) of the assay was 50 nmol L^{-1}, thus not adequate for diagnostic applications. Herein, it is reported an optimized assay displaying improved detectability and the ability to distinguish between three different B19 virus genotypes [5]. The reaction chip was designed employing capillary forces instead of pumping devices to drive the flows of samples and reagents in order to obtain a minimally instrumented portable device.

The developed miniaturized multiplex biosensor is based on oligonucleotide array and chemiluminescence (CL) lensless imaging detection for parvovirus B19 detection and genotyping. The portable device consists of a reaction chip that is composed by:

- a glass slide chemically activated and arrayed with three B19 genotype-specific probes for the capture of DNA. The slide has to be integrated with fluidic elements (reservoirs and microchannels) in polydimethylsiloxane (PDMS) to deliver samples and reagents (Fig. 1a).
- A thermoelectrically cooled CCD camera employed for detection and spatial localization of the CL emission, exploiting the “position encoding” approach, in which the spatial localization of the analytical signal provided analyte identification (Fig. 1b).

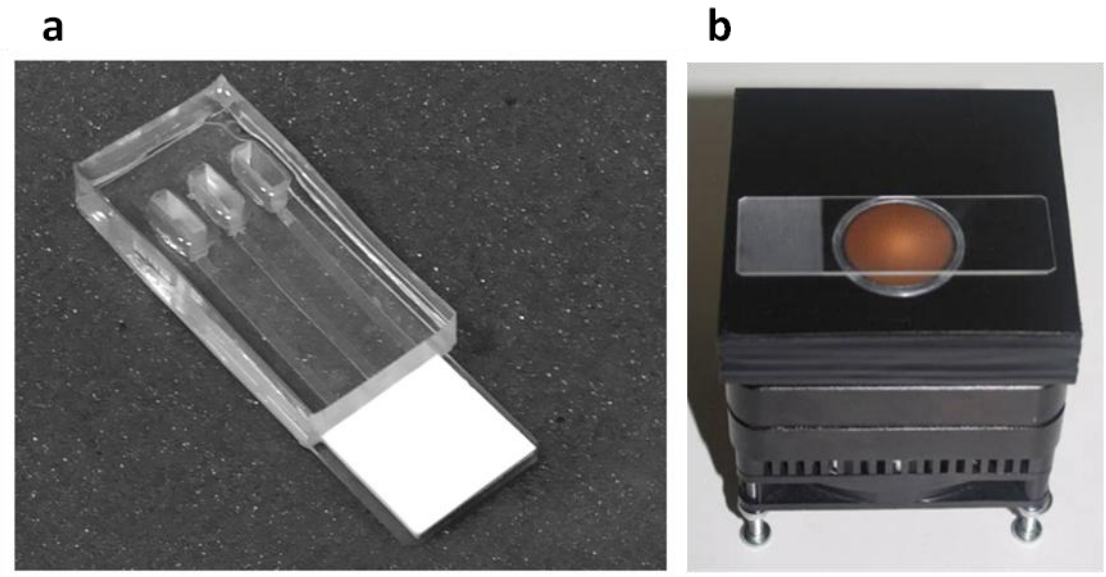

Figure 1: a) Layout of the disposable reaction chip combining a glass slide with arrayed B19 genotype-specific oligonucleotide capture probes (3×3 array) and a PDMS microfluidic layer. b) A thermoelectrically cooled CCD camera employed in "contact" imaging approach. Measurement area corresponds to the reaction chip area that is positioned on the fiberoptic taper surface.

Coupling between the functionalized glass support and the CCD camera was obtained by "contact" imaging (i.e., without employing lenses or similar optics elements) to reduce the complexity and size of the device and to improve CL signal detectability [6]. Hybrids were then detected by means of an avidin-HRP conjugate, upon addition of a CL HRP substrate. At first, artificial oligonucleotide targets, perfectly matching in sequence and length the corresponding probe sequence, were used for method development. Subsequently, biotin labeled amplified products obtained from a B19 control plasmid and from reference clinical samples were assayed to assess diagnostic applicability.

4.2 Materials and methods

4.2.1 Oligonucleotide array biosensor

The reaction chip for B19 genotyping was obtained by combining a microscope borosilicate glass slide (26× 76 mm^2, Thermo Fisher Scientific, Waltham, MA) with a polydimethylsiloxane (PDMS) microfluidic module. The disposable microfluidic module consisted of three channels (40 mm length, 1 mm width, and 0.1 mm height) with 100-µL inlet reservoirs, while the common outlet reservoir was a 4-cm^2 adsorbent cellulose pad (Whatman CF7, Whatman plc, Maidstone, UK). The bioprobe immobilization was performed by activating the slide glass surface with polyetheramine (JEFFAMINE® ED-600, generously provided by Huntsman Corporation, Everberg, Belgium) according to a reported procedure [7]. The genotype specific oligoprobes were then spotted (0.2 pmol/spot) in triplicate in an array of nine (3×3) spots, each one not exceeding 1 mm in diameter and 5 mm spacing.

4.2.2 B19 probes and artificial targets

On the basis of genomic reference sequences available in the National Center for Biotechnology Information nucleotide data base B19 probes and targets were designed. The 25-mer B19 probes were amino-modified (NH2) at 5′-end using a spacer arm of 12 carbon atoms. The complementary 25-mer B19 artificial targets were biotin labeled at the 5′-end. A biotinlabeled 25-mer B19-negative control target was also designed basing on a previously published synthetic sequence [8].

4.2.3 B19 amplified plasmid DNA and clinical samples

Using a multiplex PCR assay enabling the simultaneous amplification of the three B19 genotypes, biotin-labeled amplified products (145 base pairs) were obtained. A biotin modified forward primer and two different reverse primers were used for amplification, as reported in a published procedure [9]. Amplified products were prepared either from a B19 genotype 1 plasmid DNA or from ten purified serum samples (five positive and five negative), which were previously assayed with a reference PCRELISA method [10]. To enable construction of a calibration curve, amplified products obtained from the plasmid DNA were purified using the Wizard® PCR Clean-Up System (Promega Corporation, Indianapolis, IN) and the concentration was fluorimetrically estimated (QuantiFluor™ ds DNA System, Promega Corporation). The products were denatured by incubation at 95 °C for 5 min, and then iced before hybridization procedure.

4.2.4 Assay procedure

For hybridization procedure phosphate-buffered saline (PBS) at pH 7.6, sodium dodecyl sulfate (SDS), 0.05 M borate buffer at pH 9.6, and saline sodium citrate (SSC) buffer were used.

The analysis procedure steps are the following (Fig. 2):

- 50 µL of hybridization buffer (5× SSC, 0.1 % SDS) containing the artificial targets at different concentrations (from 1.6×10^{-2} to 10 $nmolL^{-1}$), or the denatured and purified product of amplification

from plasmid DNA (diluted at concentrations from 8×10^{-2} to 50 $nmolL^{-1}$), or 10 µL of the denatured product of amplification from a clinical sample, are dispensed in the inlet reservoir and let flowing through the channels;

- washing step is performed with 100 µL of 2× SSC containing 0.1 % SDS to remove nonspecific DNA–DNA hybrids;
- 50 µL of HRP-labeled avidin (from Sigma-Aldrich, St. Louis,MO; 50 μgL^{-1} in PBS containing 0.1%(w/v) BSA) is added in each cannel;
- another washing step is performed with 100 µL of PBS
- 20 µL of SuperSignal ELISA Femto (Thermo Fisher Scientific, Waltham, MA) are dispensed in the inlet reservoir and then the reaction chip is positioned directly on the taper surface of the CCD-based device according to the reported procedure;
- signal is imaged with 30 s acquisition time.

Samples and reagents dispensed in the inlet reservoir flore through the channels at a 15- to 20-$\mu Lmin^{-1}$ flow rate, each assay step requiring 2–3 to 5–7 min depending on the dispensed volume. Moreover after each step it is necessary to change the adsorbent pad.

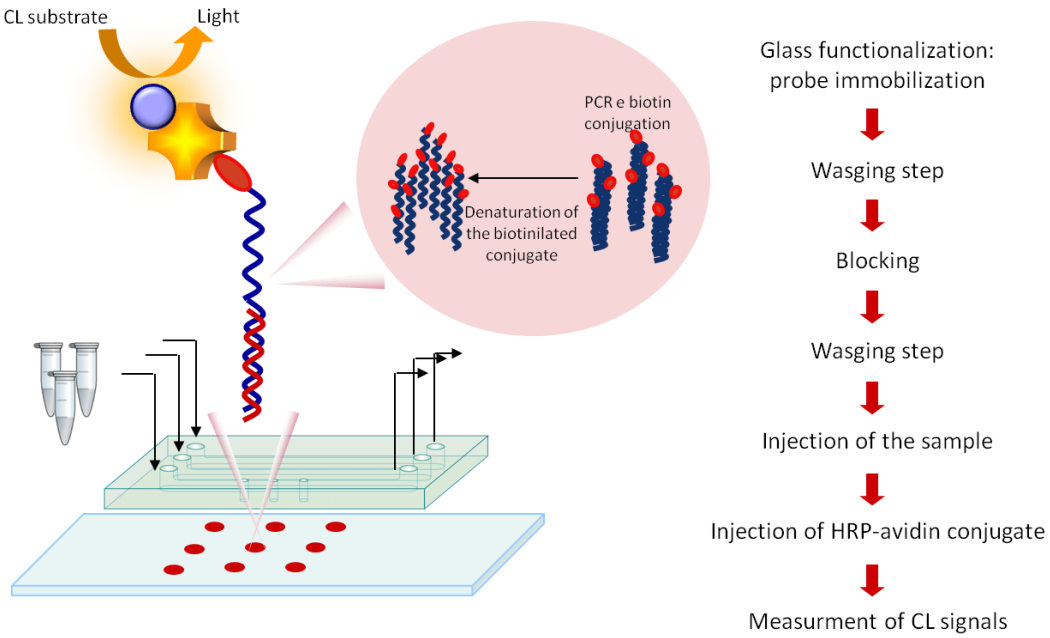

Figure 2: Scheme of the assay procedure

4.2.5 Data analysis

Quantitative analysis of CL images was performed using the WinLight software v. 1.2 (Berthold Technologies GmbH & Co KG, Bad Wildbad, Germany). The mean photon emission measured in the area corresponding to probe spots was corrected by subtracting the CL substrate background signal that was measured in the absence of target analyte and expressed in relative light units. Calibration curves were generated by plotting the net value of CL signal was plotted the target concentration. The LOD was calculated as the background signal +3 standard deviations. The same value was selected as cut-off of the assay to evaluate the clinical samples.

4.3 Results and discussion

4.3.1 Reaction chip optimization

The immobilization procedure of B19-specific oligoprobes was optimized in order to improve the detectability of the assay taking into account the previously reported studies [11].

The optimization of the concentration of the immobilizer capture probes was performed by spotting different amounts (0.04, 0.2, and 1 pmol) of each genotype specific probe along a channel, then performing hybridization procedures with the corresponding target (10 nmolL^{-1}) and it was found that the highest CL signal was observed for 0.2 pmol for all genotypes.

An higher amount of capture probes provide a decrease in the CL signals that might be due to steric hindrance. Infact in this condition capture probes are closely packed together in the spot and therefore less exposed to target hybridization [12]. Indeed the optimal surface printing density for oligonucleotide arrays [13] is approximately 105 molecules μm^{-2}, that corresepond to 0.2 pmol/spot.

4.3.2 Calibration curves

The calibration curves were generated for each B19 genotype by using standard complementary biotin-labeled artificial targets ranging from 1.6×10^{-2} to 10 nmol L^{-1} and are reported in Fig.3.

For all genotypes the dynamic range of the assay estende from 0.1 to 10 nmolL^{-1} and the LOD was 80 pmolL^{-1} that is lower when compared with

that obtained performing a conventional PCR ELISA technique (100 $pmolL^{-1}$) using the same reagents. This improvement can be due to the optimization of surface functionalization strategy, biospecific capture probes design and assay experimental conditions. It was finally ibserved that the calibration curve obtained for genotype 3 presents a different slope than those obtained for the other genotypes. Maybe this effect is caused by the different percentage content of GC couples in hybrids, which is 56 % for genotypes 1 and 2, while it is 52 % for genotype 3.

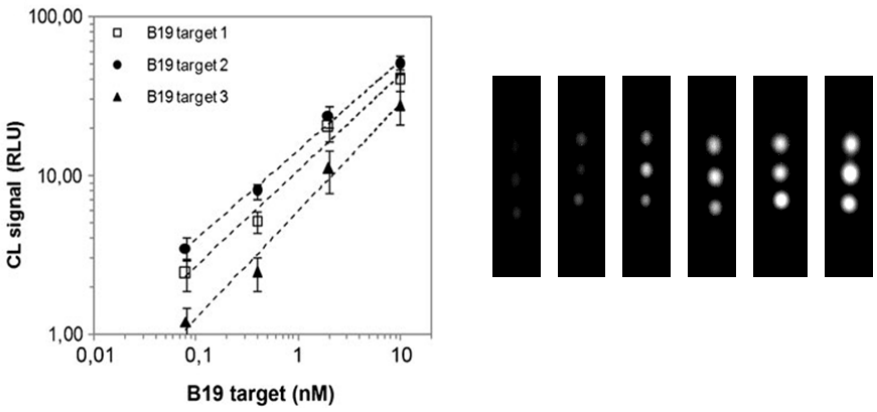

Figure 3: CL calibration curves obtained by DNA–DNA hybridization reactions between fully complementary B19 capture probe and artificial oligonucleotide targets (left) and CL images (right). The coefficient of determination (R^2) is 0.99 for genotype 1 and 0.98 for genotypes 2 and 3. CL data represent the mean values±SD of three separate experiments. RLU relative light unit.

4.3.3 Assay specificity

The specificity of the assay was evacuate by analyzing B19 targets (10 $nmolL^{-1}$) of the different genotypes in all the channels in order to prove that each B19 capture probe is specific for the detection of the specific

B19 genotype. It was found that CL signals above the cut-off value were observed only when the target analyte hybridized with the corresponding capture probe.

Moreover it was observed that there are no aspecif signals when the biotin-labeled B19 negative control target was assayed with each capture probe (Fig. 4).

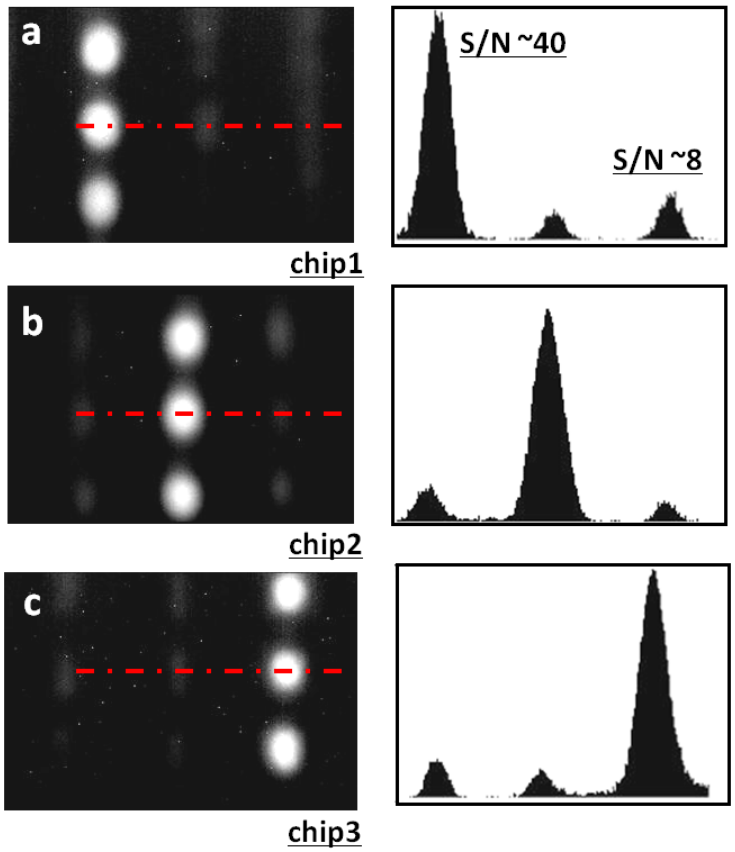

Figure 4: CL images (left) and CL-profile signals (right) obtained from hybridization reactions between the three amino-linked B19 DNA probes and the three biotin-labeled artificial oligonucleotide B19 targets. The images show three reaction chips, each one arrayed with the three B19 genotype-specific probes (three separate spots per genotype; genotype 1 along the left, genotype 2 along the middle, and genotype 3 along the right microchannel) and hybridized with a defined B19 biotin-labeled target ((a) genotype 1, (b) genotype 2, and (c) genotype 3).

4.3.4 Analysis of amplified samples

To evaluate the performance of the method, the product of amplification obtained from a B19 genotype 1 plasmid DNA was purified from reaction mix, fluorimetrically quantified, and then differently diluted (from 8×10^{-2} to 50 $nmolL^{-1}$) prior to analysis.

The assay specificity on amplified products was confirmed as a CL signal above the cutoff value was detected only in the correspondence of the B19 genotype 1 capture probe.

It was found a LOD value of 650 pmol L^{-1} that is slightly higher than that obtained for B19 targets (80 $pmolL^{-1}$). Maybe this is due to a lower hybridization efficiency between oligonucleotide probe and amplified product, with respect to hybridization between single-stranded sequences of the same length.

Finally amplified products obtained from ten reference serum samples were analyzed after PCR and scored as negative and positive, based on the cut-off value of the reaction chip. Our results (five negative and five B19 genotype 1-positive samples) were confirmed by those obtained with the reference PCR-ELISA method.

4.4 Conclusion

The developed portable biosensor based on CL lensless imaging system, is able to detect and genotype B19 DNA.

It was designed and optimized a microfluidic reaction chip that comprises a PDMS microfluidic layer coupled with a glass slide on which genotype specific B19 capture oligonucleotide probes.

Adsorbent pads facilitated the flow of the liquids along the PDMS channels exploiting capillary forces, thus realizing a selfpowered non-instrumented reaction chip.

The assay takes only 30 min that is competitive with the reference microtiter plate DNA hybridization step of PCRELISA method that takes 2 hours.

Moreover the LOD was 80 pmolL^{-1} for the three different B19 genotype oligonucleotide targets and 650 pmolL^{-1} for the amplified product of DNA genotype 1, which is comparable to that obtained with standard laboratori methodologies (e.g., PCR-ELISA) and significantly improved with respect to the previously reported feasibility study [14]. Finally the performances of the methods were also confirmed by the analysis performed on ten serum samples.

In conclusion the developed biosensor allows the simultaneous multiplexer and accurate quantification and genotypization of various DNA sequences in one sample employing relatively inexpensive instrumentation, suitable for POC applications.

In the future i twill be possible to improve this prototype and to integrate a miniaturized PCR system [15] to perform on-chip both target DNA amplification and product denaturation prior to hybridization analysis. Moreover it is also possible to use this biosensor for the diagnosis of different viral infections by changing the arrayed probes. Indeed, for

various viruses the genotypization provides important information to assess therapeutic intervention and to predict the outcome of the disease.

References

[1] Agbandje M., Kajigaya S., Mckenna R., Young N.S., Rossmann M.G.;, (1994) Virol; 203: 106-115

[2] de Jong E.P., de Haan T. R., Kroes A.C.M, Beersma M.F.C., Oepkes D., Walther F. J., (2006) J Clin Virol; 36, 1-7

[3] Roda A., Guardigli M., Michelini E., Mirasoli M., Pasini P.; (2003) Anal. Chem.; 75: 463A–470A

[4] Roda A., Mirasoli M., Dolci L.S., Buragina A., Bonvicini F., Simoni P., Guardigli M.; (2011) Anal. Chem.; 83: 3178–3185

[5] Servant A., Laperche S., Lallemand F., Marinho V., De Saint M.G., Meritet J.F., Garbarg-Chenon A.; (2002) J. Virol.; 76: 9124–9134

[6] Roda A., Mirasoli M., Dolci L. S., Buragina A., Bonvicini F., Simoni P., Guardigli M.; (2011) Anal. Chem., 83: 3178-3185

[7] Bonvicini F., Mirasoli M., Gallinella G., Zerbini M., Musiani M., Roda A., (2007) Analyst; 132: 519-523

[8] Gallinella G., Bonvicini F., Filippone C., Delbarba S., Manaresi E., Zerbini M., Musiani M., (2004) Clin. Chem.; 50:759–762

[9] Bonvicini F., La Placa M., Manaresi M., Gallinella G., Gentilomi G.A., Zerbini M., Musiani M.; (2010) Dermatology; 220:138–142

[10] Bonvicini F., Gallinella G., Cricca M., Venturoli S., Musiani M., Zerbini M.; (2004) J. Clin. Virol.; 30:134–136

[11] Roda A., Mirasoli M., Dolci L.S., Buragina A., Bonvicini F., Simoni P., Guardigli M.; (2011) Anal. Chem.; 83: 3178–3185

[12] Sheng H, Ye B.; (2009). Appl. Biochem. Biotechnol.; 152:54–65

[13] Pierik A., Dijksman J.F., Lub J., Stapert H.R., Broer D.J.; (2010) Anal. Chem.; 82:1191–1199

[14] Roda A., Mirasoli M., Dolci L.S., Buragina A., Bonvicini F., Simoni P., Guardigli M.; (2011) Anal. Chem.; 83: 3178–3185

[15] Zhang Y., Ozdemir P.; (2009) Anal. Chim. Acta; 638:115–125

CHAPTER 5

A multiplex chemiluminescent biosensor for type B-fumonisins and aflatoxin B1 quantitative detection in maize flour

---

Reproduced from: "A multiplex chemiluminescent biosensor for type B-fumonisins and aflatoxin B1 quantitative detection in maize flour"
Martina Zangheri, Fabio Di Nardo, Laura Anfossi, Cristina Giovannoli, Claudio Baggiani, Aldo Roda and Mara Mirasoli
Analyst, 2015,140: 358-365
Reproduced by permission of The Royal Society of Chemistry
http://pubs.rsc.org/en/content/articlepdf/2015/an/c4an01613k

5.1 Introduction

The development of rapid and portable analytical devices for on-field screening applications is one of the most active trends in the field of agrofood analysis, since contamination with toxic substances (e.g., natural toxins, pesticides, veterinary drug residues, environmental pollutants) or microorganisms pose severe safety issues, as well as great economic concern.

Immunochromatographic assays (also named lateral-flow immunoassays, LFIA) have shown to be particularly advantageous for such applications, since they provide rapid, simple, specific analyses with no instrumental requirement. Following their success in diagnostics, applications in agrofood screening is now an emerging field. In order to foster the use of LFIA methods as screening tools for food safety, two promising fields of research have been recently identified, namely the development of multiplex assays and their combination with portable recording devices [1]. Such features will enhance the competing ability of these portable tests with laboratory-based screening methods, directly providing on-field quantitative information on a number of analytes in a given sample. This will enable accurate screening of a large number of samples directly where they are obtained and significant savings in terms of time and costs, since only the actual suspicious samples will be transported to the analytical laboratory for confirmatory analyses. Aflatoxins and Fumonisins are secondary metabolites produced by Aspergillus and Fusarium respectively, growing on agricultural commodities in the field or after harvest [2]. Since mycotoxins represent one of the most important threat

for cereal safety [3], exhibiting acute toxic, carcinogenic, mutagenic, teratogenic, immunotoxic and estrogenic effects in man and animals [4,5], the European Commission (EC) has established maximum residue limits (MRLs) in cereals and cereal-based foods and feeds: 4000 μg kg^{-1} for type B-fumonisin and 4 μg kg^{-1} for the sum of Aflatoxins B1 (AfB1), B2, G1 and G2 as well as 2 μg kg^{-1} for AfB16.

A wide number of LFIA methods have been developed for mycotoxin detection in feed and food [1,7-9]. We recently reported a chemiluminescence (CL) LFIA-based biosensor for simple, rapid and ultrasensitive on-site quantification of type B-fumonisins in maize flour down to 25 μg kg^{-1}, which has been successfully applied to both standard and real samples [10]. It is well known that enzyme-catalyzed CL detection provides high detectability, rapidity, specificity and wide linear range in immunoassays [11,12], especially in miniaturized formats [13]. This approach has been recently extended to LFIA methods, converting them from qualitative methods (when conventional colloidal gold labelling is employed) to highly sensitive and quantitative assays [14-16].

There is a growing demand for multiplex screening assays to replace single-analyte ones, since several mycotoxins may coexist in a single product and yield to synergistic toxic effects [2,7]. Despite immunochromatography technology potentially offers easy implementation of multi-residue analysis and obvious economic encouragement for this approach, few multiplex LFIA assays have been described in the literature up to now [8,17-21], and none of them exploited the advantages of CL detection.

Herein we report the development of a biosensor for the multiplex detection of type-B fumonisins and AfB1 in maize samples. The biosensor is based on a portable ultrasensitive CCD-based “contact” imaging device coupled with a CL-LFIA strip, on which two competitive immunoassays are simultaneously performed. Aflatoxin B1 conjugated with bovine serum albumin (AfB1-BSA) and Fumonisin B1 (FmB1)-BSA conjugate were immobilized in different positions along the strip. Upon sample application, type-B fumonisins and AfB1 in the sample competed with immobilized analogues for their specific anti-fumonisin or anti-aflatoxin antibodies added to the sample. Signal detection was performed by CL contact imaging upon addition of a secondary horseradish peroxidase (HRP)-labelled secondary antibody and the suitable enzyme CL substrate. With this format, a quantitative and objective measurement of target analytes below EU regulatory levels was performed, thus enabling rapid and reliable identification of those samples requiring confirmatory analysis.

5.2 Materials and methods

5.2.1 Reagents

FmB1, AfB1, Aflatoxin B2, Aflatoxin G1, Aflatoxin G2, Ochratoxin A, Deoxynivalenol, and Zearalenone (Oekanal certified solutions), BSA, Tween-20 and HRP-labeled goat anti-rabbit immunoglobulin were purchased from Sigma Aldrich (St. Louis, MO, USA). Ultrapure water was produced by a Millipore Milli Q system (Millipore, Bedford, MA). The

Supersignal ELISA Femto CL substrate for HRP was bought from Thermo Fisher Scientific Inc. (Rockford, IL).

FmB1 and AfB1 powder were purchased from Fermentek (Jerusalem, Israel). The goat anti-rabbit antibody was purchased from AbCam (Cambridge, UK). Rabbit anti-FmB1 antibodies and rabbit anti-AfB1 antibodies were kindly supplied by Generon srl (Modena, Italy). The other reagents were of analytical grade and were employed as received. Phosphate buffered saline (PBS) was prepared as follows: 10 mmol L^{-1} Na_2HPO_4, 2 mmol L^{-1} KH_2PO_4, 137 mmol L^{-1} NaCl, 2.7 mmol L^{-1} KCl, pH 7.4. Assay strips for LFIA were prepared by immobilizing on nitrocellulose membranes, from bottom to top of the strip, the FmB1-BSA conjugate, the AfB1-BSA conjugate, and the goat anti-rabbit antibody to form the two test lines (T-lines) and the control line (C-line), respectively, keeping a distance of 4 mm between the lines (Fig. 1, Panel C). The membranes were then assembled with a sample and an adsorbent pad and cut into sections.

5.2.2 Preparation of mycotoxin-BSA conjugates

The FmB1-BSA conjugate was synthesized according to Christensen et al. [22], with slight modifications. The AfB1-oxime hapten (AfB1-CMO), synthesized according to Kolosova et al. [23], was employed for the preparation of the AfB1-BSA conjugate by the N-hydroxysuccinimide ester method as follow: 5.7 mg of AfB1-CMO were reacted overnight at room temperature with 5 mg of BSA dissolved in 0.15 M sodium bicarbonate pH 8.3 and the pure conjugate was obtained from gel-filtration, as described

above. AfB1-BSA concentration was determined through Brilliant Blue Comassie method.

Conjugates were supplemented with 0.1% sodium azide and stored refrigerated.

5.2.3 Instrumentation

The biosensor, shown in Fig. 1 (Panel B), was assembled employing a previously described CCD-based contact imaging configuration [10,24]. In particular, the LFIA strip was placed directly in contact with the thermoelectrically-cooled CCD sensor through a round fiber optic taper. A mask was used to ensure reproducible strip positioning. This assembly was enclosed in a dark box to provide shielding from ambient light. During the acquisition the CCD sensor temperature was kept at −10 ◦ C.

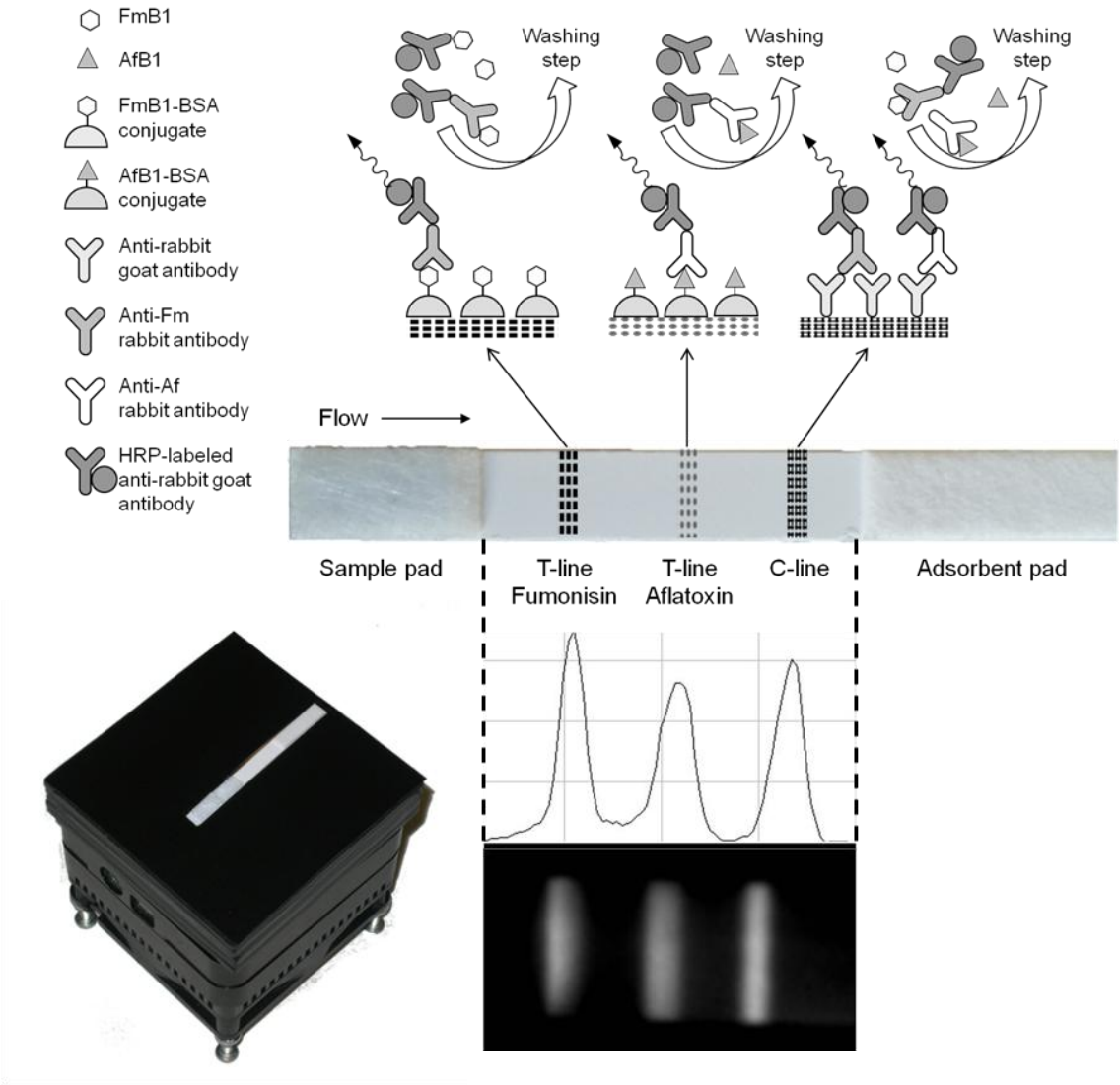

Figure 1: Top: a scheme of the multiplex CL-LFIA assay on the nitrocellulose strip. Bottom: a CCD-based device in a contact imaging detection format for acquiring CL signals from LFIA strips; a chemiluminescence image and intensity profile of a nitrocellulose membrane where adjacent lines were immobilized at a 4 mm distance.

5.2.4 Assay procedure

The nitrocellulose strip was placed horizontally on the larger fiber optic taper surface, then the LFIA assay was started by depositing on the

bottom of the strip a volume of 100 μL of solution, containing 40 μL of PBS with 3% BSA (w/v) and 0.1% Tween 20 (v/v), 5 μL of HRP-labeled goat anti-rabbit antibody diluted 1:500 (v/v) in PBS, 5 μL of rabbit anti-FmB1 and anti-AfB1 antibody, each diluted 1:500 (v/v) in PBS, and 50 μL of maize sample extract (or blank maize sample extract for the blank, or FmB1 and AfB1 standard solutions prepared in blank maize sample extract to produce calibration curves). Upon complete migration of the solution (10 min), the strip was washed by flowing 100 μL of PBS for 10 min. Then 70 μL of CL substrate was added at the bottom of the strip and let flow through the membrane (4 min), which was kept at 25 °C. The CL signal was acquired with the contact CCD-based imaging device (5-s acquisition time). Total analysis time was about 30 min. The scheme of the multiplex CL-LFIA assay on the nitrocellulose strip is showed in Fig. 1 (Panel A). To obtain quantitative information, the mean photon emission was measured in the areas corresponding to C-line and T-lines of the LFIA strip and each was subtracted of the mean background signal measured in two adjacent areas below and above the line. The T-line/C-line ratio was calculated for each analyte and then converted into B/B_0 ratio by dividing it for the T-line/C-line ratio measured in the absence of the target analyte (B0, i.e., maximum T-line/C-line value). Calibration curves were obtained by plotting B/B_0 values against the log of analyte concentration and fitting the experimental data with a four-parameter logistic equation. Linearization of the calibration curve was obtained through the logit–log transformation, by plotting the logit of the B/B_0 ratio (as a percentage)

against the log of analyte concentration. The best data fit was obtained by linear regression of the standard points.

5.2.5 Analysis of maize samples

Maize flour samples were obtained directly from producers or mills. Fumonisin content was determined by HPLC-UV as previously described [25]. AfB1 contamination was assessed by a commercial ELISA kit (EuroClone SpA, Milano, Italy).

Maize flour samples were subjected to a pre-analytical extraction procedure previously described [10]. Briefly, 1 g of maize flour was suspended in 10 mL of PBS buffer, hand-shaken for 3 min at RT and let settle for 5 min. Then, a 100-μL aliquot of the supernatant was heated for 3 min at 100 °C to inactivate endogenous maize peroxidase, then cooled to room temperature and subjected to analysis by LFIA. Heating was performed on a indium-tin oxide (ITO)-coated glass (SPI Supplies/Structure Probe Inc., West Chester, PA) employing a Frame-Seal slide chamber (Bio-Rad Laboratories, Hercules, CA) to contain the sample and avoid evaporation. To obtain the analyte concentration value for each sample, its B/B_0 value was calculated as described above and interpolated on a stored calibration curve.

5.3 Results and discussion

A duplex indirect competitive CL-LFIA was developed by depositing on a test strip AfB1-BSA and FmB1-BSA on T-lines and goat anti-rabbit antibody on a unique C-line. With this format, each of the two analytes present in

the sample competes with its corresponding immobilized hapten for binding the specific anti-AfB1 or anti-FmB1 rabbit antibodies, which are in turn detected by employing HRP-conjugated anti-rabbit antibody and CL detection. Anti-rabbit antibodies immobilized on the C-line allow confirmation of correct test development by capturing any rabbit-antibody-based signal reagent (i.e. the presence of the signal indicated the correct migration of the reactants along the strip). Moreover, normalizing the signal of T-lines respect to that of C-line, make it possible to take into account environmental and matrix factors that might affect the intensity of the CL signal (i.e. changes in ambient temperature or the presence of HRP inhibitors in the sample) providing a strip-to-strip normalization factor.

Signals were detected employing an ultrasensitive cooled CCD sensor employed in a "contact imaging" approach, as previously described. As shown in Figure 1C, 4-mm distance between adjacent lines was sufficient to prevent interference in signal detection. According to the competitive immunoassay principle, the light emission intensity of the T-lines gradually decreased up to their complete disappearance as the concentration of the respective analyte in the sample increased. The C-line intensity was employed as a normalization value, to increase assay reproducibty and compensate for test strip to test strip variability.

5.3.1 Optimization of experimental parameters

Assay parameters (concentration of immunoreagents and selection of the saturation agent) were optimised to generate assays with limits of

detection (LOD) and dynamic ranges useful for detecting AfB1 and FmB1 in maize samples below regulatory limits. Furthermore, the methods were optimized considering that, in order to detect simultaneously both analytes, the three lines on a strip should provide similar signal intensity. This ensures the possibility to use a single integration time for the simultaneous measurement of the CL signals on a strip, preventing cross-talk phenomena.

The concentrations of primary and secondary antibodies yielding the highest detectability for FmB1 and AfB1 were evaluated. The optimal concentration of anti-fumonisin (1:500 v/v), anti-aflatoxin (1:500 v/v) and HRP-labelled anti-rabbit (1:500v/v) were selected as the dilution that provides the highest detectability and the best compromise between the effects described above. Furthermore, different protocols were assayed for saturating the nitrocellulose membrane, thus reducing nonspecific adsorption of the immunoreagents and increasing the signal intensity of the lines, as previously shown [25]. In particular, different saturation agents (BSA, non fat dry milk, soybean milk) and additives in the running buffer were tested. The best performance was obtained by incubating the nitrocellulose strips with 1% BSA (w/v) in PBS buffer for 5 min at room temperature and by adding 3% BSA (w/v) and 0.1% Tween 20 (v/v) in the running buffer.

Finally, the absence of cross reactivity (CR) between the two analytes was checked by running each primary antibody in the absence of analytes in solution. As shown in Fig. 2, no CR between anti-fumonisin antibody and AfB1 (left panel), nor between anti-aflatoxin and FmB1 (right panel) was

observed, as confirmed by the absence of the upper and lower T-lines, respectively.

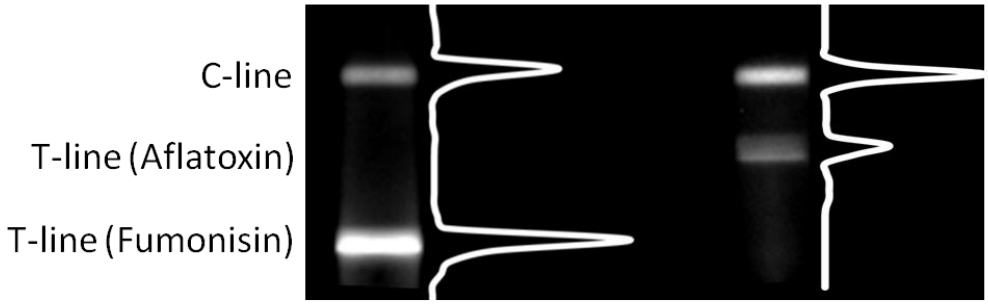

Figure 2: Chemiluminescence images and intensity profiles of nitrocellulose membranes in which anti-aflatoxin and anti-fumonisin antibodies separately ran in the absence of analytes.

5.3.2 Specificity of the immunoreagents

The specificity of the immunoassays was determined towards structurally related and unrelated mycotoxins by measuring the IC50 value for each compound of interest, i.e., the concentration of tested compound providing a response at the 50% bound (midrange of the curve). The CR values were calculated as the ratio of the IC50 value for the analyte over the IC50 value of the tested interfering compound. The anti-aflatoxin antibody showed low CR with AfG2 and AfB2 (below 2%) and higher for AfG1 (38%). The anti-fumonisin antibody showed about 100% CR with FmB2, thus showing its ability to detect type-B fumonisins present in the sample, as the sum of FmB1 and FmB2.

Both antibodies showed very low CR towards Zearalenone, Deoxynilvalenol, and Ochratoxin A, as shown in Table 1.

The characteristics of the employed antibodies make the multiplex assay particular relevant for regulatory purposes. Indeed, EU regulations define limit values for fumonisin as the sum of FmB1 and FmB26. In addition, while limit values for aflatoxins are reported as the sum of AfB1, AfB2, AfG1, and AfG2, it is important to note that the ability to singularly detect the concentration of AfB1 is particular relevant, being this mycotoxin listed as a group 1 carcinogen by the International Agency for Research on Cancer [4]. Finally, negligible CR of the antibodies towards structurally unrelated mycotoxins considerably reduces the risk for false positive results.

	Anti-fumonisin antibody	Anti-aflatoxin antibody
Fumonisin B1	100%	<0.02%
Fumonisin B2	97%	<0.02%
Aflatoxin B1	<0.02%	100%
Aflatoxin B2	<0.02%	2%
Aflatoxin G1	<0.02%	2%
Aflatoxin G2	<0.02%	38%
Zearalenone	<0.02%	0.2%
Deoxynilvalenol	<0.02%	0.8%
Ochratoxin A	<0.02%	2%

Table 1: Cross reactivity values measured for the anti-fumonisin and anti-aflatoxin antibodies

5.3.3 Calibration curves

Calibration curves were generated by using standard solutions produced in blank maize flour sample extracts in the range between 0.2 - 1500 μg L^{-1} and 0.06 - 50 μg L^{-1} of FmB1 and AfB1, respectively. Calibration curves were produced first by working in single assay; in particular both primary antibodies were added in all the strips, while the two analytes were assayed separately. As shown in Fig. 3, being a competitive type format, the decrease of T-line/C-line ratio was directly proportional to the amount of the analyte in the sample (the T-lines completely disappeared at the highest FmB1 and AfB1 concentration).

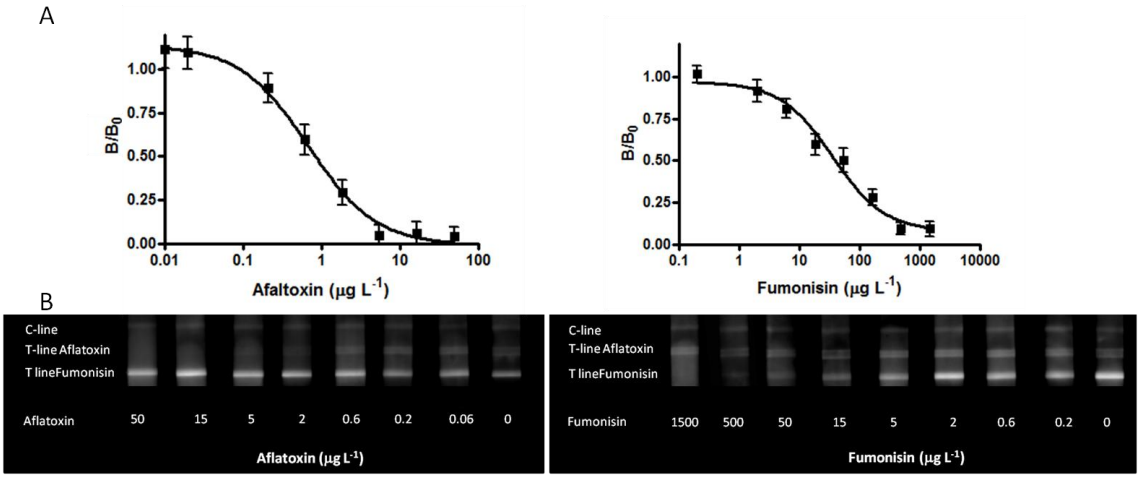

Figure 3: (A) Calibration curve obtained for AfB1 and FmB1 employing the contact imaging detection device. The curve fitting was performed employing a four-parameter logistic equation. Error bars_ ± SD, n _ 3. (B) Chemiluminescence images of LFIA membranes acquired with the contact imaging detection device.

The limit of detection (LOD) was calculated as the concentration corresponding to the blank T-line/C-line value minus three times the blank

standard deviation. The obtained values were 0.6 μg L^{-1} FmB1 and 0.15 μg L^{-1} AfB1, corresponding respectively to 6 μg kg^{-1} and 1.5 μg kg^{-1} in maize flour samples (according to the extraction procedure employed in this work). The dynamic range of the method extended from 0.6 to 1500 μg L^{-1} for FmB1 and from 0.15 to 50 μg L^{-1} for AfB1, with a midpoint value at 40 μg L^{-1} and 0.9 μg L^{-1}, respectively.

The LOD values obtained for FmB1 and AfB1 are comparable or lower than the those reported in the literature employing a CL-LFIA [10] or colloidal gold based LFIA assays [25-28], as well as when compared with commercial assays. The obtained results are comparable with those of recently published articles which describe the use of indirect competitive LFIA based on colorimetric detection for a multiple semi-quantitative determination of Fusarium mycotoxins in cereals [19] and for the simultaneous quantification of ZEA and FmB1 in corn and wheat [18]. The results of repeated calibration curves demonstrated a good reproducibility, the relative standard deviation associated to each point of the calibration curve being 0.5-12 % for FmB1 and 0.5-7% for AfB1, respectively (3 calibration curves produced in separate runs for each analyte). Finally, calibration curves obtained separately for each analyte (although in the presence of both primary antibodies) were compared with those obtained by working in multiplex format, adding in the same sample known amounts of both FmB1 and AfB1. To evaluate the possibility of accurately detecting each analyte, even when one is present at a higher concentration with respect to the other, multiplex calibration curves were generated either by increasing the amount of both analytes

simultaneously, or by increasing the concentration of one analyte while decreasing that of the other. A representative series of CL images and the obtained calibration curves are shown in Fig. 4.

Results show that the simultaneous presence of the two analytes in the sample, even in disproportionate amounts, does not affect the light emission intensity of the other test line.

The LOD and the dynamic range obtained in monoplex format were confirmed also by working in multiplex assay, making it possible to detect and quantify the two mycotoxins in a unique analysis. This indicates that multiplex competitive assays on a single test strip can produce quantitative assays without loss in assay detectability as compared with single tests.

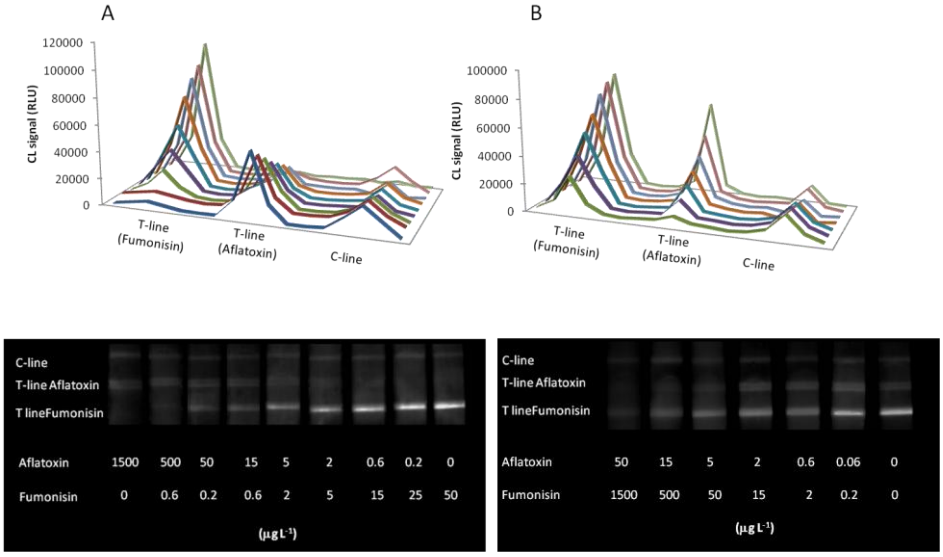

Figure 4: Chemiluminescence images and intensity profiles of LFIA membranes obtained by increasing the concentration of one analyte and decreasing the other (A) and increasing the amount of both analytes simultaneously (B).

5.3.4 Maize flour samples

To enable multiplex assays in a point-of-use format, a simple and rapid sample preparation procedure, providing good recovery for all the analytes of interest, must be employed. It has been previously shown that extraction in aqueous media at close to neutral pH values provides good recovery for both aflatoxins [26] and fumonisins [25]. Furthermore, the absence of organic solvents in the extraction solution makes the procedure more environmental-friendly and avoids problems of disruption of antigen-antibody binding. Thus, maize flour samples were subjected to extraction in PBS buffer, followed by rapid extract heating to inactivate peroxidase enzymes naturally present in maize (which was performed employing a portable system suitable for point-of-use applications). The whole analytical procedure, including sample preparation, lasted 30 min.

The assay analytical performance was evaluated by analyzing pooled extracts from blank maize flour samples (previously analyzed by ELISA) fortified by adding known amounts of both FmB1 (166, 18 and 2 $\mu g\ L^{-1}$) and AfB1 (1.8, 0.6 and 0.2 $\mu g\ L^{-1}$), corresponding approximately to 0.9, 0.6 and 0.3 B/B0 values on the respective calibration curve. Recovery ranged from 79 to 119%, while coefficients of variation below 20% were obtained (Table 2). The performance of the multiplex LFIA method was also evaluated on real samples and results were compared with those obtained by confirmatory analyses, performed by HPLC-UV (FmB1 + FmB2 content) and a commercial ELISA kit (AfB1). Results, reported in Table 3 show a good agreement between CL-LFIA and reference methods for both

mycotoxins in all samples, with recovery values ranging from 89 to 120% and coefficient of variation below 20%. A picture of the membranes used for the analyses of the maize samples is reported in Fig. 5.

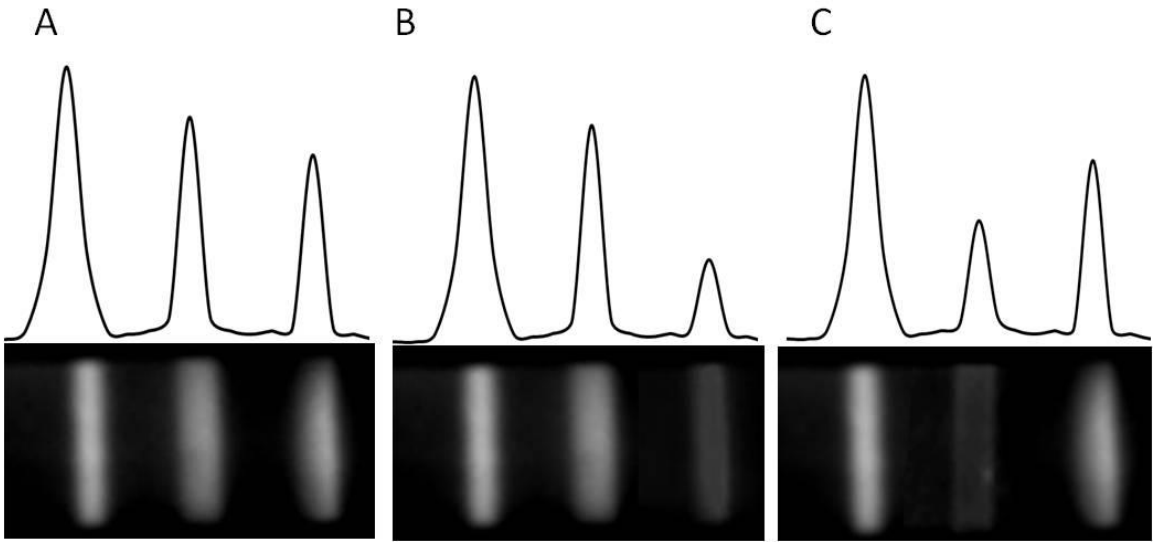

Figure 5: Chemiluminescence images of LFIA membranes used for analyses of maize samples. The membrane A is negative for all toxins, B is positive for AfB1 and C is positive for typeB-Fm.

5.4 Conclusions

The results show that the multiplex biosensor provides reliable, with performances comparable with those obtained employing reference methods. The extraction procedure fulfils the requirements for the development of a method that can be applied on site. The co-extraction of the two mycotoxins, although based on a simple manual extraction with aqueous buffer and rapid heating system employing a portable manifold, shows satisfactory recoveries. The method is rapid (total analysis time 30 min), simple, cost effective and can be performed in a non-laboratory environment by non-specialists.

The possibility to detect simultaneously two analytes, providing quantitative results within current regulatory limits, reduces the number of analysis and allows to screen on site a large number of samples, thus reducing the costs for transporting and analyzing samples in the laboratory. This allows performing frequent analyses monitoring the entire production chain (e.g., on field, at harvest, during storage and transportation) according with the HACCP procedures. In the future, it will be possible to further increase the number of analytes by adding other test lines, provided the compatibility with the antibody employed in the immunoassay.

Ongoing work is devoted to the development of a ready-to-use cartridge containing the LFIA strip and all the reagents necessary per a complete analysis, in order to facilitate on-field applications.

Expected concentration (μg L^{-1})	CL-LFIA (μg L^{-1})	Recovery (%)	Expected concentration (μg L^{-1})	CL-LFIA (μg L^{-1})	Recovery (%)
(A) Maize flour extracts fortified with Fumonisin B1 and Aflatoxin B1			(B) Maize flour samples		
Fumonisin			**Fumonisin**		
166	148 (CV%=5)	89	470	480 (CV%=20)	102
18	15 (CV%=15)	83	80	87 (CV%=12)	109
2.0	2.3 (CV%=13)	115	10	12 (CV%=15)	120
Aflatoxin			**Aflatoxin**		
1.8	1.7 (CV%=19)	94	0.45	0.43 (CV%=10)	96
0.60	0.69 (CV%=12)	116	0.57	0.58 (CV%=10)	102
0.21	0.20 (CV%=14)	95	0.50	0.44 (CV%=15)	88

Table 2: Results obtained in the analysis of maize flour samples by CL–LFIA biosensor. (A) Fortified samples were produced by adding known amounts of fumonisin B1 and aflatoxin B1 to a blank maize sample extract. (B) Maize flour samples, previously analyzed by HPLC-UV and ELISA, were subjected to extraction and analyzed by CL–LFIA biosensor. CL–LFIA data are expressed as mean and CV% of three independent measurements.

References

[1] Dzantiev B.B., Byzova N.A., Urusov A.E., Zherdev A.V.; (2014) Trend Anal Chem; 55: 81-93

[2] Krska R., Schubert-Ullrich P., Molinelli A., Sulyok M., MacDonald S., Crews C.; (2008) Food Addit Contam; 25: 152-163

[3] Codex Alimentarius, (1991). Codex standard for durum wheat semolina and durum wheat flour 178-1991 (Rev. 1-1995). Rome: FAO/WHO

[4] International Agency for Research on Cancer, IARC, 1993, pp.301-366 IARC (1993) International Agency for Research in Cancer, Lyon, France. IARC 57:427–794

[5] Edite Bezerra da Rocha M., Freire F.daC.O., Erlan Feitosa Maia F., Izabel Florindo Guedes M., Rondina D.; (2014) Food Control; 36: 159-165

[6] Commission Regulation EC No 1881/2006 (2006) Off J Eur Union 364:5–24; Commission regulation (EC) No 1126/2007 (2007) Off J Eur Union 255:14–17

[7] Goryacheva Y., De Saeger S., Eremin S.A., Van Peteghem C.; (2007) Food Addit Contam; 24, 1169–1183

[8] Anfossi L., Baggiani C., Giovannoli C., D'Arco G., Giraudi G., (2013) Anal Bioanal Chem; 405: 467–480

[9] Krska R., Molinelli A.; (2009) Anal Bioanal Chem; 393: 67–71

[10] Mirasoli M., Buragina A., Dolci L.S., Simoni P., Anfossi L., Giraudi G., Roda A.; (2012) Biosens. Bioelectron; 32: 283– 287

[11] Roda A., Mirasoli M., Guardigli M., Michelini E., Simoni P., Magliulo M.; (2006) Anal Bioanal Chem, 384: 1269-1275

[12] Magliulo M., Mirasoli M., Simoni P., Lelli R., Portanti O., Roda A.; (2005) J Agric Food Chem; 53: 3300-3305.

[13] Mirasoli M., Guardigli M., Michelini E., Roda A., (2014) J Pharm Biomed Anal; 87: 36-52.

[14] Cho I.H., Paek E.H., Kim Y.K., Kim J.H., Paek S.H.; (2009) Anal. Chim. Acta; 632: 247–255

[15] Mirasoli M., Buragina A., Dolci L.S., Guardigli M., Simoni P., Montoya A., Maiolini E., Girotti S., A. Roda; (2012) Anal Chim Acta; 721: 167– 172

[16] Joung H-A., Oh Y.K., M-G. Kim, (2014) Biosens Bioelectron; 53: 330–335

[17] Ngom B., Guo Y., Wang X., Bi D.; (2010) Anal Bioanal Chem; 397: 1113–1135

[18] Wang Y., Yan Y., Ji W., Wang H., Li S., Zou Q., Sun J., (2013) J Agric Food Chem; 61: 5031-5036

[19] Lattanzio V.M.T., Nivarlet N., Lippolis V., Della Gatta S., Huet A.C., Delahaut P., Granier B., Visconti A.; (2012) Anal. Chim. Acta; 718: 99-108

[20] Li P., Zhang Z., Zhang Q., Zhang N., Zhang W., Ding X., Li R., (2012) Electrophoresis; 33: 2253–2265

[21] Njumbe Ediage E., Di Mavungu J.D., Goryacheva I.Y., Van Peteghem C., De Saeger S.; (2012) Anal Bioanal Chem; 403: 265–278

[22] Christensen H.R., Yu F.Y.,Chu F.S., (2000) J Agric Food Chem; 48: 1977-84

[23] Kolosova A.Y., Shim W.B., Yang Z.Y., Eremin S.A., Chung D.H., (2006) Anal Bioanal Chem; 384: 286-294

[24] Roda A., Mirasoli M., Dolci L.S., Buragina A., Bonvicini F., Simoni P., Guardigli M., (2011) Anal Chem; 83: 3178–3185

[25] Anfossi L., Calderara M., Baggiani C., Giovannoli C., Arletti E., Giraudi G., (2010) Anal Chim Acta; 682: 104–109

[26] Anfossi L., D'Arco G., Calderara M., Baggiani C., Giovannoli C., Giraudi G., (2011) Food Addit Contam Part A Chem Anal Control Expo Risk Assess; 28: 226-234

[27] Molinelli A., Grossalber K., Krska R., (2009) Anal Bioanal Chem; 395: 1309–1316

[28] Wang S., Quan Y., Lee N., Kennedy I.R., (2006) J Agric Food Chem; 54, 2491–2495

CHAPTER 6

A simple and compact smartphone accessory for quantitative chemiluminescence-based lateral flow immunoassay for salivary cortisol detection

---

Reproduced from: "A simple and compact smartphone accessory for quantitative chemiluminescence-based lateral flow immunoassay for salivary cortisol detection"
Martina Zangheri, Luca Cevenini, Laura Anfossi, Claudio Baggiani, Patrizia Simoni, Fabio Di Nardo, Aldo Roda
Biosensors and Bioelectronics, 2015, 64:63-68
Reproduced by permission of Springer (License number 3580670111372)

6.1 Introduction

The development of an accurate and user-friendly diagnostic device for "point-of-care" (POC) applications is one of the most challenging objectives in field of analytical chemistry. The requirements for POC devices are the portability, quickness, and easiness to use. Moreover in an integrated, self-standing device, they should be able to perform the entire analytical process, from sample pretreatment to measurement and data processing. Among the different analytical techiniques, the methods based on immunological reactions are suitable for this purpose because their high specificity and sensitivity makes it possible to detect clinical biomarkers even at low concentrations and in complex matrices. A suitable platform for immunological methods is the paper-based technology. Infact this devices are low cost and easy to handle, thanks to the use of capillary force for fluid transport and delivery without external power [1-6]. Of the paper-based analytical methods, lateral flow immunoassays (LFIAs), are one of the most commercially feasible analytical tools for rapid and portable clinical immunodiagnostics [2,7] such as diagnosing blood infections or contamination, drug abuse, or for ascertaining pregnancy [5].

Since LFIA was principally used for qualitative analysis, in recent years, this format has been combined with portable instruments that provide quantitative sensing based on the use of portable photometric strip readers to measure the lines' colour intensity [8-10] or by using alternative labels, such as enzymes [11], fluorescent nanoparticles [12-14],

electrochemical measurements [15,16], and more recently chemiluminescence detection of horseradish peroxidase (HRP) labelled reagents [17-21]. The use of CL detection is ideal for miniaturization and POC biosensor development because of its inherent sensitivity and simplicity. Organic photodiodes (OPDs) [22] and miniaturized hydrogenated amorphous Silicon photodiode array [23] and have been recently proposed as a versatile and low-cost technology that allow to develop miniaturized devices with high detectability and sensitivity. Another approach for CL detection is light imaging with a charge-coupled-device (CCD) or complementary metal-oxide semiconductor (CMOS) sensor, providing not only a measurement of emitted photons, but also the 2D image of the reaction chip [24] allowing spectral and spatial resolution. Nowadays, the sensitivity of the back side illuminated CMOS (BSI-CMOS) used in new generation of smartphone camera mean it can be used as a CL detector. Moreover, it is possible to exploit the connectivity and data processing offered by smartphones to perform analysis directly at the point of need with simple procedures. A system like this could eventually be used to monitor patient health and directly notify the physician of the analysis results in real time leading to a decrease costs and increase the healthcare availability and accessibility [25,26].

The use of smartphone for colorimetric LFIA method was recently reported [27,28] but until now, the use of CL detection and smartphone technology for LFIA methods has not been reported.

The aim of this work was to developed a portable analytical device that transforms a smartphone into a CL detector for quantitative LFIA analysis.

Using a low cost desktop 3D printer, we developed the analytical device that comprises a smartphone equipped with custom-designed accessories. The accessories are a cartridge that houses the LFIA membrane and a smartphone adaptor, containing a plano-convex lens aligned with the camera and a slot for inserting the cartridge. Once the operator has carried out the assay on the LFIA strip, both the smartphone and the cartridge are inserted into the assembled cradle to perform the measurement. A specific photography Application and the camera's autofocus system were used to obtain an high quality image of the sensing surface.

The performance of the system were evaluated by quantitative detection of salivary cortisol, which is considered a biomarker of stress, anxiety, and depression [29,30]. Since salivary levels of cortisol are very low in saliva matrix (at least a factor 10 with respect to plasma levels) [31], the developed assay must be highly sensitive and accurate. We optimized a competitive immunoassay, in which cortisol in saliva and horseradish peroxidise (HRP)-cortisol conjugate compete for anti-cortisol antibody immobilized on the nitrocellulose membrane. The HRP-cortisol bound to antibody will be detected using a chemiluminescent substrate based on luminol/H_2O_2 and enhancers.

6.2 Materials and methods

6.2.1 Reagents

The Supersignal ELISA Femto CL substrate for HRP was purchased from Thermo Fisher Scientific Inc. (Rockford, IL). Polyclonal anti-cortisol antibody produced in rabbit was purchased from Analytical Antibodies (Bologna, Italy). HRP-conjugate cortisol was obtained from Diametra (Milano, Italy). Cortisol standard solution, polyclonal anti-peroxidase (HRP) antibody produced in rabbit, bovine serum albumin (BSA), and Tween-20 were purchased from Sigma Aldrich (St. Louis, MO, USA). Salivettes cotton swabs for the saliva sampling were purchased from Sarstedt, Germany. The Silgard 184 polydimethylsiloxane prepolymer and the curing agent were obtained from Dow Corning (Midland, MI). The other reagents were of analytical grade and were used as received.

Assay strips for LFIA were prepared by immobilizing on nitrocellulose membranes the rabbit anti-cortisol antibody (T-line) and the rabbit anti-peroxidase antibody (C-line) keeping a distance of 5 mm between the two lines. The membranes were then assembled with a sample and an adsorbent pad and cut into sections.

6.2.2 Preparation of immunochromatographic test strip

Nitrocellulose membranes (Hi-flow plus 180 membrane cards from Merck Millipore, Billerica, MA) for LFIA strip were prepared employing a XYZ3050 platform (Biodot, Irvine, CA), equipped with two BioJet Quanti™ 3000 Line Dispenser for non-contact dispensing. In particular, from bottom to top of

the strip, the anti-cortisol antibody (1:50 v/v) and the anti-HRP antibody (1:500 v/v) diluted in PBS (20 mM phosphate buffer, pH 7.4), were dispensed to form the T-line and the C-line, respectively. Reagents were deposited at 1µL cm^{-1}, keeping a distance of 5 mm among the lines. Membranes were dried at 37°C for 60 minutes under vacuum, then the nitrocellulose surface was saturated with 1% BSA (w/v in PBS), washed with PBS supplemented with 0.05% of Tween 20, and finally dried at 37°C for 120 min under vacuum. Membranes were assembled with a glass fiber pad as the sample pad (Whatman Standard 14® from GE Healthcare Europe, Milan, Italy) and a cellulose pad as the adsorbent pad (Merck Millipore, Billerica, MA), with 1-2 mm of overlap between one and the other. Assembled membranes were cut into strips (5 mm width) by means of a CM4000 guillotine (Biodot, Irvine, CA) and stored in a desiccator at room temperature.

6.2.3 LFIA assay principle and format

It was developed an indirect competitive CL-LFIA assay. Cortisol in sample or standard solutions and HRP-cortisol conjugate migrate along the nitrocellulose membrane strip by capillarity. Upon the reaching the area corresponding to T-line, where the anti-cortisol antibody was immobilized, the cortisol in the sample compete with HRP-cortisol for binding a fixed and limited amount of immobilized anti-cortisol antibody. The unbound reagents HRP-cortsol conjugate are then captured by immobilized anti-HRP antibody (C-line). In the detection step, a CL substrate for HRP was

added to the strip and the resulting CL signal was imaged using the smartphone camera.

The intensity of the CL signal of the T-line is inversely related to the amount of cortisol and allowed to quantify the amount of cortisol in the sample. For quantitative analysis, the CL signal of the T-line was normalized with respect to that of the C-line of the same strip inorder to take into account environmental and matrix factors that might affect the intensity of the CL signal, such as changes in ambient temperature or the presence of HRP inhibitors in the sample. As with qualitative colorimetric LFIAs, the CL signal of the C-line was also used to assess the validity of the assay (i.e. an intense signal indicated the correct migration of the reactants along the strip).

6.2.4 Smartphone accessory

Smartphone adaptor and LFIA cartridge were made using the Makerbot Replicator 2X (Makerbot, Boston MA, USA). As printing material thermoplastic black and yellow acrylonitrile butadiene styrene (ABS) polymers were used. 3D models were created using the browser-based 3D design platform Tinkercad. The MakerWare slicer software was used to define printing options and settings. The smartphone accessories are showed in Figure 1. The smartphone adaptor was designed for the Samsung Galaxy SII Plus smartphone (Fig. 1c). It holds a plano-convex lens of 6mm diameter (Edmund Optics, York, UK) in contact with the phone objective and houses an LFIA cartridge (8 cm length, 2.5 cm width and 1cm thickness), preventing ambient light interference in the camera objective.

The LFIA cartridge (Fig. 1a) houses a nitrocellulose strip (Fig. 1b) and contains a 25 µl reservoir for HRP-cortisol conjugate solution, two separate 100 µl reservoirs for CL substrate and PBS, and an inlet for sample injection. The cartridge was printed in two separate pieces in order to insert the strip and reagents. A lid provides an optical window for signal acquisition and a grid allows evaporation of the absorbent pad.

The analytical performance of the smartphone camera was compared with that of a conventional laboratory ultrasensitive imaging instrument, the Night OWL LB 981 luminograph (Berthold Technologies GmbH & Co KG, Bad Wildbad, Germany) equipped with a conventional lens-based optics and a highly sensitive, back-illuminated, double-Peltier-cooled, black and white CCD camera previously developed in our laboratory [32,33], since this approach has not previously been used to acquire CL signals from LFIA membranes.

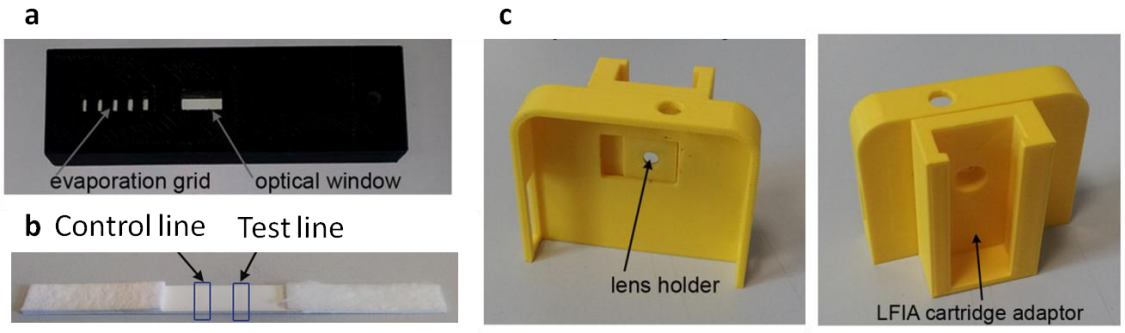

Figure 1: (a) 3D printed (ABS) cartridge, housing the LFIA strip; (b) LFIA nitrocellulose strip with control- (C-line) and test-lines (T-ine); (c) 3D printed smartphone accessory comprising a plano-convex lens holder and the LFIA cartridge adaptor.

6.2.5 Sample and spiked sample preparation

Saliva samples were collected from healthy volunteers at 8 AM before eating, while the saliva used for the calibration curves was collected at 9 PM, when cortisol concentration is usually lower due to circadian variation. To establish the calibration curves in saliva, several dilutions of cortisol were added to saliva to obtain the desired concentrations (between 0 and 100 ng/mL). The confirmatory analysis on real samples were performed using a commercial ELISA kit (Cortisol saliva ELISA, Diametra, Milan, Italy).

6.2.6 Assay procedure

Firstly saliva samples were collected by resting an adsorbent swab inside mouth until it was saturated (60-90 seconds) and then, the swab was placed into a syringe for immediate compression. A small volume of saliva sample (25μL) was transferred into a prefilled well, positioned near to the sample pad, through a PDMS-based injection septum. The syringe needle penetrated through the PDMS layer and the sample was mixed up with the prefilled solution of HRP-cortisol conjugate diluted 1:100 (v/v) in PBS containing BSA 6% and Tween 0.2%.

Upon the injection of the sample, the mixed solution reached the sample pad and it began to flow across the membrane where the immunoreactions take place. After the complete migration of the solution (15 min), a washing step was performed by flowing 50 μL of PBS for 10 min. Then, the strip was wetted by 100 μL of CL substrate, stored in a

reservoir placed near the nitrocellulose membrane. Finally the cartdtrige is inserted into the slot on the phone's cover (Fig. 2) and then the CL signals were acquired (10 seconds) using a professional camera application for mobile devices (Camera FV-5 Lite). To obtain quantitative information, a calibration curve was generated using cortisol standard solutions prepared in saliva matrix.

The elaboration of the signal was performed using Using ImageJ software v.1.46 (National Institutes of Health, Bethesda, MD). In particular, the mean photon emission intensity was measured in the areas corresponding to C-line and T-line of the LFIA strip. Each was subtracted from the mean background signal measured in adjacent areas. The T-line/C-line ratio was calculated for each concentration and then converted into B/B_0 ratio by dividing it for the T-line/C-line ratio measured in the absence of the target analyte (B_0, i.e. maximum T-line/C-line value). By plotting B/B_0 values against the log of analyte concentration calibration curves described by a four-parameter logistic function were obtained.

To obtain the analyte concentration in real samples, B/B_0 value was calculated as described above and interpolated on a stored calibration curve.

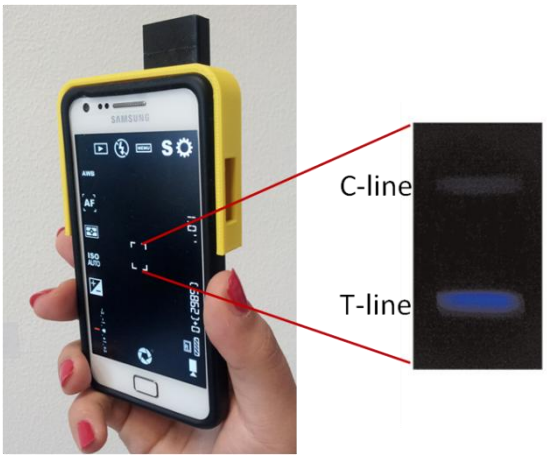

Figure 2: The integrated cortisol LFIA smartphone based device with running Camera FV-5 lite application for CL signal acquisition and the CL image of the sensing surface.

6.3Results and discussion

6.3.1 Smartphone camera detectability and resolution

To evaluate the imaging resolution and assess the possibility of accurately measuring the photon emission from a T-line on the strip without any significant interference from the adjacent C-line, the strips were imaged using both the reference LB-981 luminograph and the smartphone's camera (Fig.3) equipped with the developed mini darkbox accessory. It was observed that there is no significant crosstalk measuring the CL intensity of each line using smartphone camera. The performances showed by smartphne camera are comparable to those obtained using a bench-top luminograph. The peaks of the CL intensity profiles measured across the lines are resolved at the baseline, even in the case of a disproportion of CL intensity between the light intensities of the two adjacent lines. The detectability offered by smartphone camera is only one

decade less compared with those obtained using the CCD camera or organic photodiodes [22]. It is important to point out the fact tat the CCD, differently from the smartphone camera, is cooled at -40 °C and presents larger pixel size. Anyway the detectability offered by BSI-CMOS smartphone camera is adequate for measuring the light signal from the LFIA strip at the relevant cortisol concentration. New generation of smartphones is based on colour BSI-CMOS that is much more sensitive than previous front-illuminated sensors, with an increase of the amount of captured light from about 60% to over 90% (Swain and Cheskis, 2008), making it possible to improve low-light imaging performance. Moreover, the smartphone could be used as an integrated platform that allows to acquire and also to process the signal together with the possibility of direct connectivity (bluetooth, wifi) for data managing and sharing.

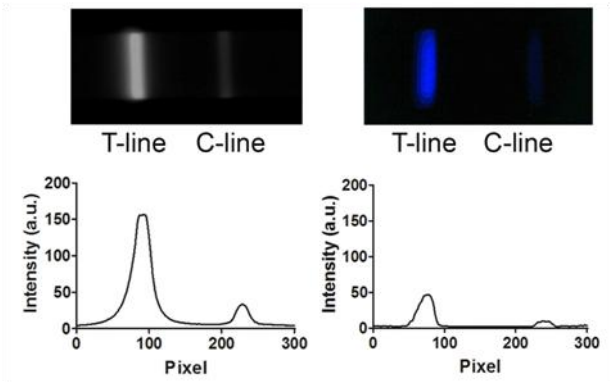

Figure 3: Comparison of CL images acquired with a Berthold Nigh Owl luminograph (left) or the smartphone camera (right). The insensity profile and image resolution of the two instrumentation are presented.

6.3.2 Concentration of immunoreagents

In order to generate an assay with a detection limit and dynamic range suitable for measuring cortisol in the relevant physiological range in saliva samples, concentration of HRP-cortisol conjugate was optimized. For preventing the interferences between CL signals of C-line and T-line, they must have similar signals in order to use a single integration time to be simultaneously measured. For the optimization of HRP-cortisol conjugate concentration, blank samples and samples containing 1 and 10 ng/ml were assayed in presence of different dilutions of HRP-cortisol conjugate. As shown in Fig. 4 a decrease in the concentration of the HRP-cortisol conjugate employed in the assay in the range between 1:50 and 1:1000 (v/v) caused a decrease in the CL emission of the T-line. This was associated to an increase in the ability of cortisol to displace the HRP-cortisol conjugate from the immobilized anti-cortisol antibody, as shown by a decrease in the ratio T-line/C-line obtained in the presence and in the absence of cortisol in the sample. An higher dilution of the HRP-cortisol conjugate results in a significant decrease in the CL signal for the concentration of 10 ng/mL cortisol, shortening the dynamic range and making not possible to quantify higher cortisol levels. The dilution that provides the best compromise between these effects was 1:100 v/v.

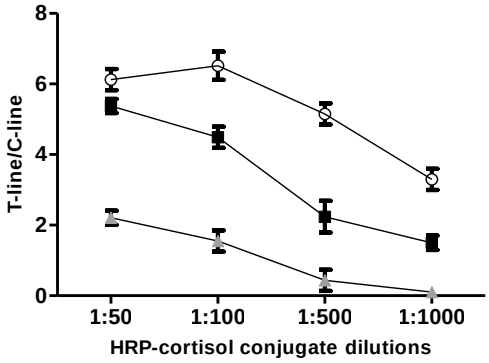

Figure 4: Chemiluminescence signals obtained employing different dilutions of HRP-cortisol conjugate. Assays were performed in the absence of cortisol (white symbols) or in the presence of cortisol 1 ng/mL (black symbols) and 10 ng/mL (grey symbols).

6.3.3 Chemiluminescent signal kinetics

The kinetics of the HRP-catalyzed CL emission in the presence of luminol-based substrates containing suitable enhancers reaches a steady state CL intensity in a short time [34,35]. Since the migration along the whole LFIA membrane requires 15 minutes, it might result in partial inactivation of HRP, especially in the presence of intense CL signals. In order to overcome this problem, the CL substrate was applied directly to the nitrocellulose membrane, avoiding excessively long migration times along the whole strip. To estabilish the suitable integration time, measurement of the CL signals at different integration times (from 2 to 20s) were performed, founding that 10 s was sufficient to achieve the maximum CL signal, thus this time was used for the analysis. Infact, using an integration time lower than 10 s, the intensity of the CL signal decreases considerably, while a higher integration time does not significantly enhance the intensity of the

signal itself. Upon the achievement of the steady state it lasts for about 1 min, confirming that an excess of substrate was present on the LFIA membrane and ensuring that the CL signal intensity was proportional to the enzyme amount. The kinetic of the CL signal is reported in Fig. 5.

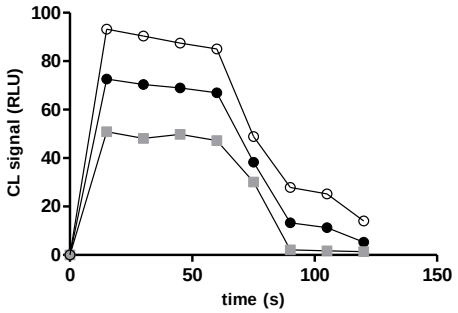

Figure 5: Kinetics of the chemiluminescence signals obtained in correspondence of the T-line obtained in the absence of cortisol (white symbols) and in the presence of cortisol 1 ng/mL (black symbols) and 10 ng/mL (grey symbols).

6.3.4 Calibration curve

Using cortisol standard solutions in the range of 0.5 - 100 ng/mL, calibration curves were generated. Calibration curves were generated by adding known amounts of cortisol standard solutions to saliva cortisol free (Fig.6a) and also to PBS in order to evaluate the matrix effect. The comparison between the calibration curves is reported in Fig. 6b. Since we exploited a competitive type format, the decrease of the T-line/C-line ratio was directly proportional to the amount of the analyte in the sample. Repeating calibration curves several times, it was demonstrated a good reproducibility with an average of the relative standard deviation

associated with each point of the calibration curve of 10% in buffer and 16% in saliva matrix. The limit of detection (LOD) was estimated as the concentration corresponding to the blank T-line/C-line value minus three times its standard deviation. The LOD values were 0.3 ng/mL in saliva matrix and 0.1 ng/mL in buffer while the dynamic ranges of the method extended from 0.3 to 60 ng/mL for saliva and from 0.1 to 60 ng/mL in PBS. Even if the LOD value was slightly influenced by matrix effect, the dynamic range obtained in saliva was still adequate for evaluating cortisol concentrations in human saliva in both normal and pathological conditions.

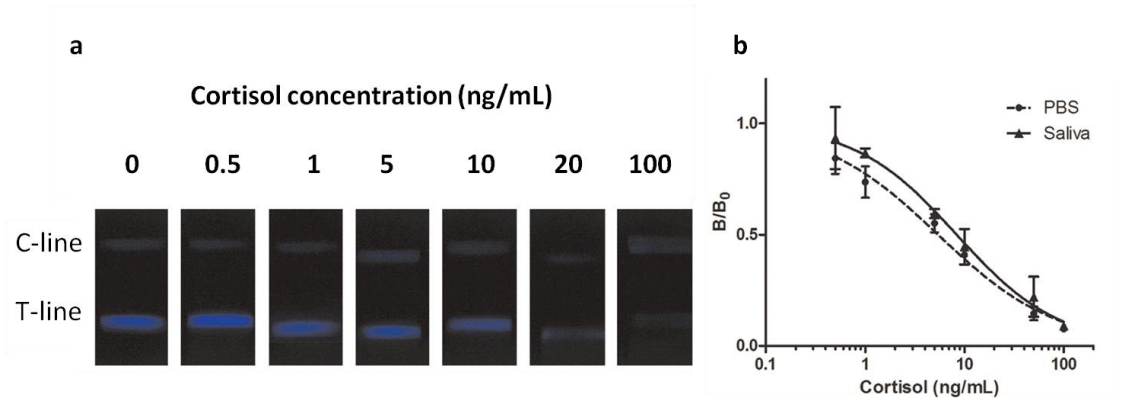

Figure 6: (a) CL images acquired with the smartphone at increasing concentrations of cortisol. (b) Calibration curves for cortisol obtained in phosphate buffer and in saliva using the smartphone camera. Images were elaborated with imageJ software to quantify the CL signal of the C- and T-line and plotted as described in material and methods section.

6.3.5 Determination of cortisol in real samples

Saliva samples belonging to 11 subjects were analysed, to further confirm the accuracy of the proposed method. The calibration curve obtained for

the saliva matrix described by a nonlinear four-parameter logistic calibration plot was used for interpolation in order to evaluate the concentration of cortisol in real saliva samples. The analysis for each sample was repeated four times and the results were compared with those obtained using a confirmatory method (Fig. 7a). In Fig. 7b are reported chemiluminescence images of LFIA membranes used for analyses of salva samples. It was found a good agreement between CL-LFIA and commercial ELISA kit results for all samples. Recovery values were in the range from 88% to 116%, and a coefficient of variation below 20% was obtained, proving the practical applicability and reliability of the proposed CL-LFIA for quantitative determination of cortisol in saliva samples.

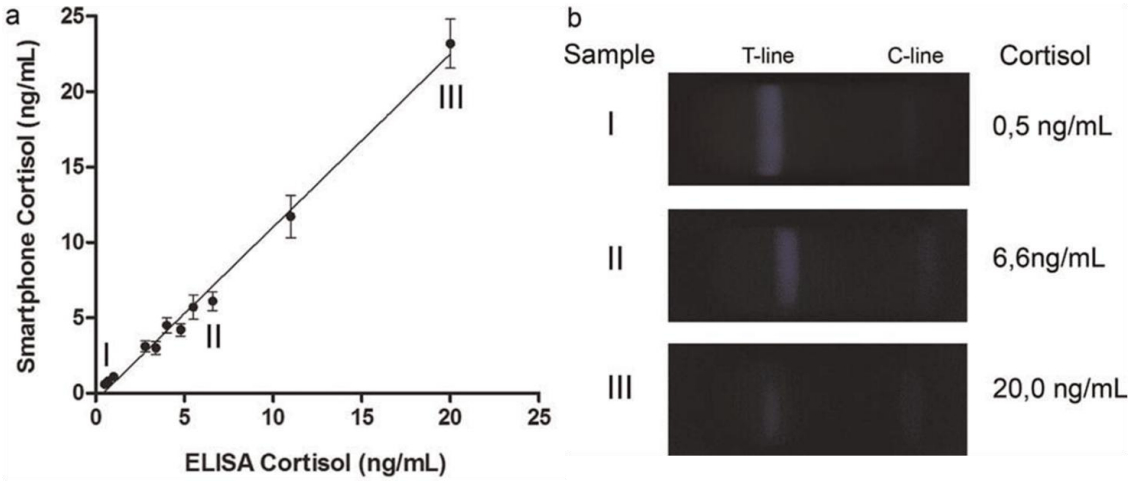

Figure 7: a) Correlation between cortisol concentrations in saliva samples, obtained with commercial ELISA kit and the smartphone CL-LFIA device. b) CL images of saliva samples from healthy patients at low (I), medium (II) and high (III) cortisol concentration.

6.4 Conclusion

We have developed and optimized a simple and sensitive device, which uses ready-to-use analytical cartridges and a smartphone as a CL imaging system to quantify human cortisol level in saliva. We exploited 3D printing technology to design and realize accessories that were easily inserted into the smartphone and could be adapted for any kind of mobile platforms such as smartphone or tablet.

The use of CL as a detection principle allows to work with simple accessories, that compose a mini dark box to prevent interference from ambient light, equipped with a small lens aligned with the smartphone camera to focus the CL emission from the LFIA strip. Moreover, CL detection allows to obtain high sensitivity making it possible to detect and quantify cortisol in real saliva samples in the relevant physiological range. The method is simple, rapid (total analysis time 30 min) and could be performed by unskilled personnel. In addition, the device enabled a point-of-need analysis approach (i.e. the analysis can be performed directly at home), reducing response time and analysis cost. This smartphone-based salivary cortisol testing device, could be valuable to assess patient stress level as well as other pathology such as depression. This device could thus pave the way for a new generation of analytical devices in the clinical diagnostic field.

References

[1] Ballerini D.R., Li X., Shen W.; (2012) Microfluid Nanofluid; 13: 769-787

[2] Li C.Z., Vandenberg K., Prabhulkar S., Zhu X., Schneper L., Methee K., Rosser C.J., Almeid E.; (2011) Biosens Bioelectron; 26:4342-4348

[3] Martinez A.W., Phillips S.T., Carrilho E., Thomas S.W., Sindi H., Whitesides G.M., (2008); Anal Chem; 80, 3699-3707

[4] Martinez A.W., Phillips S.T., Whitesides G.M., Carrilho E.; (2010) Anal Chem; 82: 3-10

[5] Posthuma-Trumpie G.A., Korf J., Van Amerongen A.; (2009) Anal Bioanal Chem; 393: 569-582

[6] Zhao W., Van der Berg A.; (2008) Lab Chip; 8: 1988-1991

[7] Qin Z., Chan W.C., Boulware D.R., Akkin T., Butler E.K., Bischof J.C.; (2012) Angew Chem; 51: 4358-4361

[8] Anfossi L., Calderara M., Baggiani, C. Giovannoli, C. Arletti, E. Giraudi G.; (2010) Anal Chim Acta; 682: 104-109

[9] Molinelli A., Grossalber K., Krska R.; (2009) Anal Bioanal Chem; 395: 1309-1316

[10] Salter R., Douglas D., Tess M., Markovsky B., Saul S.J.; (2006) J Aoac Int; 89: 1327-1334

[11] Cho J.H., Han S.M., Paek E.H., Cho I.H., Paek S.H.; (2006) Anal Chem; 78: 793-800

[12] Li Z., Wang Y., Wang J., Tang Z., Pounds J.G., Lin Y.; (2010) Anal Chem, 82:7008–7014

[13] Xia X.H., Xu Y., Zhao X.L., Li Q.G.; (2009) Clin Chem; 55: 179–182

[14] Zou Z.X., Du D., Wang J., Smith J.N., Timchalk C., Li Y.Q., Lin Y.H.; (2010) Anal Chem; 82: 5125–5133

[15] Fernandez-Sanchez C., McNeil C.J., Rawson K., Nilsson O.; (2004) Anal Chem; 76: 5649–5656

[16] Muhammad-Tahir Z., Alocilja E.C.; (2003) Biosens Bioelectron; 18: 813–819

[17] Mirasoli M., Buragina A., Dolci L.S., Simoni, P. Anfossi, L. Giraudi G., Roda A.; (2012) Biosens Bioelectron, 32: 283– 287.

[18] Mirasoli M., Buragina A., Dolci L.S., Guardigli M., Simoni P., Montoya A., Maiolini E., Girotti S., Roda A.; (2012) Anal Chim Acta; 721: 167– 172

[19] Roda A., Guardigli M., Michelini, E. Mirasoli, M. Pasini P.; (2003) Anal Chem; 75:463A–470A

[20] Wang X., Hofmann O., Das R., Barrett E.M., De Mello A.J., De Mello J.C., Bradley D.D.C.; (2007) Lab Chip; 7: 58–6

[21] Zangher..

[22] Pires N.M.M., Dong T.; (2014) Biomed Mat Eng; 24: 15-20

[23] Caputo D., De Cesare G., Dolci L.S., Mirasoli M., Nascetti A., Roda A., Scipinotti R.; (2013) IEEE Sensors J; 14: 2595-2601

[24] Roda A., Mirasoli M., Dolci L.S., Buragina A., Bonvicini F., Simoni P., Guardigli M.; (2011) Anal Chem; 83: 3178–3185

[25] Ozdalga E., Ozdalga A., Ahuja N.; (2012) J Med Internet Res; 27: 14:e128

[26] Zhu H., Isikman S. O., Mudanyali O., Greenbaum A., Ozcan A.; (2012) Lab Chip; 13: 51–67

[27] Mudanyaly O., Dimitrov S., Sikora U., Padmanabhan S., Navruz I., Ozcan A.; (2012) Lab Chip; 12: 2678–2686

[28] Sangdae L., Giyoung K., Jihea M.; (2013) Sensors; 13: 5109-5116

[29] Hellhammer D.H., Wüst S., Kudielka B.M.; (2009) Psychoneuroendocrino; 34: 163–171

[30] Tlili C., Myung N.V., Shetty V., Mulchandani A.; (2011) Biosens Bioelectron; 26: 4382–4386

[31] Roda A., Girotti S., Lodi S., Preti S.; (1984) Talanta; 31: 895-900

[32] Roda A., Pasini P., Musiani M., Girotti S., Baraldini M., Carrea G., Suozzi A.; (1996) Anal Chem; 68: 1073–1080

[33] Roda A., Mirasoli M., Venturoli S., Cricca M., Bonvicini F., Baraldini M., Pasini P., Zerbini M., Musiani M.; (2002) Clin Chem; 48: 1654–1660

[34] Marzocchi E., Grilli S., Della Ciana L., Prodi L., Mirasoli M., Roda A., (2008) Anal Biochem; 377: 189–194

[35] Kricka L.J., Voyta J.C., Broinstein I.; (2000) Methods Enzymol; 305: 370-390

CHAPTER 7

Multiwell cartridge with integrated array of amorphous silicon photosensors for chemiluminescence detection: development, characterization and comparison with cooled-CCD luminograph

---

Reproduced from: "Multiwell cartridge with integrated array of amorphous silicon photosensors for chemiluminescence detection: development, characterization and comparison with cooled-CCD luminograph"
Mara Mirasoli, Augusto Nascetti, Domenico Caputo, Martina Zangheri, Riccardo Scipinotti, Luca Cevenini, Giampiero de Cesare, Aldo Roda
Analytical and Bioanalytical Chemistry, 2014, 406:5645–5656
Reproduced by permission of Springer (License number 3580690805264)

7.1 Introduction

Lab-on-chip (LOC) devices have recently found progress in the fields of life sciences and microtechnology. This devices are characterized by the ability of performing analysis of small amounts of sample, employing portable and miniaturized analytical instrumentation [1]. However currently there are just few LOC devices commercially available and they often require the use of laboratory equipment for their operation. Thus the objective of the research in this field is directed towards the fully integration of all the necessary components into a single analysis tool in order to produce a true LOC system [2-5].

Bioluminescence (BL) and chemiluminescence (CL), are very suitable for the development of LOC system, offering high detectability even in small volumes (due to the very low background) and large dynamic range of the signal [6-9]. Moreover equipment required for signal detection is rather simple, with no necessity for excitation light sources, focusing optics, wavelengths selectors, and specific geometry of the measurement cell [9-10]. However, BL and CL usually require highly sensitive detectors, such as cooled CCDs or photomultiplier tubes [11] since the light level emissioni s very low and in most cases integrated detectors did not offer suitable detectability. In the previous chapter devices based on a cooled charge-coupled-device (CCD) exploiting a lensless contact imaging approach were reported. This detection system, coupled with a microfluidic module, allow to perfrom multiplex CL bioanalytical assays achieving high detectability that is comparable with those obtained with reference

laboratory instrumentation [12-14]. However, although the portability and compactness, the detector requires power consumption that is not compatible with the developmet of a real LOC system. An interesting alternative for simultaneous detection of different parallel reactions, is amorphous silicon (a-Si:H) and its alloys. They are characterized by low deposition temperature (<250 °C), that is compatible with a wide range of support materials, and moreover thanks to the use of microelectronics technologies, a-Si:H a good candidate for application in microfluidic devices [15]. In addition, the a-Si:H physical characteristics make the use of this material suitable for different devices, such as electronic switching [16], solar cells [17], physical [18] and optical sensors. In particular, a-Si:H photosensors provide very low dark currents and a high quantum efficiency in the wavelength range from ultraviolet [19] to near infrared [20-21]. Thin-film a-Si:H photosensors has been already used [22], for measuring the optical absorbance in the UV range [23], fluorescence [24,25], or CL signals[26-28]. In this work we proposed a a LOC system with integrated photosensors and applied it to two different "model" bioassays in order to state the suitability of a-Si:H photodiodes as ultrasensitive detection devices for LOC systems. The system is composed by an array of 16 a-Si:H photodiodes deposited on a glass substrate (Fig. 1a) and a PDMS unit containing 16 wells that was placed directly in contact with the photosensor in order to obtain an integrated microcartridge (Fig. 1b). In this way the CL signal is generated and measured in close proximity, providing efficient photon transfer between the sample-well and the photosensors and a miniaturization of the

system. A custom portable readout electronic board was employed. The devices performances were first characterized in terms of sensitivity, noise and detectability with different CL and BL systems, comparing the analytical performances with reference laboratory instrumentation. Finally, the device functionality was successfully tested on two model bioanalytical BL (cell toxicity assay) and CL (total antioxidant capacity measurements) assays.

7.2 Materials and methods

7.2.1 Reagents

Alkaline phosphatase (ALP) from bovine intestinal mucosa, horseradish peroxidase (HRP) type VI-A and activated charcoal and ascorbic acid were purchased from Sigma-Aldrich (St. Louis, MO). Firefly luciferase (Luc) stock solution (5 mg mL^{-1}) was purchased from the ATP Determination Kit (Molecular Probes). The Lumiphos Plus CL cocktail for ALP was from Lumigen (Southfield,MI) and the Super Signal ELISA Femto CL cocktail for HRP was purchased from Thermo Fisher Scientific (Rockford, IL). Polydimethylsiloxane (PDMS) Silgard 184 pre-polymer and curing agent were from Dow Corning (Midland, MI). The BL cocktail for Luc measurements was Britelite plus (PerkinElmer Inc., Waltham, MA). In all the microelectronic processes, water for last rinsing was purified with a Milli-Q Plus (Millipore, R=18.2 MΩ·cm) ultra-pure water system. All solutions were prepared in 0.1 M phosphate buffered saline (PBS) pH 7.7 employing Milli-Q Plus ultra-pure water. Materials for photolithography process (photoresist AZ- 1518, developer AZ351B remover AZ100 and

etchants for metals) were purchased from Sigma-Aldrich, while SU-8 2005 photoresist, its developer and its remover were purchased from Micro Resist Technology GmbH (Germany).

7.2.2 Instrumentation

As a reference instrumentation The Night Owl LB 981 (Berthold Technologies, Bad Wildbad, Germany) was employed. To reduce the background noise, the system is equipped with a 512×512-pixel back-illuminated slow-scan CCD sensor, thermoelectrically cooled to −50 °C. For image acquisition and processing The Winlight 1.2 (Berthold Technologies) software was used. All images were acquired employing a 4-s integration time. Varian Eclipse spectrofluorimeter (Varian Inc., Palo Alto, CA) was used for recording chemiluminescence and bioluminescence spectra.

7.2.3 Photosensor array fabrication

The photosensors are p-doped/intrinsic/n-type stacked structure deposited on a glass substrate covered with an indium tin oxide (ITO) layer that acts both as transparent window layer for the BL and CL signal and as electrical bottom contact for the a-Si:H diodes. Metal films deposited on the a-Si:H layers behave both as photosensor top electrode and electrical contact lines. Amorphous silicon layers were deposited by a three UHV chambers plasma- enhanced chemical vapor deposition (PECVD) system (from Glasstech Solar Inc.), metal film were deposited by a BALZERS 510 vacuum evaporation system while ITO layer was grown by a magnetron

sputtering system from Materials Research Corporation (Orangeburg, NY, USA).

The fabrication of the photosensor array was performer through the following steps:

1. Deposition of 150-nm-thick ITO by magnetron sputtering and its pattering by wet etching (solution of H_2O_2:HCl=1:3) for definition of the bottom electrode;

2. Deposition by PECVD of the three a-Si:H layers. The deposited thicknesses were 10, 400 and 50 nm for the ptype, intrinsic and n-type material, respectively;

3. Deposition by magnetron sputtering of a three metal layer stack (30 nm-thick Cr/150 nm-thick Al/30 nm-thick Cr) acting as back electrode of the sensors;

4. Mesa patterning of the device structure by wet and reactive ion etching for the metal stack and a-Si:H layers respectively (the area of each photodiode is 2×2 mm^2);

5. Deposition of a 5 μm-thick SU-8 layer acting as insulation layer between the back metal and the front TCO contacts;

6. Opening of via holes over the diodes on the passivation layer;

7. Sputtering of a 100 nm-thick TiW metal layer over the passivation layer;

8. Patterning of the TiW external contacts for the definition of the back contact and the external connection of the photodiodes.

The photolithographic processes were performed using a TAMARACK 152R mask-aligner for mask reproduction, a Reactive Ion Etching system (from IONVAC PROCESS, Italy) for dry etching of amorphous silicon films

and a chemical bench for wet etching of metal films. All the microelectronic processes have been performed in a clean room. After fabrication, the photodiodes have been individually tested to evaluate their electrical and electro-optical characteristics. The photosensor current-voltage characteristics were evaluated using a Keithley 236 Source Measure Unit (SMU), while the sensor responsivity was measured by using a quantum efficiency setup, which includes a tungsten light source, a monochromator (model Spex 340E from Jobin- Yvon), a UV-enhanced crystalline silicon diode (model DR 2550-2BNC from Hamamatsu) used as reference, a beamsplitter and focusing optics (from Melles-Griot). For the characterization of the sensor array as a whole and for the subsequent experimental part, portable custom readout electronics has been used for the simultaneous measurement of the current of the 16 photodiodes [29]. The a-Si:H photosensor array was connected to the custom readout electronic board using a flex connector. The low-noise readout electronics is based on eight ACF2101 dual-channel charge sensitive preamplifiers from Texas Instruments that integrate the sensor current providing a proportional output voltage that is converted to digital by a MAX180 12-bit analog to digital converter fromMaxim. The sensor bias is sourced by a 12-bit digital to analog converter whose output has been buffered with a AD8510 operational amplifier to ensure correct driving of the large capacitive load represented by the 16 photodiodes in parallel. The entire front-end board is controlled by a TUSB3210 microcontroller that also provides the USB link to an external computer where a graphical user

interface allows to easily operate the entire system from acquisition setup to data storage.

7.2.4 Microwell cartridges fabrication

Coupling a 10-mm-thick black PDMS unit comprising an array of 16 through holes with the glass support where the 16-photosensor array had been deposited a disposable 16-well cartridges with integrated photosensors was obtained. Activated charcoal (3 %, w/w) was added to a mix of pre-polymer and curing (at a 10:1 ratio(w/w)) in order to obtain black PDMS mixture, which was vacuum treated for 15 min to remove air bubbles. Then it was casted in a mold containing 16 pillars (2×2 mm) in positions corresponding to the photosensors in the array. The polymerization took 16 h at room temperature and then the structured PDMS was peeled off from the mold and coupled with the glass substrate aligning the wells with photosensors and exploiting the sticky nature of partially cured PDMS, as previously reported [28].

7.2.5 Chemiluminescence measurements

The chip of photosensors was placed inside the CCD-based Night Owl LB 981 luminograph light-shielded box to ensure dark conditions during the experiments and to acquire luminescent signals simultaneously with the two instruments. A picture of the measurement setup is reported in Fig. 1c. The performances of photosensors in providing quantitative measurement of the emitted photons down to low light levels was

evaluated by generating the calibration curve in a concentration range significant for each specific enzyme.

The background signal was measured for both detection systems in absence of luminescent solutions at the beginning of each experiment. For each measurement 2 µL of enzyme solution (HRP, ALP, or Luc) at different concentrations (buffer for the blank) and 8 µL of the respective luminescent cocktail were dispensed in the wells. To ensure that the signal measured by the photosensors was not affected by a memory effect due to exposure to ambient light [30], the measurements of the luminescence signals were performed with a delay of 20 s after the closure of the dark box. Consecutive acquisitions of the same integration time for both luminograph and photosensors simultaneously enable a comparison of analytical performance of the two devices.

The integration time used for each acquisition was 4 s for images acquired with the CCD (with a frame rate of one image every 15s as a trade-off between time resolution of process monitoring and data-storage requirements) and 3.98 s for the photosensors (enabling a measurement of photocurrent every 4 s). The calibration curve was generated by plotting plateau values of photocurrent measured during the entire luminescent reaction kinetics averaged over three independent measurements against enzyme concentration.

The limits of detection (LOD) were calculated as the enzyme concentration whose signal corresponds to three times the standard deviation of the blank signal, which is the signal measured in the absence of the enzyme. Such standard deviation accounts for electronic noise, photodiodes shot

noise, as well as the variation of the low autoluminescence of the CL cocktail.

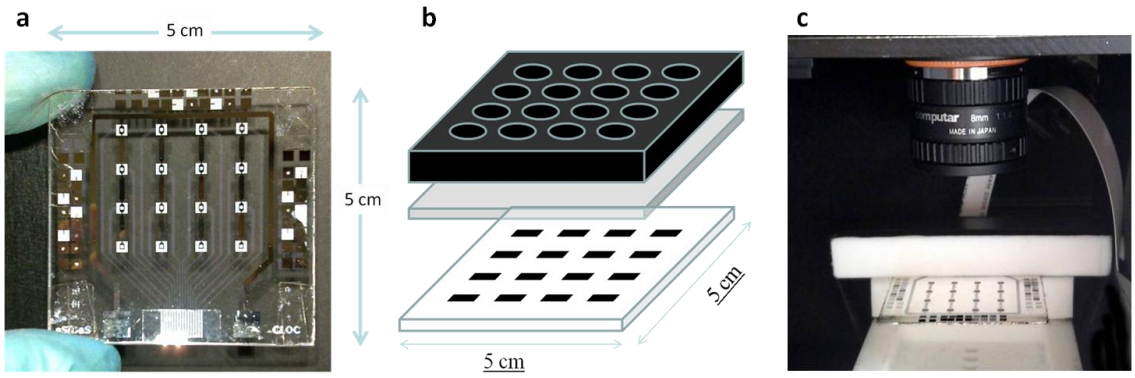

Figure 1: (a) View of photosensors array; (b) Schematic overview of the 16-well microcartridge with integrated a-Si:H photosensors ; (c) Measurment setup for comparison between photosensors array and CCD camera.

7.2.6 Cytotoxicity test

A volume of 100 µL of human embryonic kidney cells (HEK293) genetically modified to stably express Luc (6,000 cells suspended in liquid culture medium) was incubated with 100 µL of dimethyl sulfoxide (DMSO) at different concentrations (in the range 2–50 %, v/v in culturemedium, only culture medium for the blank) for 90 min at 37 °C. Then, 20 µL of the mixture were transferred in the PDMS cartridge wells andphotons emission was acquired as reported above (4 s consecutive acquisitions for a total of 10 min) after the addition of 20 µL of BL cocktail.

7.2.7 Total antioxidant activity measurements

Ten microliters of ascorbic acid solutions (between 0 and 50 µM, only buffer for the blank) was dispensed into each well of the PDMS microcartridge in duplicate, then 20 µL of Super Signal ELISA Femto CL cocktail containing the enzyme HRP (4 pg μL^{-1}) was added. In parallel, 10 µL of two red grape must extract samples (one ethanol extract and one aqueous extract) were assayed in triplicate, upon dilution with water (1:500 and 1:100, v/v, respectively). Photons emissions were acquired at 4-s frame rate for a total of 10 min in order to assess the kinetics of CL emission.

7.3 Results and discussion

A disposable microcartridges for BL and CL-based bioassays integrating arrayed a-Si:H photosensors was proposed. Custom portable readout electronics has been used for the simultaneous measurement of the currents of the 16 photodiodes in order to enable out-of-laboratory applications. Custom readout electronics design and sensors architecture have been optimized for reaching the required detectability and ensuring adequate reproducibility of response between sensors in the array. The PDMS unit was coupled with a-Si:H photosensors to obtain disposable cartridges containing 16 black wells with clear bottom (40 µL each) in which chemical reactions are performed in close proximity to the sensors, fabricated on the opposite glass substrate side to avoid issues of chemical compatibility.

Electrical and electro-optical characteristics of photodiodes were first tested. Then, the analytical performance of the arrayed a-Si:H photosensors in the measurement of BL and CL emissions was evaluate and compared with reference cooled slow-scan CCD-based imaging instrumentation.

Finally, model luminescent bioassays, namely a BL based cytotoxicity assay and a CL enzyme-based assay for total antioxidant capacity measurement, were used to test their ability to provide real-time measurement of evolving BL and CL reactions.

7.3.1 Photosensor characterization

In order to determine the dark current noise in the operation condition and the sensor sensitivity at the different wavelengths, measure of the current-voltage (I-V) curve in dark condition and the spectral response in the visible range were performed (Fig. 2). Fig. 2a reports the average I-V characteristics of three different diodes of the array, measured in dark conditions. A value of the dark current in the order of 10−10A cm^{-2} in reverse bias conditions was found for all the photodiodes. The root-meansquared (rms) dark current noise was calculated to be around 1.6 fA, taking into account that the photosensor area is 4 mm^2 and that the measurements have been taken with a signal bandwidth of 1 Hz. This value is below the experimental noise introduced by the experimental characterization setup that is around 10 fA. In Fig. 2b are reported quantum efficiency curves averaged over three different photosensors of the array and it was found a good uniformity of response over the array.

In order to enable the use of different BL and CL reactions with the same device, the thickness and doping of the different a-Si:H layers have been designed in order to achieve a wide spectral response. The firefly Luc-luciferin ATP Mg^{2+} BL reaction has a maximum emission at 565 nm. The CL reaction catalyzed by ALP in the presence of Lumiphos Plus cocktail displays a maximum emission at 470 nm while the luminol/ peroxide/enhancer CL reaction catalyzed by HRP has a maximum emission at 425 nm. A comparison of the normalized spectra of the three luminescent reactions are reported in Fig.2b. It was observed that all the considered luminescence emission spectra match reasonably well with the response of the photodiodes, considering the range from violet-blue to yellow-greenish light. It is also possible to extend applications also to red-shifted BL and CL reactions and to tune spectral response for other specific wavelengths of interest by proper sensor design. The photosensor responsivity at the emission wavelength of the investigated molecules can be derived, according to the QY curve.

Since the responsivity (R) can be described as :

$R(\lambda)= QY(\lambda)\ \lambda/1,240(nm)$

we deduct that the photosensor responsivity is equal to 140, 235 and 320 mAW^{-1} for the luminescent reactions catalyzed by HRP, ALP and Luc, respectively.

Comparing the main characteristics of our photosensor with other optical detectors integrated in microfluidic chip in terms of responsivity, dark level,size and noise level of devices based on both organic and inorganic materials, it is possible to find out that the performances of our

photosensor are within those of the other proposed systems. Our device demostrates a lower responsivity at 425 nm with respect to that reported by Pereira et al. [31], but it presents lower dark current and better noise performances. The graphene-based photosensor shows very high responsivity, due to its internal gain, but it also present a much higher dark current, higher thermal budget and more complex fabrication process [32]. Finally photodetectors based on organic materials present good performances in terms of both responsivity and dark current levels, but their fabrication and technology processes are not completely assessed [33,34].

In the next sections the characteristics of the proposed system are discussed in detail in order to evidence its suitability for lab-on-chip analysis requirements, since its analytical performances are very close to that of cooled backilluminated CCD-based reference instrumentation.

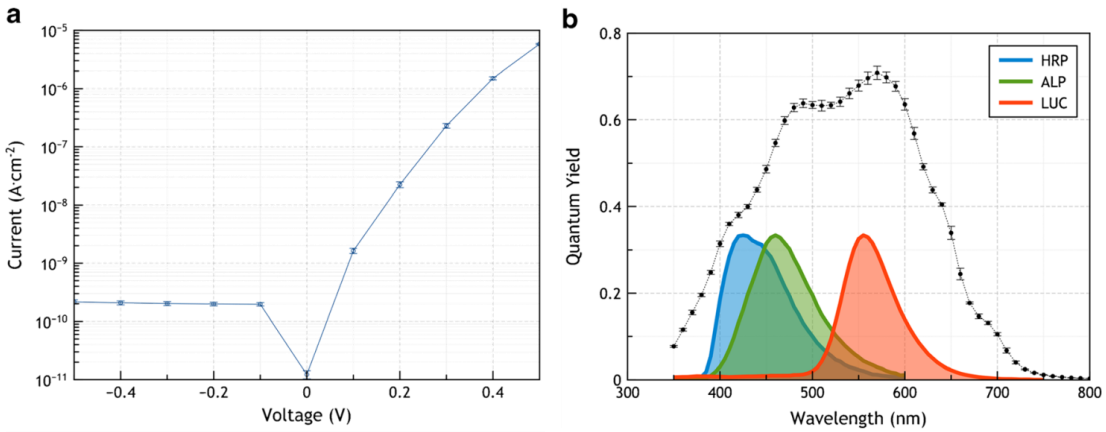

Figure 2: Characteristics measured for three diodes of the a-Si:H array: (a) current-voltage curves; (b) normalized quantum efficiency curve. The maximum of the quantum efficiency curve, occurring at 580 nm, is equal to 0.72. In the same graph, the emission spectra of the luminescent reactions studied in this work are shown: each spectrum is normalized to its maximum emission value

7.3.2 Bio- and chemiluminescence measurements

Three luminescent systems that are widely used in bioanalytical applications were used for evaluating performances of the photosensors. The luminescent systems are CL reactions catalyzed by HRP or ALP enzymes (widely used in enzyme-based assays and binding assays as gene probe hybridization and immunoassays), and the BL reaction catalyzed by firefly Luc (employed as a reporter gene in recombinant cell-based biosensors). A summary of the obtained results is showed in Table 1. When the enzyme is employed as a label, the enzymatic substrate is added in excess to obtain light emission proportional to enzyme amount and, in the chimical luminescence reactions, light detected is a transient product of the reaction that is only present while the reaction between enzyme and enzymatic substrate is occurring.

By measuring light emission in parallel with the a-Si:H photosensors and the CCD-based luminograph we generated calibration curves for each enzyme. It has to be considered that the a-Si:H photosensors were employed at room temperature (about 25 °C) in view of their use in a on-the-field application as well as to avoid cooling down of biological reactions that occur on the opposite side of the same glass substrate, which would largely affect their kinetics, while the CCD sensor was thermoelectrically cooled down to −10 °C, which decreases the background signal (both in terms of absolute value and instrumental noise) due to the thermal generation of electrons.

	a-Si:H photosensors array	CCD-based luminograph
Alkaline phosphatase		
R^2 value	0.998	0.997
Sensitivity	0.012 pA $pmol^{-1}$ L	29 RLU $pmol^{-1}$ L
LOD	30 pmol L^{-1}	19 pmol L^{-1}
Firefly Luciferase		
R^2 value	0.999	0.998
Sensitivity	0.0067 pA $pmol^{-1}$ L	30 RLU $pmol^{-1}$ L
LOD	500 pmol L^{-1}	160 pmol L^{-1}
Horseradish peroxidase		
R^2 value	0.989	0.999
Sensitivity	0.45 pA $pmol^{-1}$ L	1300 RLU $pmol^{-1}$ L
LOD	1.6 pmol L^{-1}	0.7 pmol L^{-1}

Table 1: Parameters of the calibration curves obtained for the three assayed reactions and two types of detection system employed

7.3.3 Alkaline phosphatase

ALP is a enzyme of 160 kDa that is often employed as a marker for CL assays employing 1,2-dioxetane derivatives as enzymatic substrates. The CL cocktail employed for ALP in this work contains 4-methoxy-4-(3-phosphatephenyl)spiro [1,2- dioxetane-3,2'-adamantane] disodium salt (AMPPD) and an enhancer (which increases the duration and intensity of the emission). The enzyme catalytic action on AMPPD consists in dephosphorylation of the aryl phosphate with subsequent cleavage of the 1,2- dioxetane ring and the production of a phenolate in its excited state leads to photons emission [35]. The kinetics of photon emission measured with on-chip a-Si:H photosensors is reported in Fig. 3. Each measured solution contains 2 µL of a 3×10^{-4} mg mL^{-1} ALP solution (corresponding to 2 fmol of deposited enzyme), and 8 µL of Lumiphos plus CL cocktail. In the figure is reported the sensor photocurrent calculated as the total measured current minus the dark current value measured before adding the enzyme, which was stable for more than 10 min (CV 0.7 %). Upon enzyme addition, the photocurrent response rapidly increased during the first 5 min and then remained at plateau for at least 5 min (10.8±0.1 pA, inset in Fig. 3). The CL signal decreases very slowly to the baseline level in approximately 2 h, due to the consumption of CL reagents and/or inactivation of the enzyme. The observed behavior was confirmed by the reference CCD system and it reflects the typical kinetics of the CL reaction of 1,2-dioxetane compounds catalyzed by ALP [36]. All the photodiodes of the array shows a dark current around 8 pA. This baseline value also

accounts for the very weak spontaneous light emission of the CL cocktail in the absence of enzyme. The intrinsic photodiode current shot noise, the preamplifier noise and the switching (kTC) noise contributions cause the variance of the baseline signal and they corresponds to the practical noise of the system. Results show that the a-Si:H photosensors enables real-time detection of evolving CL reactions infact they rapidly respond to changes in the CL signal and return to dark signal levels upon completion of the reaction, without any memory effect. Moreover the amount of data corresponding to the entire kinetic curve using 4-s time resolution, occupies about 64 kB of memory, while the 480 raw images, acquired by the CCD camera every 15 s, occupy at least 235MB (495 kB for each frame).

This has a significant impact on the algorithm complexity and computing time for data analysis and also on the data-storage and data-transmission bandwidth. Calibration curves were obtained in the range between 5 and 100 pg μL^{-1} employing the 1,2-dioxetane-based CL cocktail and in Fig. 4 are reported the data measured with the a-Si:H photosensors and with the CCD-based detector. Both curves present an excellent linearity in the investigated range of concentration. Each point referring to the specific ALP concentration is taken from the maximum of the kinetic curve with respect to the signal baseline, averaged over three different experiments.

The measured sensitivity of the a-Si:H photodiodes is 38.5 fA pg^{-1} and the calculated LOD at three sigma is 5 pg μL^{-1} (corresponding to 65 amol of deposited enzyme considering that the measured standard deviation of the blank signal is 120 fA. The LOD obtained using the CCD (2.8 pg μL^{-1})

demonstrates that a-Si:H photodiodes shows equivalent performances with state-of-the-art laboratory instrumentation.

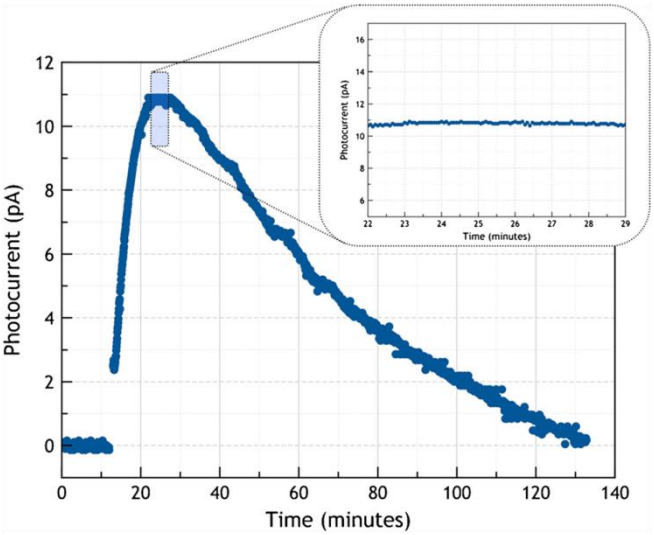

Figure 3: Kinetics of photon emission of ALP CL system measured with on-chip a-Si:H photodiodes

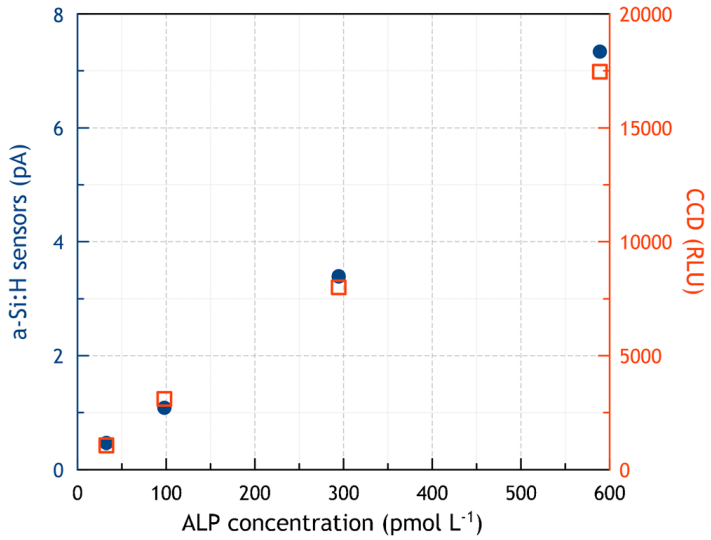

Figure 4: Calibration curve for ALP employing the Lumiphos Plus CL cocktail. Circle and squares refer to the measurements achieved with a-Si:H photosensors and CCD camera, respectively.

7.3.4 Luciferase

Firefly Luc is one of the most widely used reporter proteins for reporter gene-based whole-cell and biosensors for the study of gene expression. Wildtype Photinus pyralis luciferase is a 62-kDa protein that in the presence of Mg^{2+}, ATP and molecular oxygen oxidizes its enzymatic substrate, firefly luciferin, emitting yellow-green light (emission maximum ~560 nm). The quantum efficiency of the a-Si:H photosensors is maximum at this wavelength, around 0.72, as shown in Fig. 2b.

Calibration curves for Luc were generated in the range between 20 pg μL^{-1} and 2 ng μL^{-1} employing the luciferin/ATP-based BL cocktail (Fig. 5). It was found a LOD of 30 pg μL^{-1} that corresponds to 1 fmol of deposited enzyme, while 10 pg μL^{-1} was the LOD obtained with the CCD-based detection. This extends possible applications to BL-based assays, such as recombinant whole-cell biosensors for environmental or life science applications and it is the first report about the measurement of Luc signals with integrated a-Si:H photosensors.

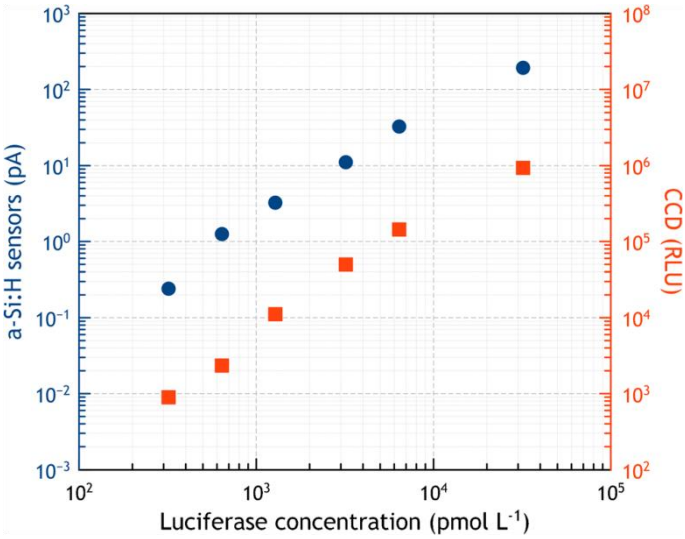

Figure 5: Calibration curve for Luc employing the Britelite plus BL cocktail. Blue and red symbols refer to the measurements achieved with a-Si:H photosensors and CCD camera, respectively

7.3.5 Horseradish peroxidase

Another enzyme widely used in bioanalytical assays is Horseradish peroxidase which is characterized by low dimension (44 kDa) and high turnover rate. It catalyzes the reaction between a hydrogen acceptor (such as hydrogen peroxide) and a hydrogen donor, namely luminol in CL systems. Luminol is oxidized producing 3-aminophthalate in its excited state and when it decays to the ground state it releases photons with maximumemission at 425 nm. Adding some enhancers to the CL cocktail such as substituted phenols, substituted arylboronic acid derivatives and other molecole it is possible to increase the enzyme turnover number and the equilibrium concentration of the key intermediate luminol radical anion, providing more intense, prolonged and stable light emission [37,38].

In Fig. 6 is reported the calibration curves, obtained for the enzyme HRP (between 0.025 and 50 pg μL^{-1}) via CCD camera and photosensors. The calibration curves obtained employing the photosensors are consistentwith CCD results. Limits of detection of 70 fg μL^{-1} (corresponding to 3 amol of deposited enzyme) was found for the photosensors, which was only 2.3 times higher than the LOD obtained for the CCD measurement in the same experimental conditions and consistent with previously reported LOD values [39]. Each curve is the average of three independent measurements. The linear response extends up to 5 pg μL^{-1}. At higher concentrations it was observed a slight deviation from linearity that is probably due to the fact that the CL reagents are not in sufficient excess with respect to enzyme amount as previously reported [28]. However the dynamic range of the curve covers three orders of magnitude of enzyme concentrations.

By comparing the calibration curves obtained employing different a-Si:H photosensor chips produced in different sessions, very high inter-chip reproducibility was observed.

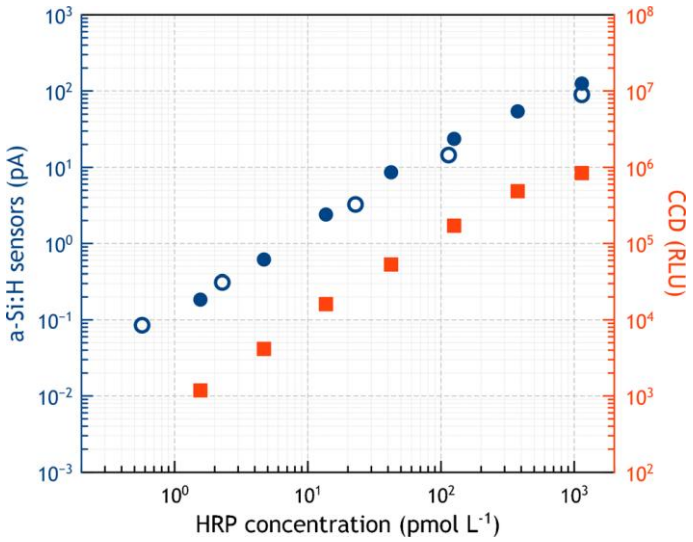

Figure 6: Calibration curve for HRP employing the SuperSignal ELISA Femto CL cocktail. Open and solid circles refer to the measurements achieved with a-Si:H photosensors produced in two different fabrication runs and acquired with the Keithley 236 SMU and with the custom readout electronics, respectively. Squares refer to the measurements achieved with the CCD camera

7.3.6 Sensors array characterization

The design of the array of photosensors allows the simultaneous measurement of 16 different luminescent reactions. In this way the system is suitable for multiplex bioassays in which the reaction areas are spatially resolved. It is necessary to verify absence of crosstalk phenomena among adjacent photosensors and to ensure that all the photosensors can uniformly respond to a given light signal independently on their position on the array.

7.3.7 Inter-sensor reproducibility

Inter-sensor reproducibility was evaluated by depositing an aliquot of the same CL cocktail containing HRP at low (0.2 pg μL^{-1}) and high (2 pg μL^{-1}) levels on each photodiode.

Acquiring the CL signals simultaneously for all the photosensors, it was observed a maximum variability of the signal between photosensors of 3%.

7.3.8 Crosstalk

The evaluation of crosstalk phaenomenon was performed by pouring HRP CL solutions at different concentrations in the highest investigated range (between 0.2 and 50 pg μL^{-1}) in one of the black PDMS wells and by comparing the signal of the selected site with that of the all neighboring sites.

It was observed that the crosstalk signal between photosensors was well below the noise level of the sensors, thus proving that combining the design of the array (size and spacing of the photosensors) and the use of black PDMS structure for sample confinement is correct making the device suitable for the simultaneous measurement of multiple analytes with negligible crosstalk between the photosensor.

7.3.9 Model luminescent bioanalytical assays

Applying model BL cytotoxicity assay and a CL total antioxidant capacity assay it was demonstrated the applicability of the integrated a-Si:H photosensor array to real bioanalytical assays. In these kind of assay, the possibility to follow the CL emission in real-time over a large number of consecutive acquisitions is crucial for assay performance.

7.3.10 Bioluminescence cytotoxicity assay

HEK293 cells genetically modified to stably express Luc were treated with DMSO at different concentrations (in the range 2–50 %v/v) as a model toxic compound. The addition of the toxic compound to the cells suspension causes cell membrane disruption, leading to a reduction in cell metabolism and viability, thus lowering the BL signal. The BL emission of treated cells was normalized accordingly to the blank that was set to 100 % and plotted against DMSO concentration, as reported in Fig. 7.

As expected, the decrease in the BL signal attested the toxic effect of DMSO and it was found that the half lethal concentration (LC50) of 13 % (v/v) DMSO is the concentration that produces a 50 % reduction in light.

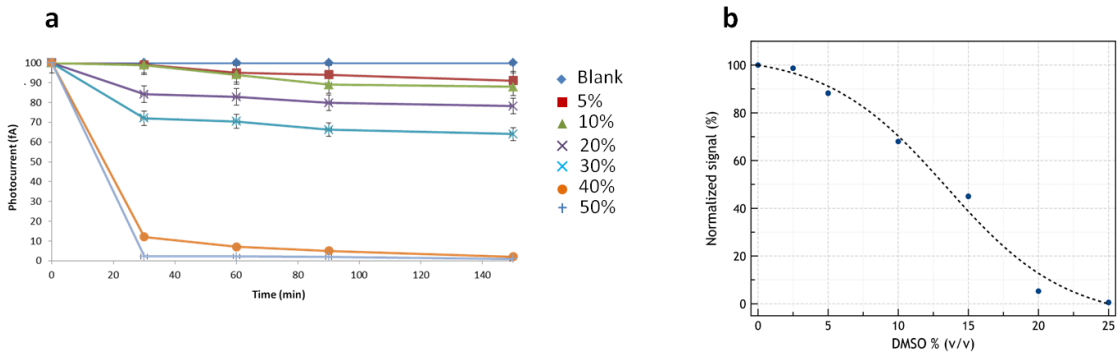

Figure 7: (a) DMSO effects on the BL signal as a function of toxic compound concentration (in the range between 5% and 50%) and treatment time (from 30 to 150 min). The signal is normalized respect to BL signal measured for the non-treated cells; (b) Normalized cytotoxicity curve for DMSO, asmeasured employing a-Si:H photosensors.

7.3.11 Chemiluminescence measurement of total antioxidant capacity

The assay is based on the ability of antioxidants (i.e. compounds with a reduction potential lower than that of luminol) to quench the enhanced HRP-catalyzed luminol CL reaction [38]. CL emission is quenched as long as antioxidants are present in the mixture and it recovers as soon as all antioxidants are oxidized. To determine the total antioxidant capacity of a sample, the recovery time is employed and compared with the response of a standard antioxidant (in this work ascorbic acid).Since the analytical information is given by the time of the 50 % signal, in this type of assay, the possibility to simultaneously record in real-time the evolving CL reactions is crucial. The evolving signals measured for the CL cocktail in the presence of different amounts of ascorbic acid is reported in Fig. 8 (top). A linear calibration curve was obtained by plotting the time of 50 % signal recovery against ascorbic acid concentration. Finally two extracts

from red grape juice were assayed, one obtained through extraction in water and one in ethanol. Preliminary experiments showed that that the optimal dilution factor to obtain signal recovery within 10 min was 1:100 (v/v) and 1:500 (v/v) for the aqueous and the alcoholic extracts, respectively. As shown in Fig. 8 (bottom), for samples containing a mixture of different antioxidant compounds, a smooth increase of the CL signal is observed as compared with sharp increase of the CL signal observed in the presence of the standard antioxidant ascorbic acid. By interpolating the time of 50 % signal recovery of each sample on the calibration curve previously reported, it was found the total antioxidant capacity of the sample expressed as ascorbic acid equivalents, that corresponds to 14 mM for the ethanol extract and 3.5 mM for the aqueous extract. These results showed, as expected, a higher antioxidants extraction ability of alcoholic solutions with respect to aqueous ones.

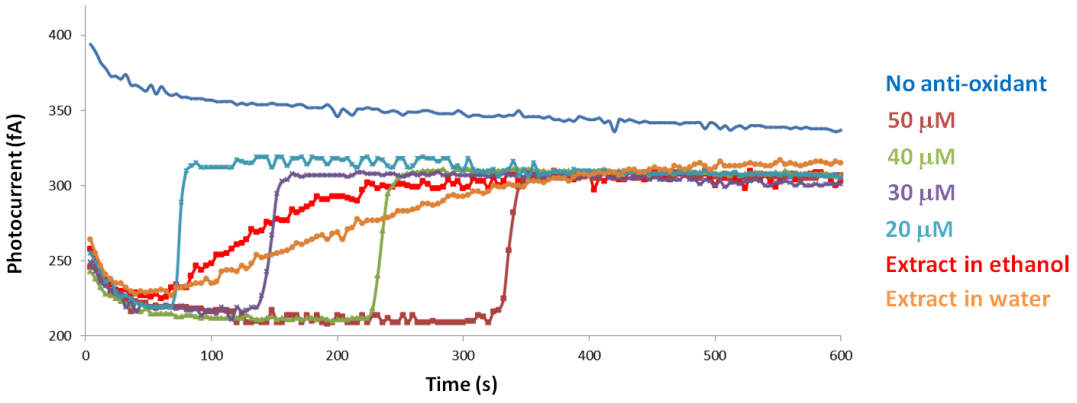

Figure 8: Real-time monitoring of CL emission of the HRP/CL cocktail in the presence of ascorbic acid standard solutions and red grape juice extracts.

7.4 Conclusions

In view of the development of integrated of a BL and CL-based LOC device that combine the analytical detection system and the transduction into a simle chip, the performance of a new photosensors chip was evaluated. In order to allow multiplex analyses, the a-Si:H photosensors used in this work were deposited on a glass support and patterned in a 4×4 matrix. The opposite side of the support was coupled with a multiwell PDMS microcartridge that allow to carry out the luminescence reactions in positions corresponding to the sensors. The a-Si:H photosensors are are amenable to fabrication in different sizes and inexpensive to manufacture. For multiplex applications, they can be produced in arrays, in which the number of sensors is limited by the size of the glass substrate and their density by the crosstalk phenomena, that can be controlled by careful design of the array geometry [40]. The photosensors were tested on BL and CL-enzyme based reactions showing a good inter-sensor reproducibility within the array, low instrumental noise levels, LOD values comparable with those obtained employing reference laboratory instrumentation and negligible crosstalk between adjacent sensors. In particular, the limits of detection for HRP, AP and firefly Luc enzyme labels were found in the order of attomoles to femtomoles and the linearity of response extended up to three orders of magnitude making the a-Si:H photosensors suitable for analytical applications in BL and CL-based LOC devices.

The a-Si:H photosensor array are comparable with respect to cooled CCD detectors not only regards detectability but even device dimensions and costs. Moreover it is important to point out that , while the CCD results refer to thermally cooled device, the a-Si:H photosensor performances were achieved at room temperature (about 25 °C) showing the suitability of the proposed system for in-the-field applications.

In addition, the digital memory occupancy of the measured data is significantly lower than those of image-based systems, which have positive effects not only on the data storage but also on the algorithm complexity and computing time for data analysis.

In the future it will be possible to extend the multiwell cartridge with integrated photosensors applicability to the development of rapid heterogeneous assays, which require a different microfluidic device. We can state therefore that the proposed a-Si:H photosensor array, when integrated with microfluidic chips, provides sensitive, compact and potentially low-cost microdevices for BL- and CL-based bioassays with a wide range of possible applications for in-field and point-of-care bio-analyses.

References

[1] Abgrall P., Gue A.M.; (2007) Lab chip technol; 17:R15–R49

[2] Arora A., Simone G., Salieb-Beugelaar G.B., Kim J.T., Manz A.; (2010) Anal Chem; 82: 4830–4847

[3] Costantini F., Nascetti A., Scipinotti R., Domenici F., Sennato S., Gazza L., Bordi F., Pogna N., Manetti C., Caputo D., de Cesare G.; (2014) RSC Adv; 4:2073– 2080

[4] Seidel M., Niessner R.; (2008) Anal Bioanal Chem; 391:1521–1544

[5] Marquette C.A., Corgier B.P., Blum L.J.; (2012) Bioanalysis; 4:927–936

[6] Marquette C.A., Blum L.J.; (2009) Bioanalysis; 1:1259–1269

[7] Roda A., Guardigli M., Pasini P., Mirasoli M., Michelini E., Musiani M.; (2005) Anal Chim Acta; 541:25–36

[8] Roda A., Pasini P., Guardigli M., Baraldini M., Musiani M.,Mirasoli M.; (2000) Fresen J Anal Chem; 366:752–759

[9] Roda A., Guardigli M., Michelini E., Mirasoli M.; (2009) Trac-Trends Anal Chem; 28:307–322

[9] Mirasoli M., Guardigli M., Michelini E., Roda A.; (2014) J Pharm Biomed Anal; 87: 36–52

[10] Kricka L.J., Park J.Y.; (2011) in: Roda A (ed) Chemiluminescence and bioluminescence—past, present and future. RSC, Cambridge

[11] Berthold F., Hennecke M., Wulf J.; (2011) In: Roda A (ed) Chemiluminescence and bioluminescence—past, present and future. RSC, Cambridge, pp 113–139 12

[12] Roda A., Mirasoli M., Dolci L.S., Buragina A., Bonvicini F., Simoni P., Guardigli M.; (2011) Anal Chem; 83:3178–3185

[13] Roda A., Cevenini L., Michelini E., Branchini B.R.; (2011) Biosens Bioelectron; 26:3647–3653

[14] Mirasoli M., Bonvicini F., Dolci L.S., Zangheri M., Gallinella G., Roda A.; (2013) Anal Bioanal Chem; 405:1139–1143

[15] Kamei T., Toriello N.M., Lagally E.T., Blazej R.G., Scherer J.R., Street R.A., Mathies R.A.; (2005) Biomed Microdevices; 7:147– 152

[16] Ibaraki N.; (1994) Materials Research Society Symposium Proceedings Cambridge Univ Press; 336:749–749

[17] Carlson D.E.; (1977) IEEE Trans Electr Dev; 24:449–453

[18] de Cesare G., Gavesi M., Palma F., Riccò B.; (2003) Thin Solid Films 427:191–195

[19] Caputo D., de Cesare G., Nascetti A., Tucci M.; (2008) IEEE Trans Electr Dev; 55:452–456

[20] Louro P., Fernandes M., Fantoni A., Lavareda G., Nunes de Carvalho C., Schwarz R., Vieira M.; (2006) Thin Solid Films; 511–512:167–171

[21] Caputo D., de Cesare G., Nascetti A., Palma F., Petri M.; (1998) Appl Phys Lett; 72:1229–1231

[22] Fixe F., Chu V., Prazeres D., Conde J.P.; (2004) Nucleic Acids Res; 329:70–75

[23] de Cesare G., Caputo D., Nascetti A., Guiducci C., Riccò B.; (2006) Appl Phys Lett; 88:083904–083906

[24] Caputo D., de Cesare G., Nascetti A., Negri R.; (2006) J Non-Cryst Solids; 352: 2004–2006

[25] Caputo D., de Cesare G., Fanelli C., Nascetti A., Ricelli A., Scipinotti R.; (2012) IEEE Sens J; 12:2674–2679

[26] Novo P., Prazeres D.M.F., Chu V., Conde J.P.; (2011) Lab Chip; 11:4063–4071

[27] Novo P., Moulas G., Prazeres D.M.F., Chu V., Conde J.P.; (2013) Sensor Actuat B-Chem; 176:232–240

[28] Caputo D., de Cesare G., Dolci L.S., Mirasoli M., Nascetti A., Roda A., Scipinotti R.; (2013) IEEE Sens J; 13: 2595–2602

[29] Nascetti A., Truglio M., Valerio P., Caputo D., de Cesare G.; (2011) Proc 4th IEEE Int Work Adv Sensors Interfaces art. no. 6004691:77–81

[30] Wieczorek H.; (1995) Solid State Phenom; 44–46:957–972

[31] Pereira A.T., Pimentel A.C., Chu V., Prazeres D.M.F., Conde J.P.; (2009) IEEE Sens J 9: 1282–1290

[32] Liu C-H., Chang Y-C., Norris T.B., Zhong Z.; (2014) Nat Nanotechnol; 9:273–278

[33] Wang X., Amatatongchai M., Nacapricha D., Hofmann O., de Mello J.C., Bradley D.D.C., de Mello A.J.; (2009) Sensor Actuat B-Chem; 140:643–648

[34] Matos Pires N.M., Dong T., Hanke U., Hoivik N.; (2013) J Biomed Opt 18:097001

[35] Adam W., Bronstein I., Edwards B., Engel T., Reinhardt D., Schneider F.W., Trofimov A.V., Vasil'ev R.F.; (1996) J Am Chem Soc; 118:10400–10407

[36] Roda A., Pasini P., Musiani M., Girotti S., Baraldini M., Carrea G., Suozzi A.; (1996) Anal Chem; 68:1073–1080

[37] Easton P.M., Simmonds A.C., Rakishev A., Egorov A.M., Candeias L.P.; (1996) J Am Chem Soc; 118:6619–6624

[38] Marzocchi E., Grilli S., Della Ciana L., Prodi L., Mirasoli M., Roda A. (2008) Anal Biochem; 377: 189–194

[39] Saleh L., Plieth C.; (2010) Nat Protoc 5:1627–1634

[40] Pereira A.T., Pimentel A.C., Chu V., Prazeres D.M.F., Conde J.P.; (2009) IEEE Sens J 9: 1282–1290

List of publications

1. A simple and compact smartphone accessory for quantitative chemiluminescence-based lateral flow immunoassay for salivary cortisol detection *M. Zangheri, L. Cevenini, L. Anfossi, C. Baggiani, P. Simoni, F. Di Nardo, A. Roda* Biosensors and Bioelectronics, (2015) 64: 63-68

2. A multiplex chemiluminescent biosensor for type B-fumonisins and aflatoxin B1 quantitative detection in maize flour *M. Zangheri, F. Di Nardo, L. Anfossi, C. Giovannoli, C. Baggiani, A. Roda, M. Mirasoli*Analyst, (2015) 140 (1): 358-365

3. Multiwell cartridge with integrated array of amorphous silicon photosensors for chemiluminescence detection: development, characterization and comparison with cooled-CCD luminograph *M. Mirasoli, A. Nascetti, D. Caputo, M. Zangheri, R. Scipinotti, L. Cevenini, G. de Cesare, A. Roda* Analytical and bioanalytical chemistry, (2014) 406 (23): 5645-5656

4. Chemiluminescence-based micro-total-analysis system with amorphous silicon photodiodes *D. Caputo, G. de Cesare, R. Scipinotti, M. Mirasoli, A. Roda, M. Zangheri, A. Nascetti* Sensors and Microsystems (edited by Springer International Publishing, (2014) 207-211

5. Chemiluminescence-based biosensor for fumonisins and aflatoxins quantitative detection in maize samples *M. Mirasoli, M. Zangheri, L.*

Anfossi, F. Di Nardo, D. Calabria, C. Giovannoli, C. Baggiani, A. Roda Luminescence, (2014) 29: 31-32

6. Localization of proteins in paint cross-sections by scanning electrochemical microscopy as an alternative immunochemical detection technique *G. Sciutto, S. Prati, R. Mazzeo, M. Zangheri, A. Roda, L. Bardini, G. Valenti, S. Rapino, M. Marcaccio* Analytica chimica acta, (2014) 831: 31-37

7. Performances of on-chip integrated amorphous silicon photodiodes for chemiluminescence and bioluminescence-based assays *M. Mirasoli, A. Nascetti, M. Zangheri, D. Caputo, R. Scipinotti, G. De Cesare, A. Roda* Luminescence, (2014) 29: 31-31

8. Performances of amorphous silicon photodiodes integrated in chemiluminescence based μ-TAS *D. Caputo, M. Nardini, R. Scipinotti, G. de Cesare, M. Mirasoli, M. Zangheri, A. Roda, A. Nascetti* SPIE Optics+ Optoelectronics,(2013) 87740W-87740W-8

9. Portable chemiluminescence multiplex biosensor for quantitative detection of three B19 DNA genotypes *M. Mirasoli, F. Bonvicini, L.S. Dolci, M. Zangheri, G. Gallinella, A. Roda* Analytical and bioanalytical chemistry, (2013) 405 (2-3): 1139-1143

10. Gravitational field-flow fractionation integrated with chemiluminescence detection for a self-standing point-of-care compact device in bioanalysis *S. Casolari, B. Roda, M. Mirasoli, M. Zangheri, D. Patrono, P. Reschiglian, A. Roda* Analyst, (2013) 138 (1): 211-219

11. Single and multiplexed immunoassays for the chemiluminescent imaging detection of animal glues in historical paint cross-sections *G. Sciutto, L.S. Dolci, M. Guardigli, M. Zangheri, S. Prati, R. Mazzeo, A. Roda* Analytical and bioanalytical chemistry, (2013) 405 (2-3): 933-940

12. Parvovirus B19 DNA detection in serum samples employing a microfluidic device based on chemiluminescence contact imaging *M. Mirasoli, L.S. Dolci, F. Bonvicini, A. Buragina, F. Di Furio, M. Zangheri, M. Guardigli, G. Gallinella, A. Roda* Luminescence, (2012) 27 (2): 141-142

Acknowledgments

The present works have been performed in the Laboratory of Analytical and Bioanalytical Chemistry headed by Prof. Aldo Roda. I thank him and his co-workers, especially my supervisor Prof. Mara Mirasoli.

I also thank the following research groups for the profitable collaborations:

- Analytical Chemistry group directed by Prof. Claudio Baggiani (University of Turin)
- D. Caputo, G. de Cesare, R. Scipinotti - Dept. of Information Engineering, Electronics, Telecommunications ("Sapienza" University of Rome)
- A. Nascetti - Aerospace and Astronautics Engineering ("Sapienza" University of Rome)
- Analytical Chemistry group directed by Prof. Pierluigi Reschiglian (University of Bologna)
- Virology group directed by Prof. Giorgio Gallinella (University of Bologna)
- Microchemistry and Microscopy Art Diagnostic group directed by Prof. Rocco Mazzeo (University of Bologna)